REPUBLIC OF TURKEY

GRADUATE SCHOOL OF NATURAL AND APPLIED SCIENCES

DEPARTMENT OF ELECTRICAL AND ELECTRONIC ENGINEERING

INVESTIGATION AND IMPROVEMENT OF ULTRAWIDEBAND ANTENNA CHARACTERISTICS

DUYGU NAZAN GENÇOĞLAN

MASTER OF SCIENCE

Adana 2017

REPUBLIC OF TURKEY

GRADUATE SCHOOL OF NATURAL AND APPLIED SCIENCES

DEPARTMENT OF ELECTRICAL AND ELECTRONIC ENGINEERING

INVESTIGATION AND IMPROVEMENT OF ULTRAWIDEBAND ANTENNA CHARACTERISTICS

DUYGU NAZAN GENÇOĞLAN

MASTER OF SCIENCE

SUPERVISOR

ASSIST. PROF. DR. ŞULE ÇOLAK

Adana 2017

Approval of the Graduate School of Natural and Applied Sciences

Director

Assoc. Prof. Dr. Osman SİVRİKAYA

I certify that this thesis satisfies all the requirements as a thesis for the degree of Master of Science.

Chairman of the Department

Asst. Prof. Dr. Mahmut Yusuf TANRIKULU

This is to certify that I have read this thesis and that in my opinion it is fully adequate, in scope and quality, as a thesis for the degree of Master of Science.

Supervisor

Asst. Prof. Dr. Şule ÇOLAK

Adana Science and Technology University

Examining Committee Members

Assoc. Prof. Dr. Muharrem KARAASLAN

İskenderun Technical University

Assoc. Prof. Dr. Sami ARICA

Çukurova University

ABSTRACT

INVESTIGATION and IMPROVEMENT OF ULTRAWIDEBAND ANTENNA CHARACTERISTICS

GENÇOĞLAN, Duygu Nazan

Master of Science, Department of Electrical and Electronic Engineering

2017, 112 Pages

In this study, antenna design is performed for Ultra-Wideband (UWB) communication systems and antenna parameters are analysed for determining the antenna performance in UWB systems. Various Ultra- Wideband antenna structures, including half wave dipole, bowtie antenna, and microstrip antenna, are designed and examined in the entire UWB frequency range, i.e. 3.1-10.6 GHz. All of the proposed antenna types are simulated through CST Microwave Studio programme. During the simulation and design process, the crucial antenna parameters such as Return Loss (S_{11}), Voltage Standing Wave Ratio (VSWR) and radiation pattern are investigated.

Some bandwidth enhancement techniques are applied for enhancement of the bandwidth and antenna performance over the UWB frequency range. These techniques include bevelling and truncating the arm edges for bowtie antenna, and changing the patch geometry for microstrip patch antenna. Then, some of the efficient antenna structures are selected in order to be optimized with evolutionary algorithms such as Genetic Algorithm and Particle Swarm Optimization. Furthermore, the effects of the optimization procedures are investigated to utilize the selected antenna structures more effectively in the UWB frequency range.

Key Words: *antennas, ultra-wideband (UWB), return loss, voltage standing wave ratio (VSWR), bandwidth*

ÖZET

ULTRA GENİŞ BANT ANTEN ÖZELLİKLERİNİN ARAŞTIRILMASI VE GELİŞTİRİLMESİ

GENÇOĞLAN, Duygu Nazan

Yüksek Lisans, Elektrik- Elektronik Mühendisliği

2017, 112 Sayfa

Bu çalışmada, Ultra-Geniş Bant (UGB) iletişim sistemleri için anten tasarımı yapılmış ve UGB sistemlerde anten performansını belirlemek için anten parametreleri analiz edilmiştir. Yarım dalga dipol, kelebek ve mikro şerit antenleri gibi çeşitli Ultra Geniş Bant anten yapıları, tasarlanmış ve UGB frekans aralığının tamamında, yani 3.1 - 10.6 GHz' de incelenmiştir. UGB antenlerinin tümünün benzetimi CST Mikrodalga Stüdyo programı ile yapılmıştır. Benzetim ve tasarım işlemi sırasında Geri Dönüş Kaybı (S_{11}), Duran Dalga Oranı ve radyasyon örüntüsü gibi önemli anten parametreleri incelenmiştir.

Anten bant genişliğinin ve anten performansının UGB frekans aralığında arttırılması için bazı bant genişliği iyileştirme teknikleri uygulanmıştır. Bu teknikler kelebek anten için kol kenarlarının eğilmesi ve kesilmesi, mikro şerit anten içinse yama geometrisinin değiştirilmesi şeklinde uygulanmıştır. Daha sonra verimli anten yapılarından birkaçı, Genetik Algoritma ve Parçacık Sürüsü Optimizasyonu gibi evrimsel algoritmalar ile optimize edilmek üzere seçildi. Buna ek olarak, seçilen anten yapılarını UWB frekans aralığında daha verimli bir şekilde kullanmak için optimizasyon prosedürlerinin etkisi araştırılmıştır.

Anahtar Kelimeler: *anten, ultra geniş bant (UGB), geri dönüş kaybı, voltaj duran dalga oranı(VDDO), bant genişliği*

ACKNOWLEDGEMENTS

I would first like to thank my thesis supervisor Assistant Professor Şule ÇOLAK of the Electrical and Electronic Engineering Department at the Adana Science and Technology University. The door to Asst. Prof. ÇOLAK and TUTSOY office was always open whenever I ran into a trouble spot or had a question about my research. Her encouragement, support, guidance and motivation from the initial level helped me to be more precise to our work and also helped me to develop a deep understanding on the subject. Furthermore, her constant effort to understand the underlying principles, and, create better designs has motivated me to do the same as well.

I would also like to thank my committee members, Assoc. Prof. Sami ARICA, Assoc. Prof. Muharrem KARAASLAN for serving as my committee members even at hardship. I also want to thank them for letting my defense be an enjoyable moment, and for their brilliant comments and suggestions.

I also want to express my thanks to Asst. Prof. Lütfü SARIBULUT, Asst. Prof. Önder TUTSOY and his master degree students who encourage me in my endeavours.

This thesis is supported by the Scientific Research Projects Unit (BAP) in Adana Science and Technology University. Project No: MÜHDBF.EEM.2015-18, Project Title: INVESTIGATION and IMPROVEMENT OF ULTRAWIDEBAND ANTENNA CHARACTERISTICS.

I would like to forward deep thank to all of my department lecturers, Asst. Prof. M. Yusuf TANRIKULU, Asst. Prof. Amira GÜRSEL, Asst. Prof. Esen YILDIRIM, and the staff at Adana Science and Technology University for their great help.

Finally, I must express my very profound gratitude to my parents and to my sisters for providing me with unfailing support and continuous encouragement throughout my years of study and through the process of researching and writing this thesis. This accomplishment would not have been possible without them.

TABLE OF CONTENTS

ABSTRACT ..... **i**

ÖZET ..... **ii**

ACKNOWLEDGEMENTS ..... **iii**

TABLE OF CONTENTS ..... **iv**

LIST OF FIGURES ..... **vi**

LIST OF TABLES ..... **xii**

NOMENCLATURE ..... **xiii**

1. INTRODUCTION **1**

2. ANTENNA PARAMETERS **5**

2.1 Radiation Pattern 5

2.1.1. Antenna Field Zones 6

2.2 Directivity, D 7

2.3 Gain, G 8

2.4 Polarization 8

2.5. Impedance, Z_A 9

2.6. Bandwidth 9

2.7. VSWR 9

2.8. Return Loss 10

3. HALF WAVE DIPOLE ANTENNA **11**

3.1. Results and Discussion 12

3.2. Radius Effect 16

4. BOW TIE ANTENNA **19**

4.1. Results and Discussion 20

4.1.1. Arm Length Effect on the Antenna Performance 22

5. BOWTIE ANTENNA CONFIGURATIONS **25**

6. ROUNDED BOWTIE ANTENNA **31**

6.1. Antenna Design 31

6.2. Impact of the Dielectric Substrate on the Antenna Performance 33

7. TRUNCATED ROUNDED BOWTIE ANTENNA 36

8. BEVELED EDGE ROUNDED BOW-TIE ANTENNA 42

8.1. Antenna Geometry 43

8.2. Simulation & Results 466

9. MICROSTRIP ANTENNA 60

9.1. Transmission Line Method 63

9.1.1. Design Procedure: 64

9.2. RECTANGULAR EDGE-FED PATCH ANTENNA 65

9.2.1. SIMULATION & RESULTS 67

9.3. ELLIPTIC MICROSTRIP PATCH ANTENNA 72

9.3.1. SIMULATION & RESULTS 74

9.3.1.1. *Effect of the Ground Plane Length on Antenna Performance* 76

10. OPTIMIZATION OF THE ANTENNA STRUCTURES 80

10.1. Enhancement Of Truncated Rounded Bowtie Antenna Via Genetic Algortihm Technique 81

10.2. Enhancement Of Truncated Rounded Bowtie Antenna Via Particle Swarm Optimization Technique 87

10.3. Enhancement Of Elliptic Microstrip Patch Antenna Via Genetic Algorithm 94

10.4. Enhancement Of Elliptic Microstrip Patch Antenna Via Particle Swarm Optimization 100

11. CONCLUSION 106

REFERENCES ..... Hata! Yer işareti tanımlanmamış.

VITA ..... Hata! Yer işareti tanımlanmamış.**2**

LIST OF FIGURES

Figure 1.1: Power Spectral density of UWB systems versus other conventional communication systems (Benedetto et al, 2006; Lu et al, 2003) 2
Figure 1.2: UWB EIRP Emission Level for indoor application in dB (Nekoogar, 2005)..... 3
Figure 2.1: Illustration of radiation pattern of dipole antenna a) when $\phi=90^o$ b) when $\theta=90^o$6
Figure 2.2: Directivity of different type antennas a) Half wave dipole b) Antipodal Vivaldi.. 7
c) Triangular pin fed patch 7
Figure 3.1: Half Wave Dipole Antenna Geometry a)Front View b)Top View 13
Figure 3.2: Excitation Signal-Gaussian Pulse 13
Figure 3.3: Impedance characteristic of the proposed half wave dipole antenna 14
Figure 3.4: Return loss characteristic of the half wave dipole antenna……14
Figure 3.5: VSWR against frequency for the proposed half wave dipole antenna……15
Figure 3.6: Radiation Pattern for half wave dipole antenna with frequency a) 4 GHz b) 5 GHz..... 16
c) 6 GHz, respectively..... 16
Figure 3.7: Simulated return loss curve of half wave dipole for different radius r with a) 0.07 b) 0.1025 c) 0.135 d) 0.1675 e) 0.2 mm, L=20.9 mm and g =0.1045 mm……1
8
Figure 4.1: Geometry of the proposed bow tie antenna a) Front view b) Side view c) Top view..... 20
Figure 4.2: Return loss in dB versus frequency for arm length of 45 mm..... 21
Figure 4.3: VSWR versus frequency for arm length of 45 mm 21
Figure 4.4: Radiation pattern of the proposed antenna at 3, 4.5, 6, 9 GHz respectively... 21
Figure 4.5: a) The proposed antenna with arm length of 45mm, the envisaged antenna with arm length of b) 66.67 mm c) 88.33 and d) 110 mm 23
Figure 4.6: Return Loss Characteristic of classical bowtie antenna with respect to arm length 45, 66.67, 88.33 and 110 mm, respectively..... 24
Figure 5.1: a) Classical Bowtie, b) Rounded Bowtie, c) Truncated Rounded Bowtie Antenna..... 25
Figure 5.2: Schematic diagram and the size of Classical Bowtie Antenna 26
Figure 5.3: Return loss (S11) in dB of the Bowtie Antenna 27
Figure 5.4: VSWR of the Bowtie Antenna..... 27

Figure 5.5: Schematic diagram and the size of Rounded Bowtie Antenna……...27
Figure 5.6: Return loss (S11) in dB of Rounded Bowtie……..28
Figure 5.7: VSWR of rounded Bow Tie Antenna..... 28
Figure 5.8: Schematic diagram and the size of Truncated Rounded BowTie Antenna..... 29
Figure 5.9: Return loss (S11) of the Truncated Rounded Bowtie Antenna..... 30
Figure 5.10: VSWR of the Truncated Rounded Bowtie Antenna..... 30
Figure 6.1: Rounded bow-tie antenna..... 31
Figure 6.2: Return Loss of Rounded Bow Tie Antenna..... 32
Figure 6.3: VSWR of Rounded Bow Tie Antenna 32
Figure 6.4: Return Loss of Rounded Bowtie Antenna at the three different εr values..... 33
Figure 6.5: VSWR of Rounded Bowtie Antenna at the three different εr values 33
Figure 6.6: Return Loss of Rounded Bowtie Antenna at different substrate thickness (H) values..... 34
Figure 6.7: VSWR of Rounded Bowtie Antenna at different substrate thickness (H) values 34
Figure 6.8: Radiation Pattern of Rounded Bowtie Antenna at three different frequencies 3.1GHz (red), 6.85GHz (green) and 10.6GHz (blue), respectively 35
Figure 7.1: Truncated rounded bow-tie antenna..... 36
Figure 7.2: Return Loss of Truncated Rounded Bow Tie Antenna..... 37
Figure 7.3: VSWR of Truncated Rounded Bow Tie Antenna 38
Figure 7.4: Radiation Patterns of Truncated Rounded Bow Tie Antenna at the three different frequencies 3.1GHz (red), 6.85GHz (green) and 10.6GHz (blue), respectively 38
Figure 7.5: Return Loss of Truncated Rounded Bow Tie Antenna at the three different εr values..... 39
Figure 7.6: VSWR of Truncated Rounded Bow Tie Antenna at the three different εr values 39
Figure 7.7: Return Loss of Truncated Rounded Bowtie Antenna at different substrate thickness(H)values……40
Figure 7.8: VSWR of Truncated Rounded Bowtie Antenna at different substrate thickness (H) values..... 40
Figure 7.9: Return Loss of Truncated Rounded Bowtie Antenna at different flare angle (α) values..... 41
Figure 8.1: Different views of the bevelled edge rounded bowtie antenna a) front b-c) perspective with millimeter values d) perspective with dimension labels..... 44

Figure 8.1: Different views of the bevelled edge rounded bowtie antenna e) top with dimension labels f) side view with millimetre values 44
Figure 8.2: The Fourier transform of the excitation signal 46
Figure 8.3: The Fourier series of the excitation signal 46
Figure 8.4: Return loss characteristic of the beveled edge rounded bow tie antenna…….47
Figure 8.5: Minimum return loss value in dB scale of the proposed antenna in the UWB frequency range..... .47
Figure 8.6: Minimum return loss value in linear scale of the proposed antenna in the UWB frequency range..... 47
Figure 8.7: VSWR of the proposed antenna……..48
Figure 8.8: Minimum VSWR value of the proposed antenna……..48
Figure 8.9: Real and Imaginary Part of the Antenna Impedance..... 49
Figure 8.10: The Cartesian representation of the radiation pattern at 6.85 GHz 49
Figure 8.11: The Polar representation of the radiation pattern at 6.85 GHz 49
Figure 8.12: The Cartesian representation of the radiation pattern at 10.275 GHz 50
Figure 8.13: The Polar representation of the radiation pattern at 10.275 GHz. 50
Figure 8.14: a) The Return Loss b) VSWR and c) Impedance of the beveled edge rounded bowtie antenna when the arm length is 70 mm 52
Figure 8.15: a) The Return Loss b) VSWR and c) Impedance of the beveled edge rounded bowtie antenna when the arm length is 85 mm 53
Figure 8.16: a) The Return Loss b) VSWR and c) Impedance of the beveled edge rounded bowtie antenna when the arm length is 100 mm 54
Figure 8.17: a) The Return Loss b) VSWR and c) Impedance of the beveled edge rounded bowtie antenna when the arm length is 110 mm 55
Figure 8.18: a) The Return Loss b) VSWR and c) Impedance of the beveled edge rounded bowtie antenna when the arm length is 120 mm 56
Figure 8.19: a) The Return Loss b) VSWR and c) Impedance of the beveled edge rounded bowtie antenna when the arm length is 130 mm……..57
Figure 8.20: a) The Return Loss b) VSWR and c) Impedance of the beveled edge rounded bowtie antenna when the arm length is 140 mm 58
Figure 9.1: Different Microstrip Antenna Configurations a)Circular Patch Microstrip Antenna b)Triangular Pin Fed Patch Antenna c)Rectangular Patch Microstrip Antenna (CST, 2016)..... 61
Figure 9.2: Microstip Antenna's physical parameters' labels from a) top view(Antenna Magus, 2016) 62
Figure 9.3: Front view of the microstrip antenna (Antenna Magus, 2016) 62

Figure 9.4: The Excitation Signal for input and output ports..... 65
Figure 9.5: Waveguide Representation of the proposed antenna 65
Figure 9.6: Different views of the proposed antenna obtained by CST MWS a) Perspective View b) Front View c) Back View 66
Figure 9.7: Return Loss Characteristic of the proposed rectangular patch microstrip antenna……..……68
Figure 9.8: Return Loss Characteristic of the proposed rectangular patch microstrip antenna with measure lines a) at first resonance b) at second resonance 68
Figure 9.9: VSWR Characteristic of the proposed rectangular patch microstrip antenna . 69
Figure 9.10: VSWR Characteristic of the proposed rectangular patch microstrip antenna with measure lines a) at first resonance b) at second resonance..... 69
Figure 9.11: The impedance characteristic of the proposed antenna..... 70
Figure 9.12: The group delay of the proposed antenna 70
Figure 9.13: Radiation Pattern of proposed antenna at different frequencies a) 6.165 GHz b) 6.85 GHz and c) 7.535 GHz respectively..... 71
Figure 9.14: Perspective View of a) Rectangular Patch b) Elliptic Microstrip patch Antenna from CST MWS 73
Figure 9.15: VSWR characteristic of the microstrip antenna a) rectangular patch b) elliptic patch when ground plane length is 20 mm..... 74
Figure 9.16: Return Loss characteristic of the microstrip antenna a) rectangular patch b) elliptic patch when ground plane length is 20 mm..... 75
Figure 9.17: Bandwidth characteristic of the proposed elliptic microstrip patch antenna.. 76
Figure 9.18: Bandwidth characteristic of the proposed rectangular patch microstrip antenna..... 76
Figure 9.19: Various ground plane lengths effect on return loss parameter when a) 20mm b) 40mm c) 60mm, respectively..... 77
Figure 9.20: All figures plotted in Figure 19 a, b and c, respectively 77
Figure 9.21: VSWR characteristic when ground plane length is a) 20mm b) 40mm c) 60mm, respectively..... 78
Figure 9.22: All figures plotted in Figure 21 a, b and c, respectively 79
Figure 10.1: Genetic Algorithm settings..... 82
Figure 10.2: The optimization method’s input parameter, relative permittivity setting from CST MWS 82
Figure 10.3: The goal function setting from CST MWS..... 83
Figure 10.4: Relative permittivity values of each iteration 84
Figure 10.5: Return loss characteristic of the aforementioned truncated rounded bowtie antenna at fist iteration 85

Figure 10.6: Optimized return loss characteristic of the aforementioned truncated rounded bowtie antenna 85
Figure 10.7: Minimum return loss characteristic of the aforementioned truncated rounded bowtie antenna at first iteration 85
Figure 10.8: Optimized minimum return loss characteristic of the aforementioned truncated rounded bowtie antenna 86
Figure 10.9: Relative permittivity values with 265 iterations 86
Figure 10.10: Minimum return loss characteristic of the truncated rounded bowtie obtained after 265 iterations 87
Figure 10.11: Particle Swarm Optimization settings 89
Figure 10.12: The optimization method's input parameter, relative permittivity setting from CST MWS 89
Figure 10.13: The goal function setting from CST MWS 90
Figure 10.14: Relative permittivity values of each iteration 90
Figure 10.15: Return loss characteristic of the aforementioned truncated rounded bowtie antenna at fist iteration 911
Figure 10.16: Optimized return loss characteristic of the aforementioned truncated rounded bowtie antenna 91
Figure 10.17: Minimum return loss characteristic of the aforementioned truncated rounded bowtie antenna at first iteration 92
Figure 10.18: Optimized minimum return loss characteristic of the aforementioned truncated rounded bowtie antenna 92
Figure 10.19: Relative permittivity values with 265 iterations 93
Figure 10.20: Minimum return loss characteristic of the truncated rounded bowtie obtained after 265 iterations 93
Figure 10.21: Genetic Algorithm settings 95
Figure 10.22: The optimization method's input parameter, relative permittivity setting from CST MWS 96
Figure 10.23: The goal function setting from CST MWS 97
Figure 10.24: Return loss characteristic of the aforementioned elliptic microstrip patch antenna at fist iteration by genetic algorithm 98
Figure 10.25: Optimized return loss characteristic of the aforementioned elliptic microstrip patch antenna by genetic algorithm 98
Figure 10.26: Minimum return loss characteristic of the elliptic microstrip patch antenna at first iteration by genetic algorithm 98
Figure 10.27: Optimized minimum return loss characteristic of the elliptic microstrip patch antenna by genetic algorithm 99

Figure 10.28: Relative permittivity values with 265 iterations 99
Figure 10.29: Particle Swarm Optimization settings……..102
Figure 10.30: The optimization method's input parameter, relative permittivity setting from CST MWS 102
Figure 10.31: Relative permittivity values of each iteration 103
Figure 10.32: The goal function setting from CST MWS 103
Figure 10.33: Return loss characteristic of the elliptic microstrip patch antenna at first iteration 104
Figure 10.34: Optimized return loss characteristic of the elliptic microstrip patch antenna 104
Figure 10.35: Minimum return loss characteristic of the elliptic microstrip patch antenna at first iteration..... 104
Figure 10.36: Optimized minimum return loss characteristic of the elliptic microstrip patch antenna 105
Figure 10.37: Relative permittivity values with 265 iterations 105

LIST OF TABLES

Table 3.1: Calculated antenna dimensions 13
Table 3.2: Bandwidth values with respect to the different radius 18
Table 5.1: Dimensions of Bow Tie Antenna Configurations 26
Table 6.1: Rounded Bowtie Antenna Parameters 32
Table 6.2: Comparison of Return Loss and VSWR parameter at different εr 34
Table 7.1: Truncated Rounded Bowtie Antenna Parameter 37
Table 8.1: Four Different Rounded Bowtie Antenna Structure's Dimensions 45
Table 8.2: Comparison of the antenna parameters with respect to four different antenna structures 51
Table 8.3: Beveled edge rounded bowtie antenna with different arm lengths over UWB frequency range (3-11 GHz) 59
Table 9.1: Detailed Antenna Physical Parameters 63
Table 9.2: The Rectangular Patch Microstip Proposed Antenna: Detailed Physical Parameters 67
Table 9.3: Physical Parameters of the rectangular patch and elliptic microstrip patch antenna 73
Table 9.4: Final dimensions of the proposed antenna after simulation results 79
Table 10.1- Parameters used for optimization by using genetic algorithm 83
Table 10.2- Resulted relative permittivity values after each iteration 84
Table 10.3- Parameters used for optimization by using genetic algorithm: 87
Table 10.4- Resulted relative permittivity values after each iteration: 88
Table 10.5- Parameter used for optimization by using particle swarm optimization: 94
Table 10.6- Resulted relative permittivity values after each iteration 94
Table 10.7- Parameters used for optimization by using particle swarm optimization: 100
Table 10.8- Resulted relative permittivity values after each iteration 101

NOMENCLATURE

UWB	Ultra- Wideband
FCC	Federal Communications Commission
EIRP	Equivalent Isotopically Radiated Power
DoD	Department Of Defense
dB	Decibel
S_{11}	Return Loss
VSWR	Voltage Standing Wave Ratio
R_L	Return Loss
D	Directivity
U	Radiation Intensity
U_{max}	Maximum Radiation Intensity
GHz	Gigahertz
CST	Computer Simulation Technology
λ	Wavelength
MWS	Microwave Studio
HPBW	Half-Power Beam Width
FNBW	First Null Beam-Width
G	Gain
MHz	Megahertz
e_t	Total Efficiency
e_r	Reflection Efficiency
e_c	Conduction Efficiency
e_d	Dielectric Efficiency
Z_A	Input Impedance
R_A	Input Resistance
R_r	Radiation Resistance
R_L	Loss Resistance
X_A	Input Reactance
E_{max}	Maximum measured voltage
E_{min}	Minimum measured voltage
E_i	Incident Wave Amplitude
E_r	Reflected Wave Amplitude
Γ	Reflection Coefficient
α	Flare Angle
l_e	Arm Length

ε_r	Relative Permittivity
H-d	Substrate Thickness
L	Substrate length
W	Substrate width
ε_{eff}	Effective Relative Permittivity
TEM	Transverse Electric-Magnetic
FT	Fourier Transform
FS	Fourier series
f_o	Operating frequency
f_{upper}	Upper Frequency Bound
f_{lower}	Lower Frequency Bound
f_{center}	Centre Frequency
Tanδ	Tangent Loss (Tan Delta)
TLM	Transmission Line Model
ϕ	Azimuth angle in spherical coordinates
θ	Azimuth angle in spherical coordinates
RFID	Radio Frequency Identification
WLAN	Wireless Local Area Network
IEEE	The Institute of Electrical and Electronic Engineering
dBm	Decibel-mill watt
c	Speed of light
g	Feeding Gap
mm	Millimetre
WiMAX	Worldwide Interoperability for Microwave Access
GSM	Global System for Mobile Communications
GA	Genetic Algorithm
PSO	Particle Swarm Optimization

1. INTRODUCTION

Ultra-Wideband (UWB) communication systems have a great deal of desirable properties including broad bandwidth, big data capacity, and ease of integration with other communication systems. The most crucial property among the aforementioned properties is to have broader bandwidth characteristic as compared to other conventional systems. Additionally, this broadband feature defines the UWB system characteristics. There are numerous implementations in order to clarify how the proposed UWB characteristic affects the system performance analysis. A vast quantity of research works have been analysed so as to introduce UWB communication systems (Nikookar, 2009; Win and Scholtz, 1998; Kshetrimayum, 2009; Aiello et al, 2006; FCC, 2002)

The history of UWB system development starts in 1880s with the pioneering work of Hertz, who verified Maxwell equations and used spark gap generator for short pulse transmission (Nikookar, 2009). Guglielmo Marconi established his laboratory in Italy in 1894. G. Marconi examined the spark oscillator for a while. After that, Righi developed this proposed spark oscillators between 1893 and 1896. Marconi and Sir Willian Preece tackled first UWB one mile rooftop link in London in 1896. G. Marconi reported first Transatlantic Wireless Transmission in 1901. Philip Carter exploited conical monopole antenna in 1939. Similarly, Nils E. Lindeblad originated the coaxial horn element antenna in 1941. Furthermore, Henning F. Harmuth, Gerald F. Ross, Kenneth W. Robbins and Paul Van Etten initiated experiments about Impulse UWB in 1960. Actually, the starting point of Impulse radio systems (Win and Scholtz, 1998) was started by G. Marconi owing to his spark gap transmission endeavours. On the other hand, Ultra-Wide Band term was used for the first time by U.S. Department of Defense (DoD) in 1989. Commercial time modulated impulse UWB system was discovered in 1998. Mark A. Barnes originated UWB slot antenna in 2000. Last and not least, US Federal Communication Commission confirmed UWB regulation for proposed communication systems in 2002. In other words, FCC approved the First Report and Order for commercial use of UWB technology with respect to power emission limits (Win and Scholtz, 1998; Kshetrimayum, 2009; Aiello et al, 2006).

Ultra-Wideband (UWB) systems have been currently used for several applications after the Federal Communications Commission (FCC) released the first Report and Order in February 2002 regarding the rules for using UWB technology (FCC, 2002). According to the report, FCC allows the unlicensed use of UWB communication in the frequency band from 3.1 to 10.6 GHz. Moreover, FCC has specified spectral mask in the frequency range of interest in order to protect the power loss during the data transmission

procedure. Therefore, FCC also imposes restrictions for power spectral density level in UWB applications. Figure 1.1 illustrates the FCC spectral mask in terms of power spectral density versus UWB system and other conventional systems. As can be seen from Figure 1.1, the interference might occur due to the interaction between communication system and noise layer. Therefore, power spectral mask is required in order to prevent the interferences. FCC addresses this drawback of the communication systems and regulates the emission limits for low power consumption of indoor and outdoor applications. Figure 1.2 illustrates the UWB Equivalent Isotopically Radiated Power (EIRP) level in dB for indoor applications. According to FCC regulations, EIRP level is limited as -41.3 dBm/MHz for UWB systems.

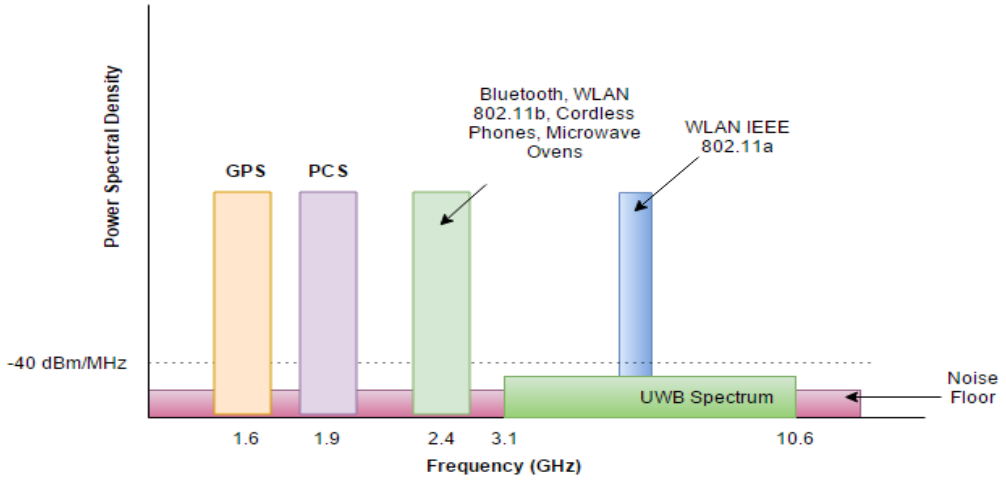

Figure 1.1: Power Spectral density of UWB systems versus other conventional communication systems (Benedetto et al, 2006; Lu et al, 2003)

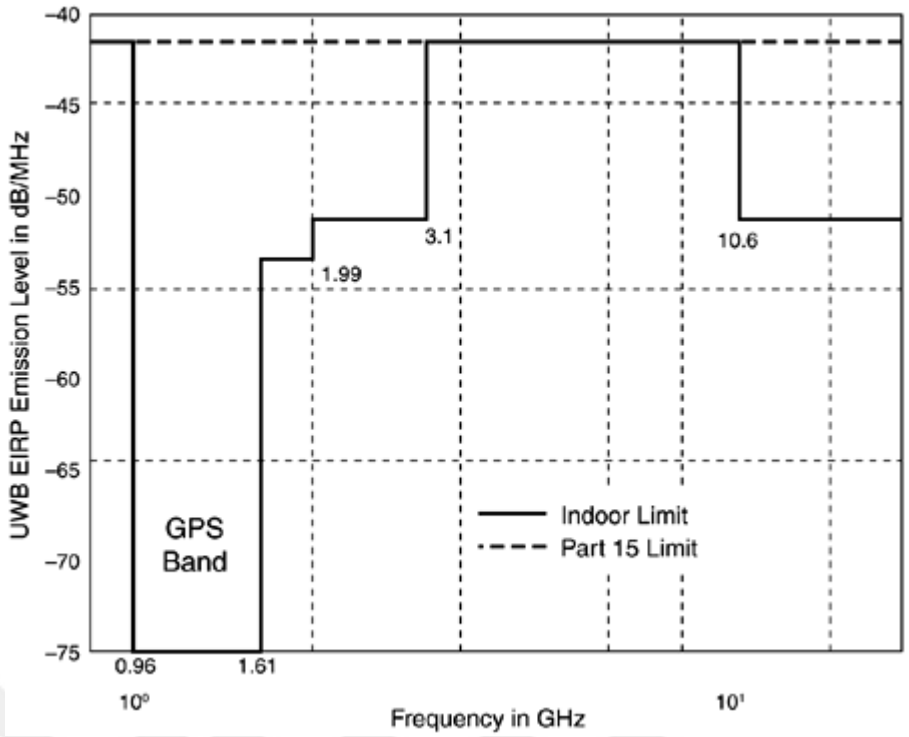

Figure 1.2: UWB EIRP Emission Level for indoor application in dB (Nekoogar, 2005)

Designing UWB transmitter/receiver has remarkable challenges so that the communication system contains simultaneously all requirements so as to have broadband characteristic, good impulse response and minimal distortion etc. At that time, an antenna becomes key component of the UWB communication systems in order to obtain maximum efficiency in the 3.1-10.6 GHz frequency range as allocated by FCC. An antenna is required not only for UWB communication system but also other application areas namely ground penetrating radar, RFID tags, biomedical application and satellite communication etc.(Sayidmarie et al, 2013; Li et al, 2010; Afyf et al, 2015; Çolak and Gençoğlan, 2016a; Çolak and Gençoğlan, 2016b; Aydın and Gençoğlan, 2016). Therefore, the variation in UWB antenna design has been attractive for researchers and scientists.

A number of UWB antenna designs have been examined and investigated in frequency range of interest in the literature (Hecimovic and Marincic; Tareq et al, 2014; Rahim and Xu, 2015; Sharma et al, 2015; Bourqui, 2010). Almost all studies have focused on antenna parameters which alter overall performance and efficiency of the communication system. The proposed antenna parameters, which influence antenna characteristic and system performance, are considered as Return Loss (S_{11} or R_L), Voltage Standing Wave Ratio (VSWR), and radiation pattern in order to exploit antenna as a transmitter or receiver (Balanis, 2005).

This thesis intends to design different antenna structures and define the basic antenna performance parameters including return loss, VSWR and radiation pattern for UWB applications. Additionally, the conventional UWB antennas are modified in order to observe the enhancement of the antenna characteristic. Generally, the main purpose of this thesis is to enhance the bandwidth and radiation characteristics of the antennas in UWB systems. The crucial treatment of proposed designs needs considerable mathematical and theoretical background. Various mathematical expressions are calculated and obtained through various chapters. Furthermore, optimization techniques are applied for determining the antenna dimensions. Half wave dipole, bow tie, rounded bow tie, truncated rounded bowtie, bevelled edge rounded bow tie, microstrip, Rectangular Edge-Fed Patch, Elliptic Microstrip patch and Horn antenna are investigated so that the aforementioned antennas might radiate in the frequency range from 3.1 to 10.6 GHz with 7.5 GHz bandwidth.

2. ANTENNA PARAMETERS

Antenna parameters are substantially important for designing and characterizing the antenna structure. In this study, a number of antennas are designed and simulated to observe fundamental antenna parameters and obtain the appropriate structure. These parameters include Return Loss, Radiation Pattern, Voltage Standing Wave Ratio, Directivity, Gain, and Polarization etc. In this chapter, antenna parameters will be examined so as to define the antenna performance. Therefore, the definitions of the proposed antenna parameters are mentioned first.

2.1 Radiation Pattern

Antenna radiation pattern is the graphical representation of radiation properties such as power density, field strength, radiation intensity, directivity and gain as a function of space coordinates or angles (θ,ϕ).The radiation pattern of dipole antenna which is obtained by using CST MWS, a commercial electromagnetic simulation programme, is illustrated with respect to angles (θ,ϕ) in Figure 2.1 a and Figure 2.1 b. The radiation pattern gives significant information about radiation characteristics of the antenna. In other words, the features, namely half-power beam width (HPBW) or 3dB beam-width, First null beam-width(FNBW), First side lobe level, front to back ratio are interpreted through radiation pattern.

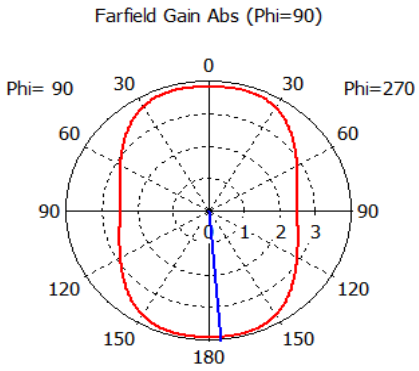

a)

Frequency = 3.425 GHz
Main lobe magnitude = 3.89 dB
Main lobe direction = 175.0 deg.

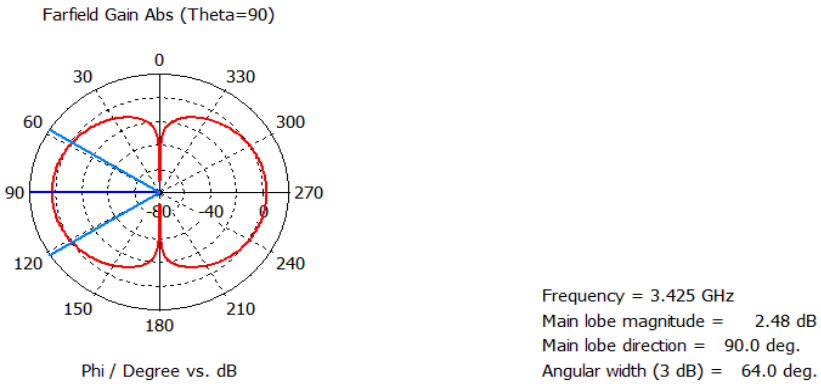

b)

Figure 2.1: Illustration of radiation pattern of dipole antenna a) when ϕ=90^o, b) when θ=90^o

Additionally, the radiation pattern might illustrate normalized values of the fields and power quantities. The antenna radiation pattern depicts how the antenna radiates into space. Furthermore, radiation pattern consists of different configurations, namely omnidirectional, directional and isotropic. An isotropic radiation pattern is generally used for determining antenna gain or directivity properties of the antenna. This type of the radiation pattern does not occur in nature. In other words, the isotropic radiation is a theoretical feature of radiation pattern configurations as a reference source. The most important distinctive feature of the isotropic radiation pattern is to radiate power evenly well in all directions. Another crucial type of radiation pattern is directional feature which radiates or receives electromagnetic waves much more in one direction than in other. This proposed radiation pattern characteristic is preferred in case maximum directivity is considerably required. Thirdly, the omnidirectional radiation pattern, which is peculiar type of directional pattern, has directionless pattern in any plane including azimuthal and elevation. Simultaneously, Figure 2.1 confirms this idea that the antenna radiates all directions when the angle of θ is 90^o.

2.1.1. Antenna Field Zones

The region, which is around proposed antenna, might be separated into three fundamental regions namely far field (i.e. Fraunhofer), reactive near field and radiating near field (i.e. Fresnel) regions. To extend these three different regions, the reactive near field occurs in the immediate vicinity of the antenna (Balanis, 2005). That is, the radiation pattern which ranges at a distance less than $0.62\sqrt{D^3/\lambda}$ gives the near field radiation pattern where *D* stands for the length of antenna and λ represents the wavelength (Balanis, 2005). Furthermore, in the near field region, the shape of the field pattern depends on the distance. Secondly, another significant region, which is called radiating near field (Fresnel), ranges between the reactive near-field and the far-field region. Similarly, the radiation pattern also still depends on the distance from the antenna. The

radiation pattern which ranges at a distance greater than $2*D^2/\lambda$ gives the far field radiation pattern. Overall, the radiation pattern consists of two main planes which are *E*-plane and *H*- plane. The electric field is measured as a function of $\theta(\text{elevation plane})$ when the angle ϕ and the distance are defined. On the other hand, the magnetic field is measured as a function of ϕ (azimuthal plane) when θ and the distances are defined.

2.2 Directivity, D

Directivity is a ratio of the radiation intensity in a given direction from the antenna to the radiation intensity averaged over all directions (Stutzman, 2012). Furthermore, the directivity indicates how the proposed antenna radiates in a specific direction. Mathematically, the directivity might be represented as Equation 2.1 (Huang and Boyle, 2008):

$$D = \frac{U(\theta,\phi)}{U(\theta,\phi)_{\max}} = \frac{4\pi U(\theta,\phi)}{P} \tag{2.1}$$

Where U stands for radiation intensity (W/ unit solid angle), U_{max} stands for maximum radiation intensity (W/ unit solid angle), and P represents total radiated power (W), D stands for directivity and its unit is dimensionless. Figure 2.2 illustrates some examples for the directivities of different antenna structures.

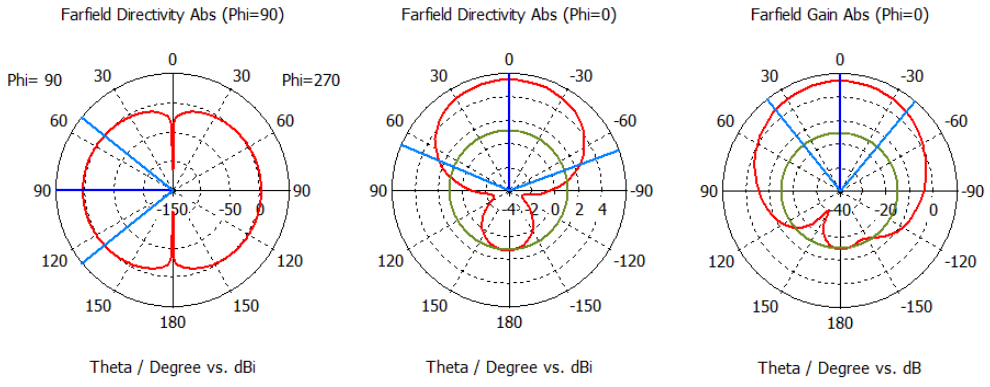

a) b) c)

Figure 2.2: Directivity of different type antennas a) Half wave dipole b) Antipodal Vivaldi c) Triangular pin fed patch

D is also the ratio of the area of a sphere to the beam area Ω_A of the antenna. The directivity is inversely proportional to the beam area. In mathematical form, it can be written as in Equation 2.2 (Stutzman, 2012):

$$D = \frac{4\pi}{\iint_{4\pi} P_n(\theta,\phi)d\Omega} = \frac{4\pi}{\Omega_A} \quad (2.2)$$

2.3 Gain, G

Directivity is proportional to the gain (G) and the radiation efficiency factor of the antenna. Gain is the crucial antenna parameter which is used for designing antenna. In other words, the goal is to construct the high or low gain which is accordance with application area, gain is one of the constraint parameter to decide the antenna performance. However, it is not enough to interpret antenna performance in terms of only gain.

$$G = e_t * D \text{ where } e_t = e_r * e_c * e_d \quad (2.3)$$

The antenna total efficiency (e_t) consists of conduction efficiency (e_c), dielectric efficiency (e_d) and reflection efficiency (e_r). Generally, the values of conduction efficiency (e_c) and dielectric efficiency(e_d) are difficult to calculate. They can be determined experimentally. Furthermore, the value of e_t is bounded from 0 to 1. e_t takes the value of 1 when the antenna is loss-free.

$$G = \eta * D \text{ where stands for efficiency} \quad (2.4)$$

Equation 2.3 and 2.4 give information about relation between Gain and Directivity. η is the ratio of the radiated power P_{rad} to the input power at the terminals of the antenna P_{in} (Hecimovic and Marincic).

2.4 Polarization

An electromagnetic wave might be represented through its frequency, magnitude, phase and polarization. Frequency, magnitude and phase are important parameters in electromagnetic wave theory and they are common for electrical and electronics engineering field. Polarization parameter is elusive electromagnetic wave parameter with respect to other parameters such as frequency, magnitude and phase. The fundamental principle of the electromagnetic wave polarization is similar to the antenna polarization. Inasmuch as the antennas are used for receiving and transmitting the electromagnetic waves i.e. radio waves. In other words, an antenna polarization is defined as the behaviour of the wave radiated in a given direction (Arokimary, 2009). When an antenna radiates, the alignment of electric and magnetic field occurs in different directions. These alignments are described as polarization of the antenna. In other words, polarization gives

information about the propagation of an electromagnetic wave, which composes of electric and magnetic field. Three types of polarization are linearly polarized, circularly polarized and elliptically polarized.

2.5. Impedance, Z_A

The input impedance (Z_A) is the ratio of the voltage to the current at the input terminals. Additionally, the input impedance of an antenna is also used to characterize the input terminal of the antenna as given in equations 2.5 and 2.6. The antenna impedance consists of real and imaginary part as shown in Equation 2.6. Input resistance R_A is composed of radiation (R_r) and loss (R_L) resistances as given in Equation 2.5. Furthermore, X_A stands for the input reactance.

$$R_A = R_r + R_L \tag{2.5}$$

$$Z_A = R_A + jX_A \tag{2.6}$$

2.6. Bandwidth

Other essential antenna parameter which describes antenna performance effectively is bandwidth. The bandwidth of an antenna gives information about the operation frequency range which varies depending on the application area. According to Balanis (Balanis, 2005), the bandwidth of an antenna is defined as “the range of frequencies within which the performance of the antenna, with respect to some characteristics, conforms to a specified standard. “ The bandwidth can be considered as the range of frequencies where the antenna characteristics (such as input impedance, pattern, beam width, polarization, side lobe level, gain, beam direction, radiation efficiency) are acceptable value of those at the centre frequency (Balanis, 2005). An UWB antenna operates in the 3.1 and 10.6 GHz range due to the fact that FCC concerns with UWB Communication Rules which are issued by Commission.

2.7. VSWR

The ratio of the maximum to minimum voltage is known as VSWR, or Voltage Standing Wave Ratio. VSWR implies that there is power being reflected back to the source. VSWR takes values between 2 and 1 for UWB applications due to FCC regulations. In other words, VSWR is useful for describing input match.There is a number

of methods for improving the VSWR of the proposed antenna. One method is to use impedance matching devices. Especially, baluns are preferred in order to match the impedance of the source to the antenna. Another way is to reduce VSWR by using attenuators. The expression for calculating VSWR can be written as:

$$VSWR = \frac{E_{max}}{E_{min}} = \frac{E_i + E_r}{E_i - E_r} \quad (2.7)$$

Where E_{max} represents maximum measured voltage, E_{min} stands for minimum measured voltage, E_i is incident wave amplitude (Volt) and E_r is reflected wave amplitude (Volt).

2.8. RETURN LOSS

Return loss is a measure of the effectiveness of power delivery from a transmission line to a load. If the power incident on the antenna is P_{in} and the power reflected back to the source is P_{ref}, the mismatch between the incident and reflected power in the travelling wave is given by the ratio $\frac{P_{in}}{P_{ref}}$. This relation explains the main concept of the return loss. The higher this power ratio is, the better the load and the line are matched. Return loss is commonly expressed in decibels (dB), as given in formula below:

$$\text{Return Loss (RL)} = 10 * \log (P_{in}/P_{ref}) \text{ dB} \quad (2.8)$$

VSWR and Return Loss are related with the Equation (2.9) as follows:

$$VSWR = \frac{1+|\Gamma|}{1-|\Gamma|} = \frac{1+S_{11}}{1-S_{11}} \quad (2.9)$$

$$\text{Where } \Gamma = \frac{E_r}{E_i} \quad (2.10)$$

3. HALF WAVE DIPOLE ANTENNA

The UWB systems have expanded rapidly after the FCC allowed the unlicensed use of frequency spectrum by ultra-short pulse signals. There has been a flourishing prospect of UWB technology in recent years for both communication and other purposes such as microwave imaging and radar applications. The design of the UWB antennas is vigorous and rigorous issue which needs considerable research effort in order to adapt to UWB requirements. Federal Communications Commission (FCC) limited the frequency band between 3.1 GHz and 10.6 GHz due to the extremely wide operating bandwidth for UWB applications. Additionally, according to FCC rules, -10 dB bandwidth should be between 3.1 and 10.6 GHz for UWB requirements. In other words, Return Loss should be below -10 dB in the 3.1 - 10.6 GHz UWB frequency range. Similarly, VSWR should be below 2 for UWB spectrum. Numerous parameters such as radiation pattern, return loss, VSWR, gain and directivity are required so as to design the UWB antenna effectively.

This section gives general overview of the design of the half wavelength dipole for UWB system applications. A dipole antenna is a linear metallic wire or rod with a feed point at the center. A dipole antenna has two symmetrical radiating arms. A half wavelength dipole antenna is also known as half wave-doublet or hertz antenna (Bakshi, 2009). Its physical length is approximately equal to half of the wavelength **(**λ/2) in free space. Its radiation resistance is 73 Ω (Balanis, 2005). Half wave dipole antennas are the most commonly used because the radiation resistance of half wavelength dipole antenna is 73 Ω which is very close to 75Ω. 75 Ω is generally the characteristics impedance of transmission lines. Half wave dipole is mostly preferred because of its radiation pattern characteristics. A half wave dipole has omnidirectional radiation pattern. Omnidirectional radiation pattern means that the antenna has the ability to radiate the signals in all directions. Omnidirectional radiation pattern is desirable because of user mobility and freedom in the transmitter or receiver position. Furthermore, this kind of antenna which has an omnidirectional radiation pattern provides the three fundamental properties such as gain, direction and polarization into the wireless system. The proposed antenna's operating frequency varies with respect to its dimensions, e.g. length of the proposed antenna. In other words, changing the length of the antenna will change the operating frequency (Tareq et al, 2014). Half wavelength is generally preferred in UWB antenna design due to its features such as reasonable size, radiation pattern uniformity, manageable input impedance, gain consistency. Many UWB half wavelength antennas have been discussed in the literature investigate the antenna characteristics (Tareq et al,

2014; Sprungle and Chen, 2008; Cerny and Mazanek, 2006; Çolak et al, 2017; Powell, 2004; Singh et al, 2012).

In this study, a half wavelength dipole antenna is designed and simulated via CST Microwave Studio. Additionally, theoretical and practical aspects are presented. The antenna is simulated in transient mode in order to observe antenna characteristics. Simulation results show that possible improvements of the antenna parameters can be achieved by selecting the optimal antenna dimensions. The center frequency of proposed antenna is calculated in the UWB frequency range (3.1GHz-10.6GHz) by using relation in Equation (3.1). According to calculation, the center frequency is obtained as 6.85 GHz. All antenna dimension parameters are calculated at the resonant frequency, 6.85 GHz, in order to obtain UWB characteristics as given (Tareq et al, 2014). Length, feeding gap, wavelength and radius of the antenna are calculated through equations (3.2-3.5) respectively as follows:

$$f_{center} = \frac{f_{upper} + f_{lower}}{2} = \frac{10.6\ GHz + 3.1\ GHz}{2} = 6.85\ GHz \quad (3.1)$$

$$L = 143/f_{center} = 143/6.85\ GHz = 20.9\ mm \quad (3.2)$$

$$g = L/200 = 0.1045\ mm \quad (3.3)$$

$$\lambda = c/f_{center} = 3x10^{8}/6.85\ GHz = 43.8\ mm \quad (3.4)$$

$$r = \lambda/1000 = 0.0438\ mm \quad (3.5)$$

3.1. Results and Discussion

Antenna size parameters are calculated with respect to the UWB frequency range. Table 3.1 presents dimensions of the proposed half wave dipole antenna. Besides, Figure 3.1 presents the designed half wave dipole with front view and top view. The antenna is simulated in transient mode by using CST Microwave Studio. Gaussian pulse is applied as the excitation signal which is shown in Figure 3.2. Global mesh properties are adjusted for obtaining more accurate results.

Table 3.1: Calculated antenna dimensions

Parameter	Value
f_{center}	6.85 GHz
Wavelength (λ)	43.8 mm
Feeding gap (g)	0.1045 mm
Radius (r)	0.0438 mm

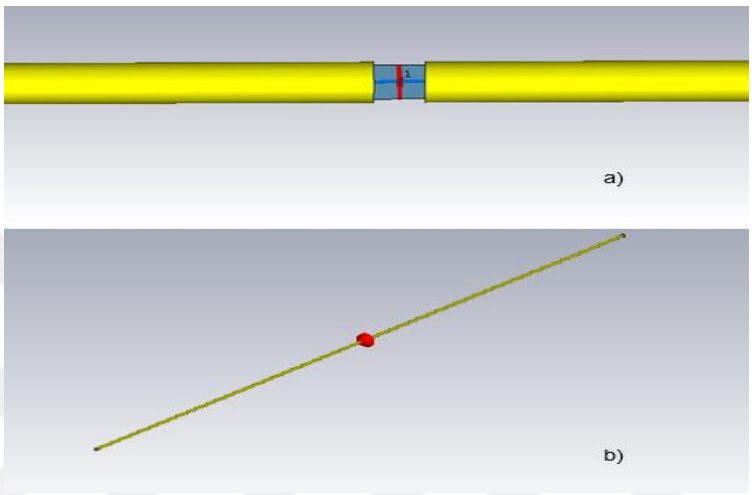

Figure 3.1: Half Wave Dipole Antenna Geometry a)Front View b)Top View

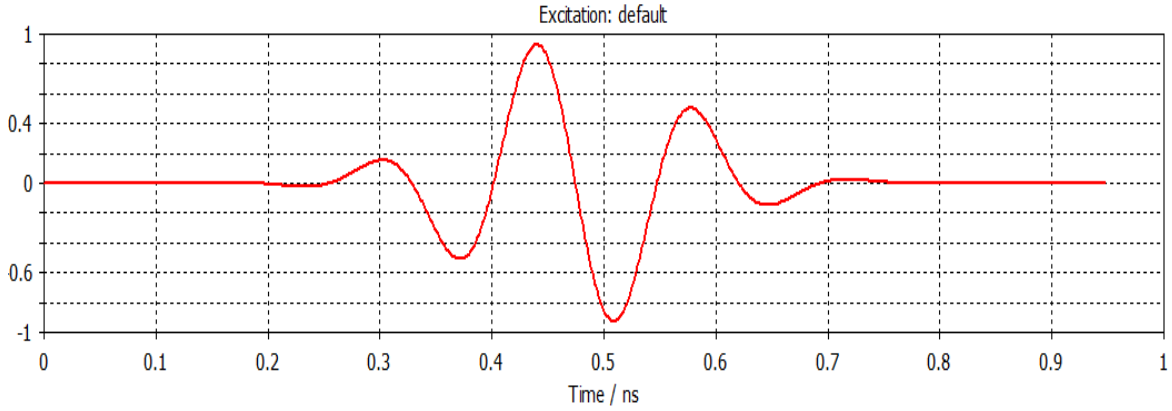

Figure 3.2: Excitation Signal-Gaussian Pulse

Figure 3.3 illutrates the impedance characteristics of the simulated antenna. The proposed antenna impedance is around 74 Ω which is so close to mathematical calculation given in the theoretical approach which is obtained in (Balanis, 2005).

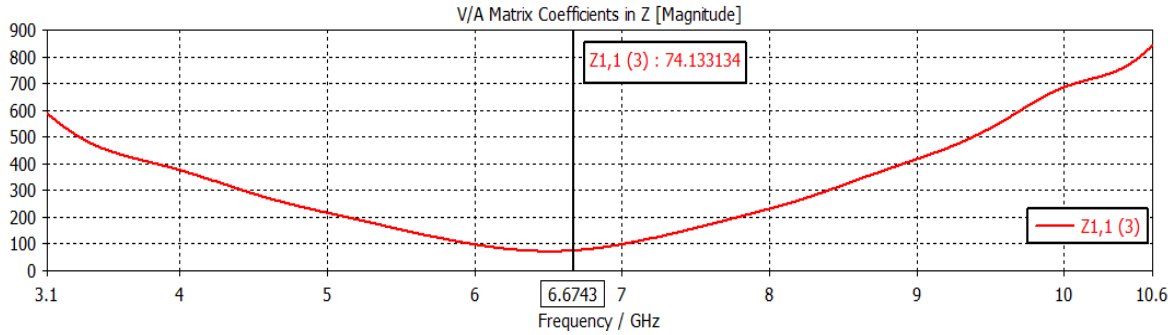

Figure 3.3: Impedance characteristic of the proposed half wave dipole antenna

Return loss and VSWR results for the half wave dipole antenna are obtained from the simulation program (CST MWS) and are shown in Figure 3.4 and Figure 3.5, respectively. As can be seen from Figure 3.4, antenna is resonating at 6.6743 GHz. The -10 dB impedance bandwidth of the proposed antenna extends in the 6.3088-7.1065 GHz range, which is about 11.89%. Corresponding bandwidth is calculated as 798 MHz. Furthermore, minimum return loss is equal to approximately -40.49 dB. As Figure 3.5 indicates, VSWR is smaller than 2 (VSWR≤ 2) and S_{11} is smaller than -10 dB (S_{11}≤ -10 dB) throughout the frequency range, i.e. 3.1 GHz-10.6 GHz. According to the simulation results, VSWR and Return Loss results are compatible with FCC regulations for UWB applications. Nevertheless, this frequency range (6.3088GHz-7.1065GHz) is narrow for UWB applications. Various enhancement techniques will be applied in order to have better antenna characteristics such as larger bandwidth, lower VSWR and return loss values over the desired frequency range in the next section.

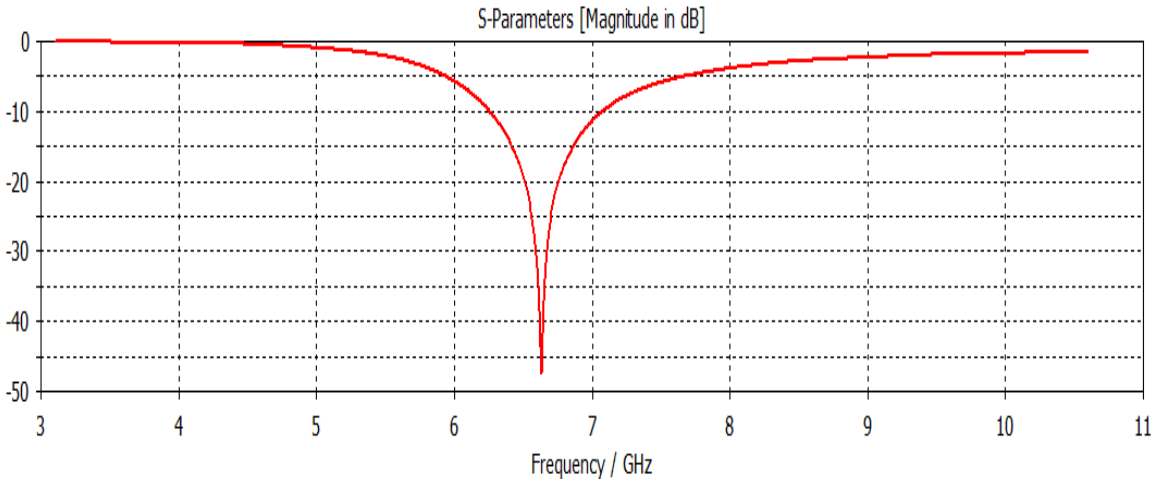

Figure 3.4: Return loss characteristic of the half wave dipole antenna

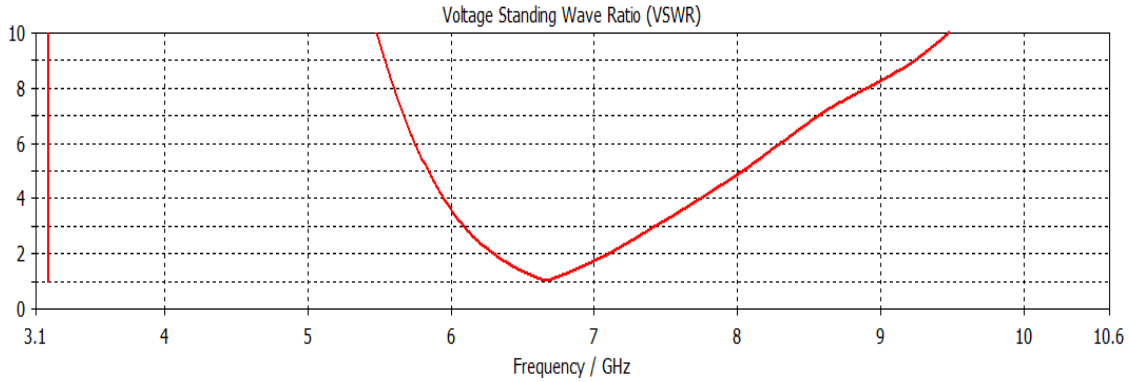

Figure 3.5: VSWR against frequency for the proposed half wave dipole antenna

The simulated radiation patterns for the dipole are sketched in Figures 3.6 a,b and c at 4, 5, 6 GHz respectively. It is apparent from these figures that proposed antenna has omnidirectional radiation pattern at different frequencies. In the figures, as the frequency increases, main lobe magnitude increases while 3 dB beamwidth decreases. Simulation results are acceptable for some applications which require omnidirectional radiation pattern.

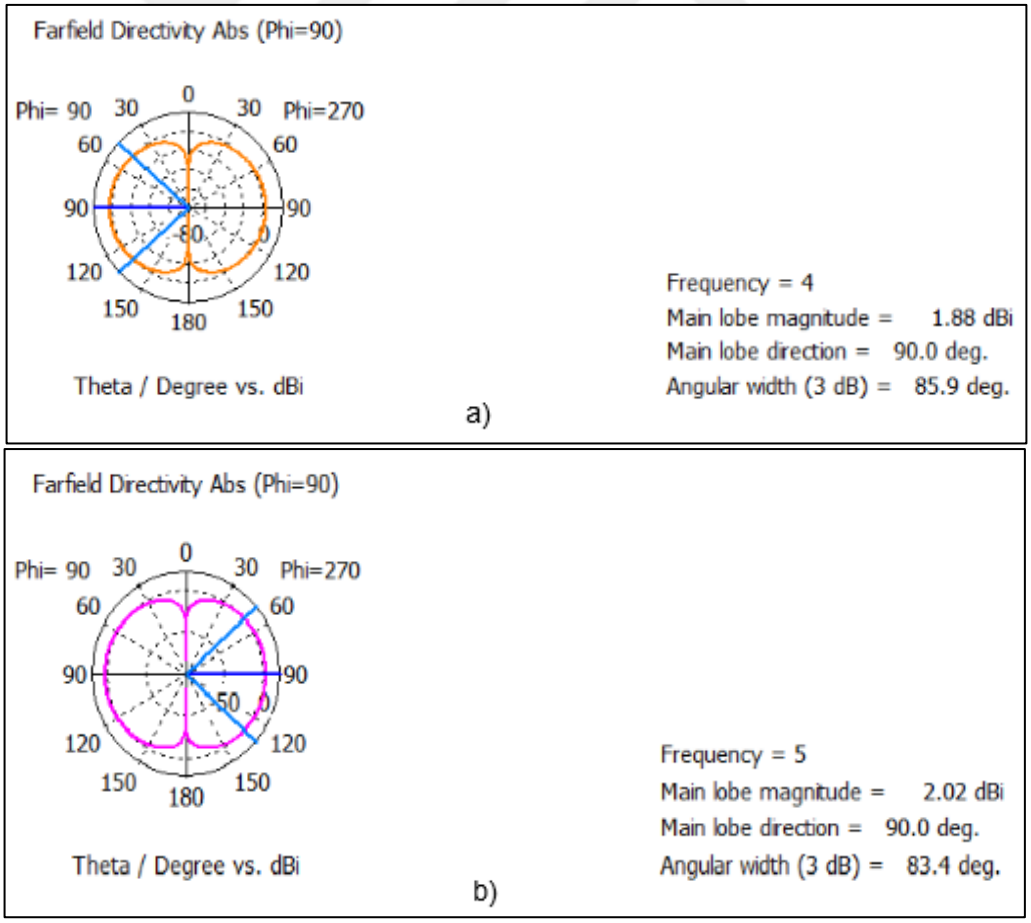

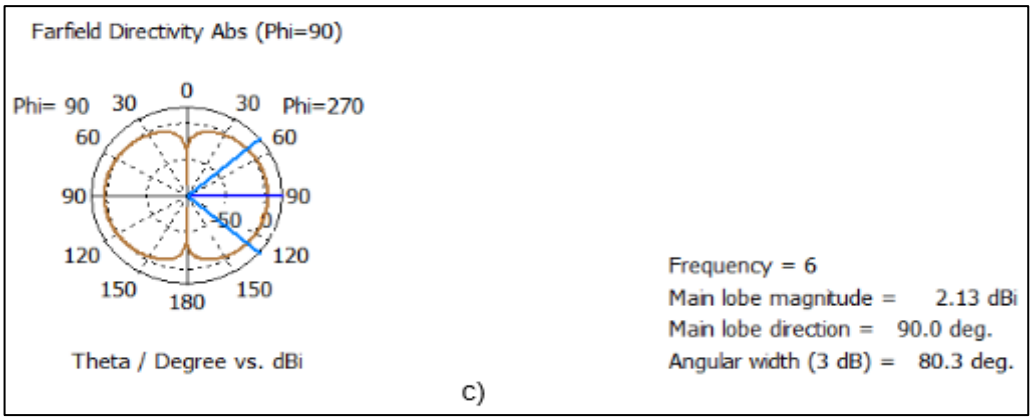

Figure 3.6: Radiation Pattern for half wave dipole antenna with frequency a) 4 GHz b) 5 GHz c) 6 GHz, respectively

3.2. Radius Effect

The dipole antenna is one of the significant antenna structures in electromagnetic compatibility problems. While thin dipole is considered, the radius of the dipole is assumed to be very small as compared to the antenna length. When thin dipoles are examined, the bandwidth of the proposed antenna reduces or increases slightly depending on the value of the dipole diameter. Various mathematical approaches are used to understand how the radius improves the bandwidth characteristics. One method is to change the length to radius ratio (L/r) in order to vary the bandwidth. This method can be achieved when the antenna length is fixed and the antenna diameter is increased. Consequently, if the wire diameter increases, its bandwidth increases (Balanis, 2005).

Figure 3.7 illustrates the return loss characteristics of the half wave length dipole with different radii (r = 0.07, 0.1025, 0.135, 0.1675, 0.2, respectively) when the other dimensions are fixed as given in Table 3.1. As seen from Figure 3.7, when radius (r) is increased, the bandwidth of the proposed antenna also increases. The bandwidth for each case has been calculated as 814.4 MHz, 844 MHz, 940.3 MHz, 984.7 MHz, 1.0217 GHz, respectively. Correspondingly, the bandwidth changes by varying dipole radius.

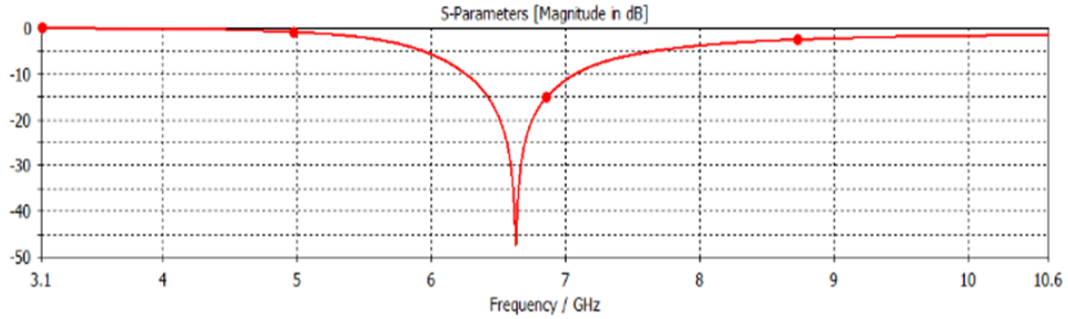

a) r = 0.07 mm

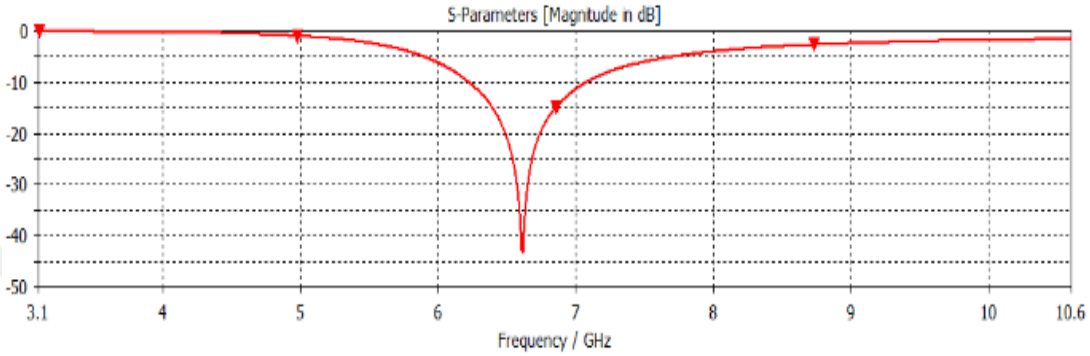

b) r = 0,1025 mm

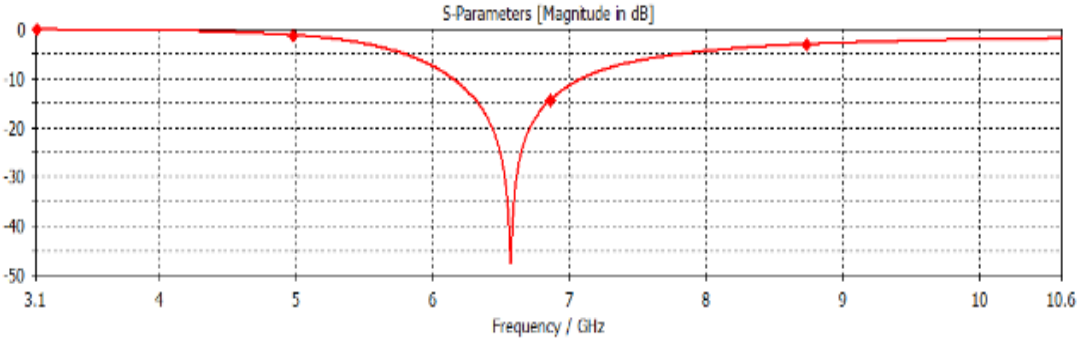

c) r = 0,135 mm

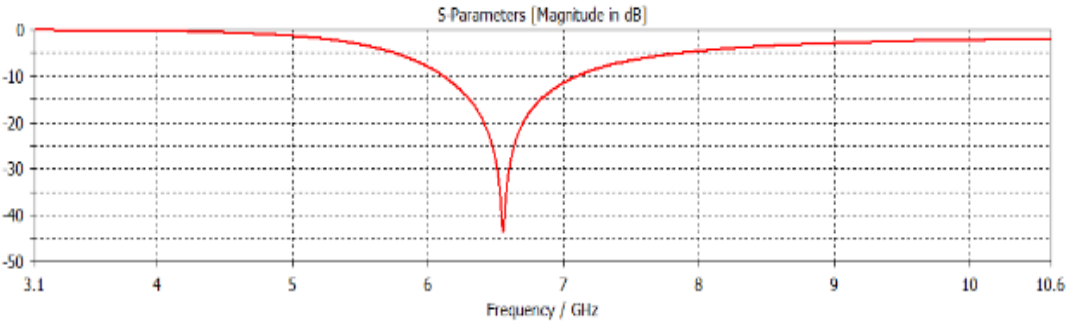

d) r = 0,1675 mm

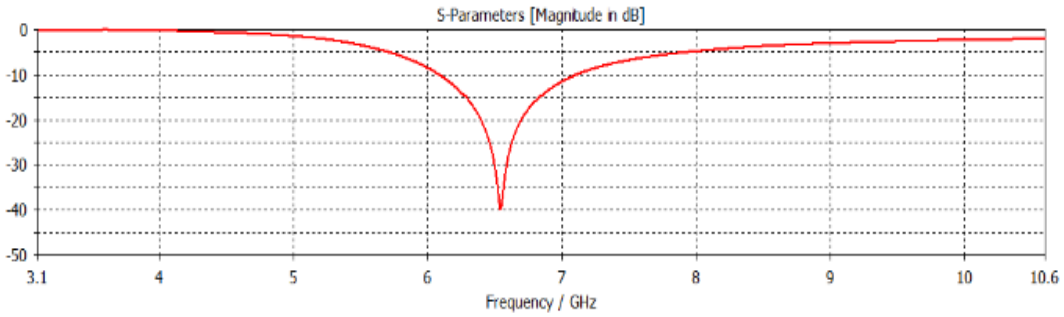

e) r = 0,2 mm

Figure 3.7: Simulated return loss curve of half wave dipole for different radius r with a) 0.07 b) 0.1025 c) 0.135 d) 0.1675 e) 0.2 mm, L=20.9 mm and *g* =0.1045 mm

The effect of radius has been explained in detail previously. To confirm this the radius effect, the radius of the proposed antenna is increased slightly in order to observe the changes in bandwidth by using CST Microwave Studio. The proposed antenna parameter namely bandwidth is improved by changing antenna diameter. Table 3.2 provides the inter correlations among the parameters of the proposed antenna. The improvement of any antenna parameter may affect the antenna characteristic. As can be seen from Table 3.2, changing the diameter of the proposed antenna improves the bandwidth. However, the VSWR and S_{11} values are not improved as much as bandwidth. As the radius increases from 0.3 mm to 0.5 mm, while dipole length is fixed, that is, as L/r ratio decreases, the bandwidth, s11 and VSWR increases. This means that although bandwidth is improved, S11 and VSWR worsens. At this stage, there is a tradeoff between the bandwidth and efficiency of the antenna. On the other hand, as the radius increases even further from 0.5 mm to 1 mm, bandwidth decreases and becomes unacceptable for UWB while s11 and VSWR increase further and get even worse. Then it would not be reasonable to increase the radius anymore. The most obvious finding to inference to make from this study is that the limitations on the antenna size should be taken into consideration during design.

Table 3.2: Bandwidth values with respect to the different radius

Radius	Bandwidth	S_{11}	VSWR
0.3 mm	1.1476 GHz	-31.349847 dB	1.0556489
0.4 mm	1.2291 GHz	-26.072863 dB	1.1045987
0.5 mm	1.2587 GHz	-20.772655 dB	1.2014034
0.6 mm	1.194 GHz	-17.229804 dB	1.3190169
0.7 mm	1.0365 GHz	-14.18651 dB	1.4853598
0.8 mm	746.4 MHz	-11.782886 dB	1.6937714
0.9 mm	Not acceptable for UWB	-9.4497215 dB	2.0104937
1.0 mm	Not acceptable for UWB	-7.8714976 dB	2.3559339

4. BOW TIE ANTENNA

The key problem with the antenna design procedure is that the proposed antenna bandwidth should comply with FCC's UWB requirements (FCC, 2002; Hecimovic and Marincic). As a previous work which is given in Section 3, the half wave dipole antenna has a great number of drawbacks due to its simple structure and narrow band characteristics. Thus, quite a few design techniques might be used to increase the bandwidth. One of the techniques for the half wave dipole antenna is to modify the structure of the dipole.

A considerable number of bowtie antenna shapes have been designed and investigated in the literature (Sayidmarie and Fadhel, 2013; Zhang et al, 2015; George et al, 2015; Çolak and Gençoğlan, 2016a; Sharma et al, 2015). Different antenna configurations, especially modifications in the dipole shape have been taken into account for the UWB requirements, i.e circular, square, diamond dipoles and bow tie (Volakis, 2007). Modified dipole configurations are generally preferred to achieve the broad band characteristic. The main point is that light weight, low cost and ease of fabrication are desired antenna features during the modification process. As mentioned before, bow tie antenna is definitely one of the modified dipole configurations. Bow tie antenna has wider bandwidth compared to the simple half wave dipole (Begaud, 2013; Brown and Woodward, 1998; Bailey, 1984).

The proposed bowtie antenna structure and its dimensions are depicted in Figure 4.1. It is clear from these views that the antenna consists of flare angle (α), arm length (l_e), substrate thickness, feeding gap and two metallic arms. All these antenna parts are crucial antenna dimension constraints, i.e. design parameters. The design parameters such as arm length, substrate width, permittivity, feed gap and flare angle are optimized to obtain better bandwidth and gain characteristics by antenna designers. Especially in UWB systems, antenna design is a crucial task due to broadband system characteristics. Therefore, any changes in antenna size affect the performance of antenna parameters.

In this chapter, two metallic sheets are assumed to be printed on a substrate with dielectric constant of 2 while the proposed antenna is simulated and designed via CST MWS. Initially, two metal sheets with lengths of 45 mm are separated by the feed gap of 0.66 mm. The overall length of antenna is almost equal to λ/2 in order to radiate efficiently and effectively. Furthermore, flare angle (α) which is the angle between two metal sheets is 60^o. Any antenna size might be considered as a constant by varying another antenna

size in order to obtain bandwidth enhancement. CST Microwave Studio is used to simulate the antenna model.

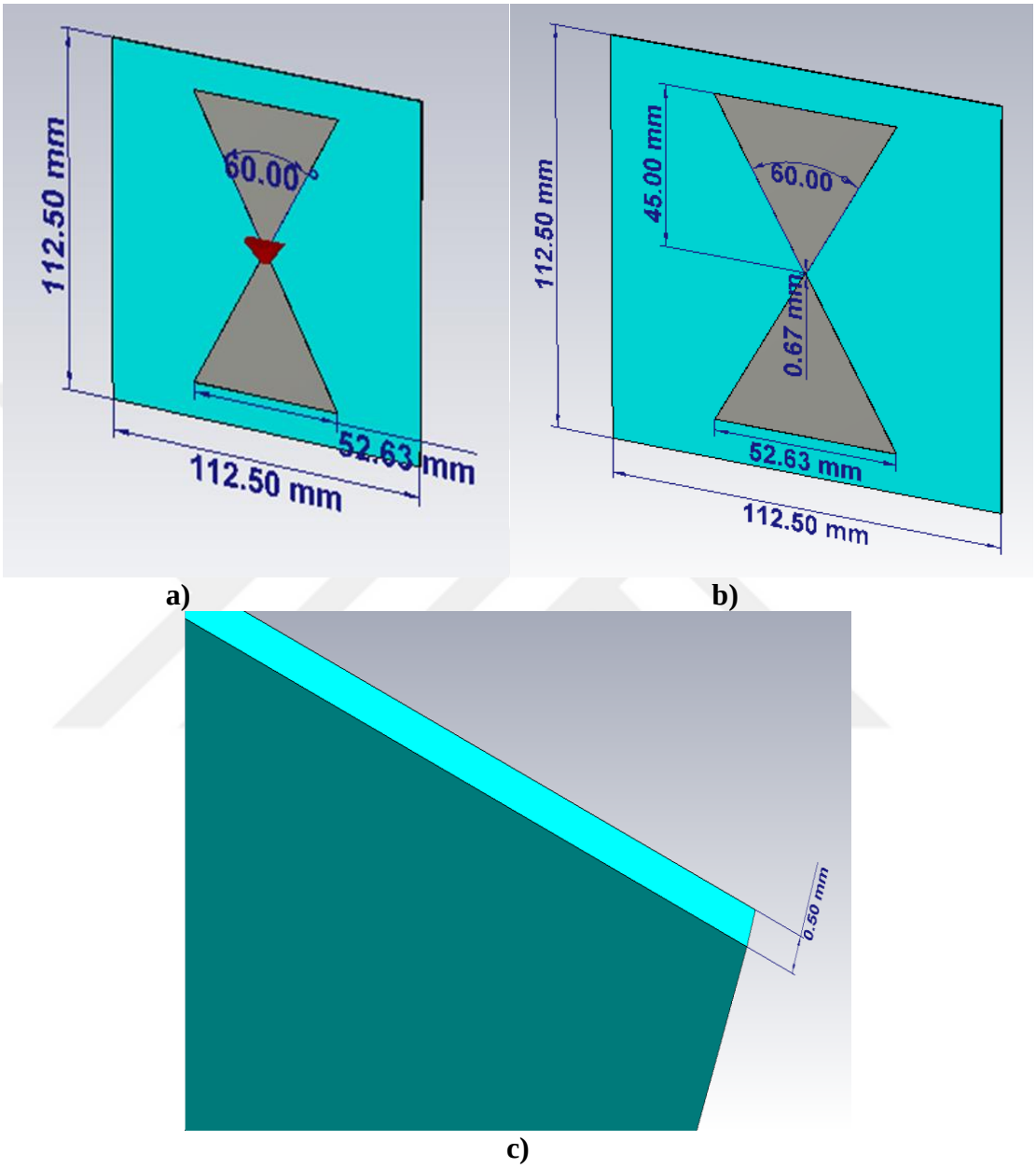

Figure 4.1: Geometry of the proposed bow tie antenna a) Front view b) Side view c) Top view

4.1. Results and Discussion

The proposed antenna is analyzed and examined in terms of its return loss and VSWR in the 3.1- 10.6 GHz range. The proposed antenna's return loss is smaller than -10 dB, in the frequency of interest of 3.1-10.6 GHz band as given in Figure 4.2. A good behavior is obtained at 4.629 GHz where the peak level of the return loss is recorded as –22.92 dB. Furthermore, as depicted in Figure 4.3, VSWR is smaller than 2 (VSWR≤ 2) in the UWB frequency range.

The simulation results show that this proposed antenna meets the UWB requirements and is regulated according to FCC restrictions i.e., VSWR≤ 2 and S11≤-10 dB, in the frequency range of interest.

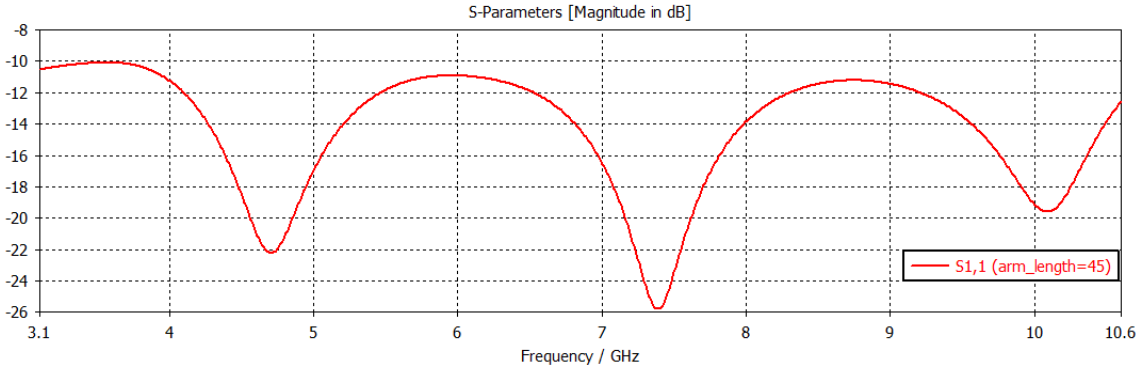

Figure 4.2: Return loss in dB versus frequency for arm length of 45 mm

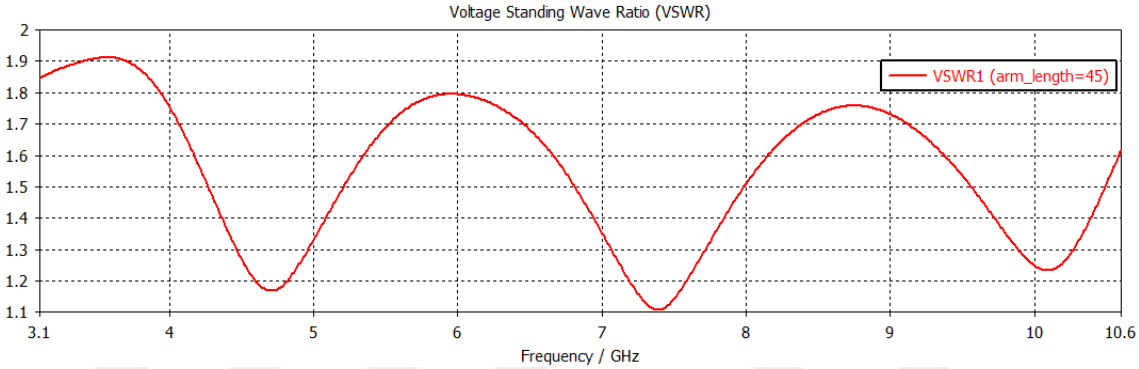

Figure 4.3: VSWR versus frequency for arm length of 45 mm

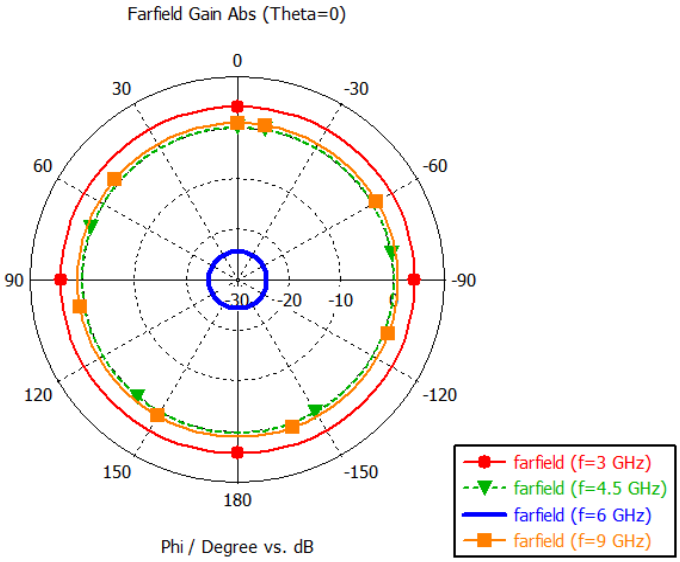

Figure 4.4: Radiation pattern of the proposed antenna at 3, 4.5, 6, 9 GHz respectively

Radiation pattern, which is another important antenna parameter describing the behavior of the antenna is also considered for the proposed bow tie antenna structure. Simulated radiation patterns are plotted in Figure 4.4 at 3, 4.5, 6, and 9 GHz, respectively. As shown in Figure 4.4, radiation patterns are omnidirectional at elevation plane. In other

words, it radiates effectively and efficiently in all directions at this plane. It is apparent from these plots that radiation characteristics are acceptable for communication systems.

To summarize, the results show that VSWR and return loss comply with the requirements for UWB communication in the 3.1GHz-10.6GHz frequency range. Furthermore, these results reveal that bow tie antenna has larger bandwidth than dipole antenna as examined in the previous chapter. In conclusion, this idea is emphasized that this proposed antenna copes up with the restriction which is related to the limitation of the frequency as mentioned in the half wave dipole section.

4.1.1. Arm Length Effect on the Antenna Performance

Initially, bowtie antenna is considered due to its simple structure and low cost. The proposed antenna is simulated in accordance with arm length in order to choose efficient antenna dimensions. The arm length is swept from 45 mm to 110 mm, i.e., with values 45, 66.67, 88.33 and 110 mm, respectively. However, the desired arm length ought to be defined as to meet the application requirements exactly. Therefore, to that end, the main restrictions are taken as cost and size while the best antenna structure is selected. Thus, in this section, different arm lengths are chosen as constraint parameters which affect cost and size. The dimensions of the proposed antenna are the same as the dimensions of the antenna structure presented in Section 4.1. The other three envisaged antennas are printed on a substrate, which has dielectric permittivity 2, with thickness 0.5 mm as shown in Figure 4.5. The substrate size is taken as 112.5x112.5 mm^2 for 45 mm arm length, 166.68x166.68 mm^2 for 66.67 mm arm length, 220.83x220.83 mm^2 for 88.33 mm arm length and 275x275 mm^2 for 110 mm arm length as presented in Figure 4.5.

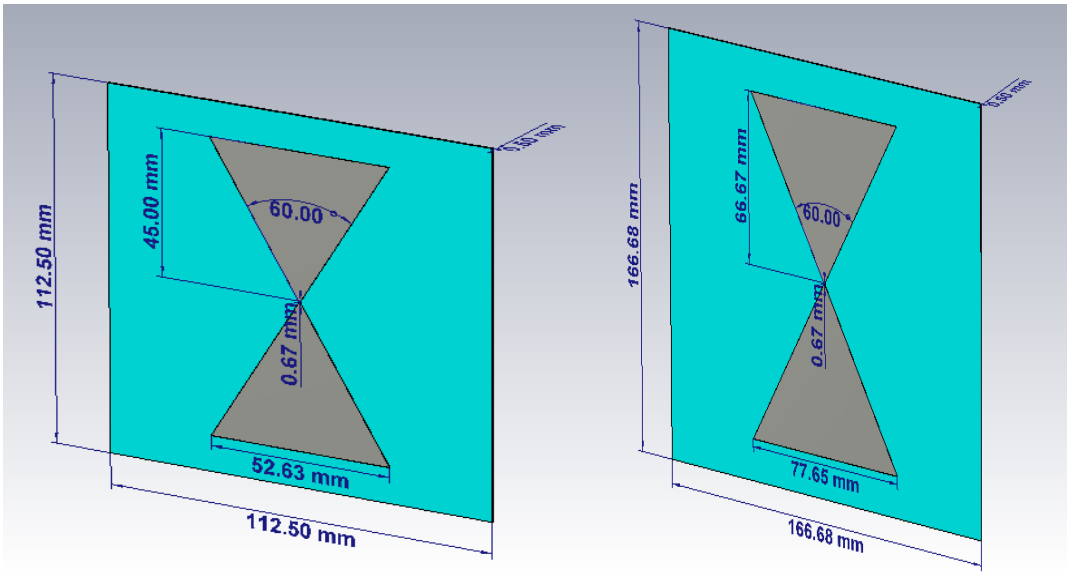

a) **b)**

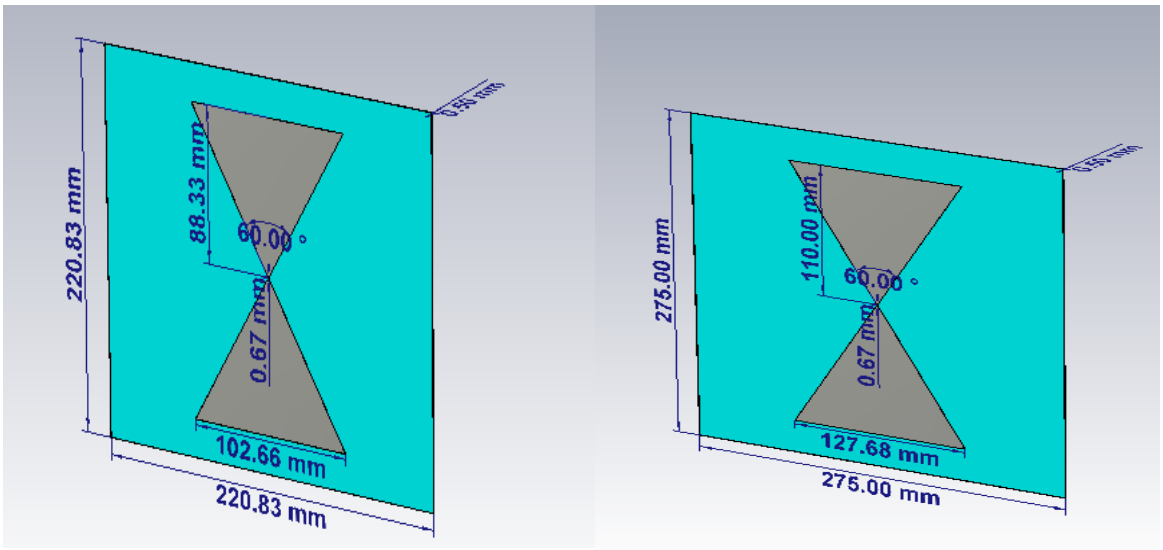

c) **d)**

Figure 4.5: a) The proposed antenna with arm length of 45mm, the envisaged antenna with arm length of b) 66.67 mm c) 88.33 and d) 110 mm

Figure 4.6 represents return loss characteristics of the proposed bowtie antennas with respect to arm length 45, 66.67, 88.33 and 110 mm, respectively. The arm length effect on antenna performance is examined through Figures 4.6 and 4.7. Figures 4.6 and 4.7 emphasize that envisaged antennas meet the UWB requirements (since S_{11} and VSWR graphs are compatible in that they both satisfy FCC rules.) due to compatibility between S_{11} and VSWR. Minimum return loss values are -23.13 dB, -29.48 dB, -36.43 dB and -47.20 dB for arm lengths, 45 mm, 66.67 mm, 88.33 mm and 110 mm, respectively. Similarly, minimum VSWR values are 1.15, 1.07, 1.03 and 1.01 for arm lengths, i.e. 45 mm, 66.67 mm, 88.33 dB and 110 mm, respectively. Additionally, there is marginally difference in bandwidth for return loss characteristic between two antennas which have arm lengths e.g., 45 and 110 mm (which are the upper and lower limits).

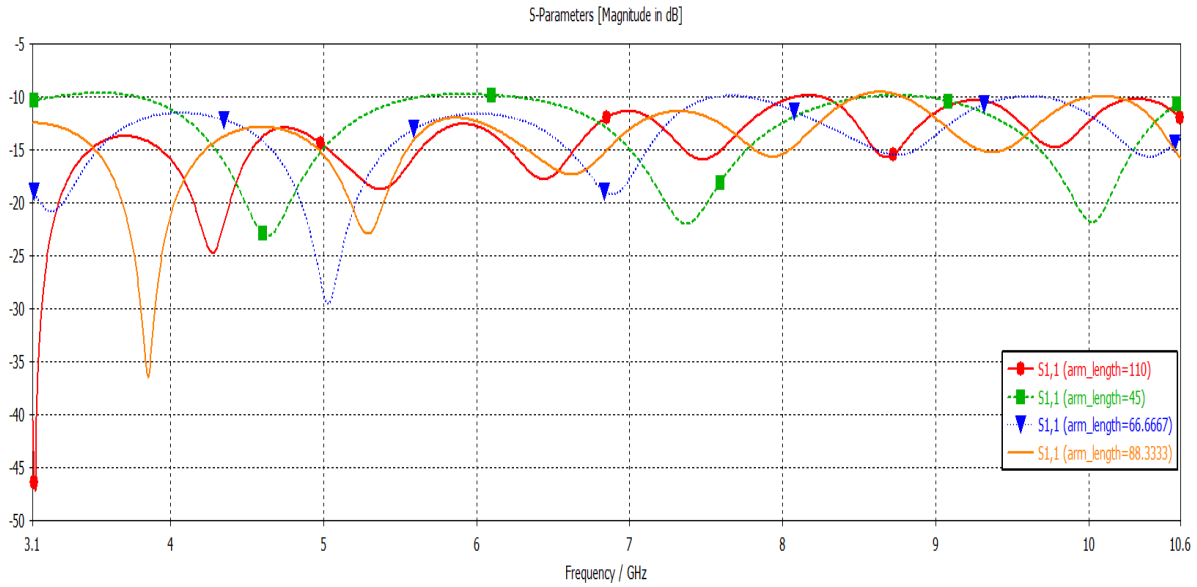

Figure 4.6: Return Loss Characteristic of classical bowtie antenna with respect to arm length 45, 66.67, 88.33 and 110 mm, respectively

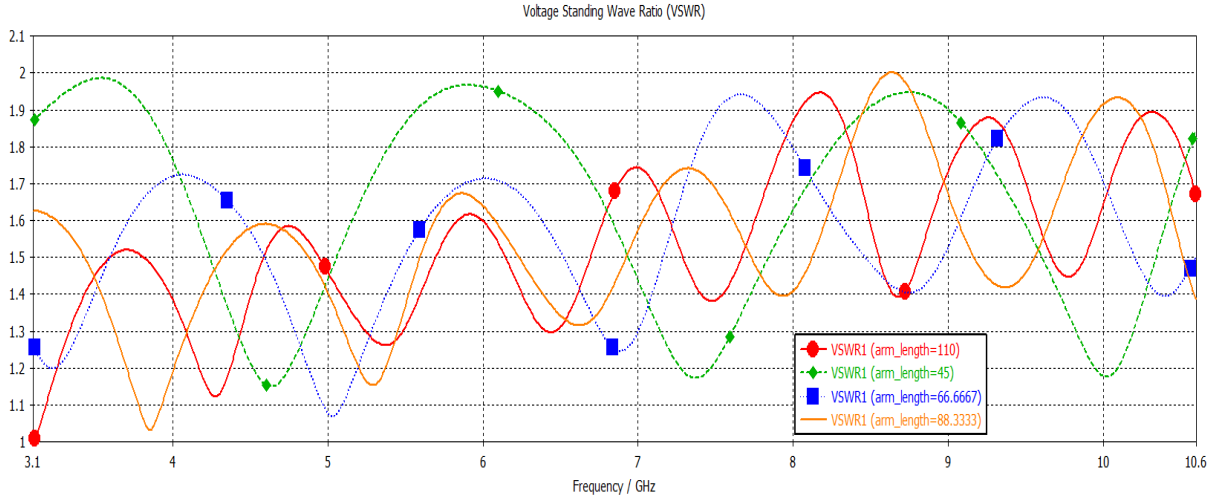

Figure 4.7: VSWR Characteristic of classical bowtie antenna with respect to arm length 45, 66.67, 88.33 and 110 mm, respectively

5. BOWTIE ANTENNA CONFIGURATIONS

Antenna design techniques for UWB applications are great deal of interest (Bourqui et al, 2010) for the researchers. There are various methods to maintain antenna characteristics stable. However, the main point is not to change input impedance for a broad range of frequencies.

Since broadband antennas are preferred in many applications, different types of antennas including frequency independent structures are investigated in the literature (Rumsey, 1966, Wiesbeck, 2009; Dyson, 1961). Different bow tie configurations are among the antenna types to broaden the bandwidth with simple design, low cost and high gain features.

One of the approaches is that the bow tie antenna ends are curved in order to improve bandwidth characteristics. This approach yields “Rounded Bowtie Antenna” structure. Another approach is that the rounded bow tie antenna is truncated from its edges to further improve the antenna behavior. This yields the “Truncated Rounded Bow Tie Antenna” structure. Three different architectural shapes of the bow tie antenna are presented in Figure 5.1.

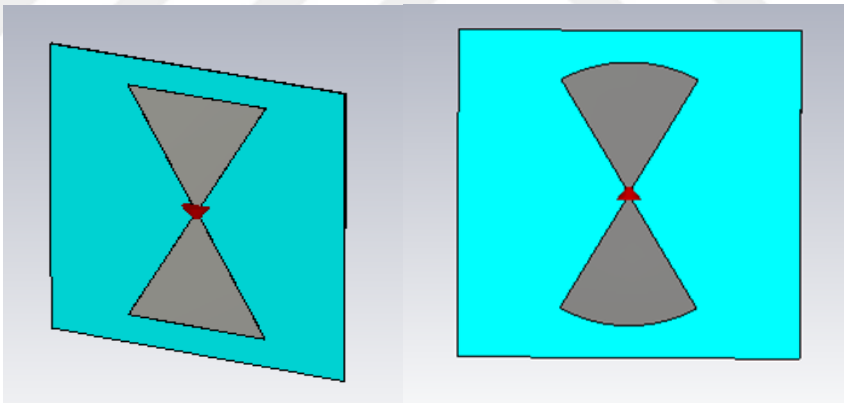

a) **b)**

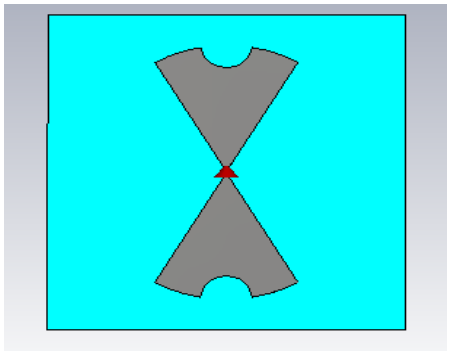

c)

Figure 5.1: a) Classical Bowtie, b) Rounded Bowtie, c) Truncated Rounded Bowtie Antenna

The three candidate antenna structures are printed on a substrate, which has dielectric constant of 2 and thickness of 0.5 mm. The substrate dimension for classical bow tie antenna is taken as 64.75 x 39.85 mm^2 while the substrate dimension is taken as 48.75 x 48.75 mm^2 for rounded bow tie and truncated rounded bow tie antennas. Flare angle, which is the angle within metal sheets (Gonzales, 2005; George et al, 2015) is 60^o. The dimensions of proposed antennas are presented in Table 5.1. CST Microwave Studio is used during the designing and modeling steps of antenna configurations.

Table 5.1: Dimensions of Bow Tie Antenna Configurations

Dimension Labels	Bowtie Antenna	Rounded Bowtie Antenna	Truncated Rounded Bowtie Antenna
Arm length	19.92 mm	19.50 mm	19.50mm
Feed Gap	0.67 mm	0.67 mm	0.67 mm
Feed Width	0.67 mm	0.67 mm	0.67 mm
Flare Angle	60^o	60^o	60^o
Permittivity	2	2	2
Substrate Thickness	0.5 mm	0.5 mm	0.5 mm
Substrate Width	39.85 mm	48.75 mm	48.75 mm
Substrate Length	64.75 mm	48.75 mm	48.75 mm
F_{min}	3 GHz	3 GHz	3 GHz
F_{max}	12GHz	12 GHz	12 GHz
F_{center}	7,5GHz	7,5 GHz	7,5 GHz

Initially, classical bowtie antenna is represented with its dimensions in Figure 5.2.

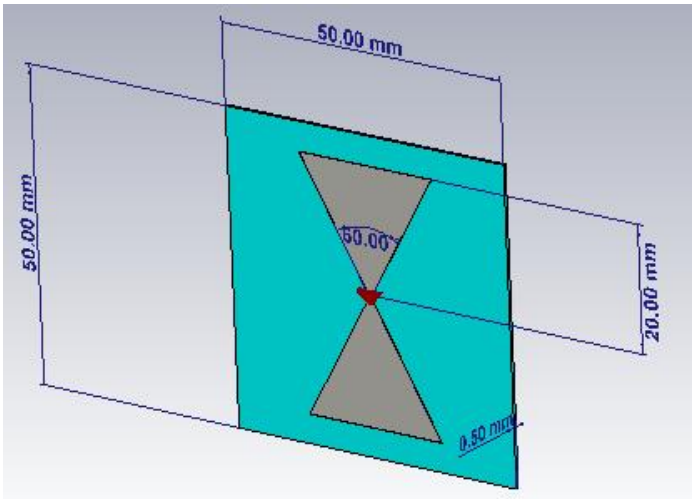

Figure 5.2: Schematic diagram and the size of Classical Bowtie Antenna

The results obtained from the simulation analysis of classical bow tie antenna are presented in Figure 5.3. From the data in Figure 5.6, S_{11} of the bow tie antenna is smaller than -10 dB in the frequency range from 3.5 GHz to 6.43 GHz and 9 GHz to 12 GHz. The

S_{11} is recorded as -41.68 dB and –15.46 dB at the first and second resonances. From this result, it is apparent that the proposed bow tie structure behaves as a dual band antenna

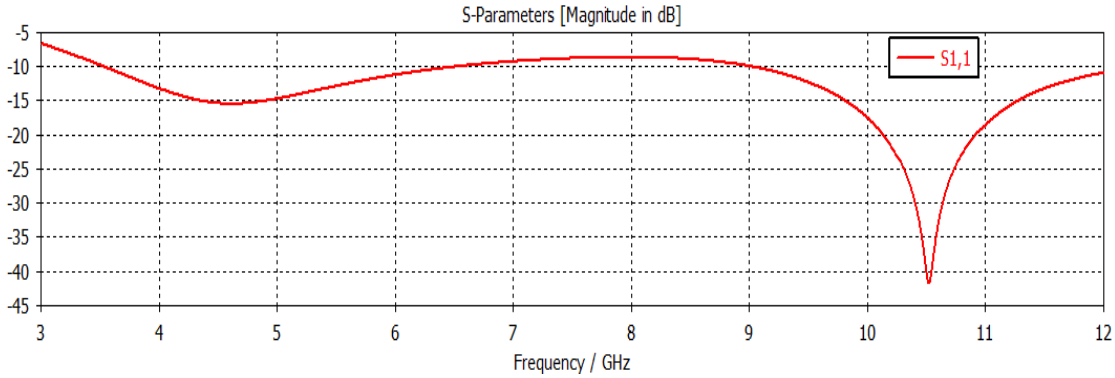

Figure 5.3: Return loss (S_{11}) in dB of the Bowtie Antenna

Figure 5.4 illustrates the VSWR vs frequency graph of the classical bow tie antenna. According to the graph in Figure 5.4, there is an excellent agreement between return loss and VSWR characteristics (Figure 5.3 and Figure5.4).

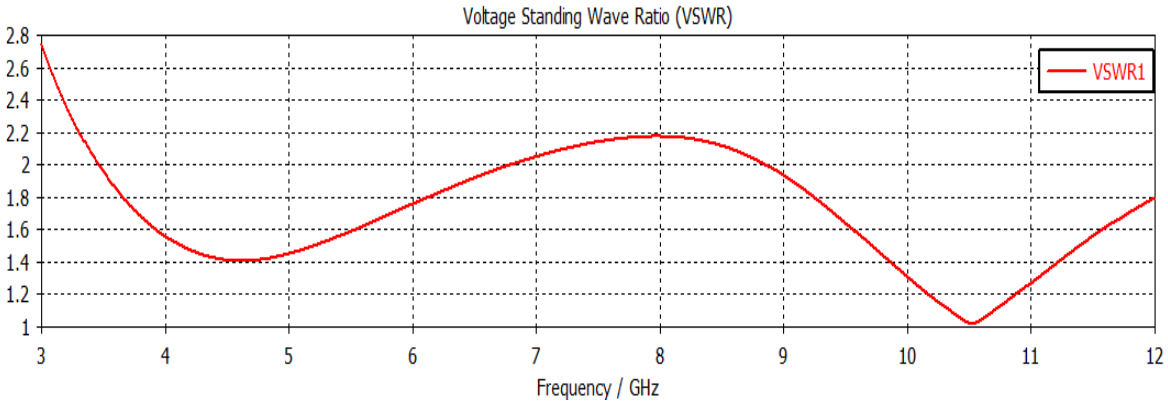

Figure 5.4: VSWR of the Bowtie Antenna

Rounded bowtie antenna is represented with its dimensions in Figure 5.5.

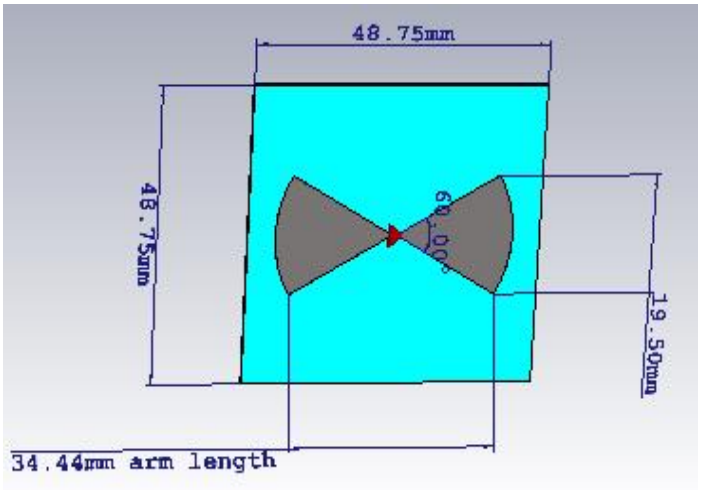

Figure 5.5: Schematic diagram and the size of Rounded Bowtie Antenna

Figure 5.6 present the return loss of the rounded bow-tie antenna which is obtained by using CST tool. It can be seen from the data in Figure 5.3 that S_{11} is smaller than -10 dB ($IS_{11}I$<-10 dB) in the frequency range from 3.89 GHz to 7.53GHz and from 8.5883 GHz to 12 GHz. The S_{11} is recorded as -27.75 dB and -14.07 dB at the resonance frequencies. The most striking result to emerge from the Figure 5.3 is that this proposed antenna behaves as a dual-band structure. Hence, this result is acceptable for some applications e.g. WİMAX, but not UWB.

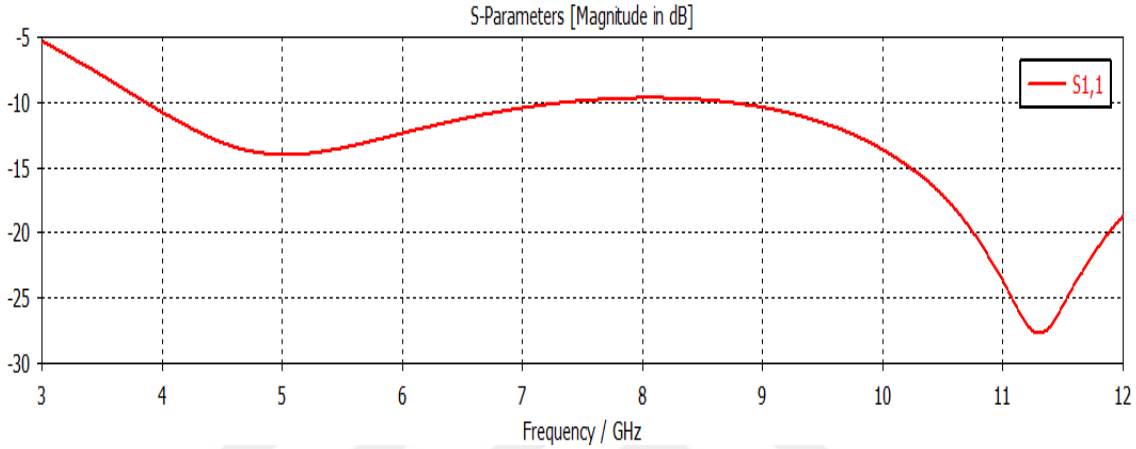

Figure 5.6: Return loss (S11) in dB of Rounded Bowtie

Figure 5.7 illustrates the VSWR characteristic of the Rounded Bow-Tie Antenna. As shown in Figure 5.7, it provides the intercorrelation among the return loss (S_{11}) characteristic which doesn't meet the requirements for UWB applications. Contrary to expectations, this proposed antenna does not cover the whole UWB frequency range which is defined by FCC (FCC, 2002). Consequently, the proposed rounded bowtie antenna needs to be improved in order to cover 3.1-10.6 GHz.

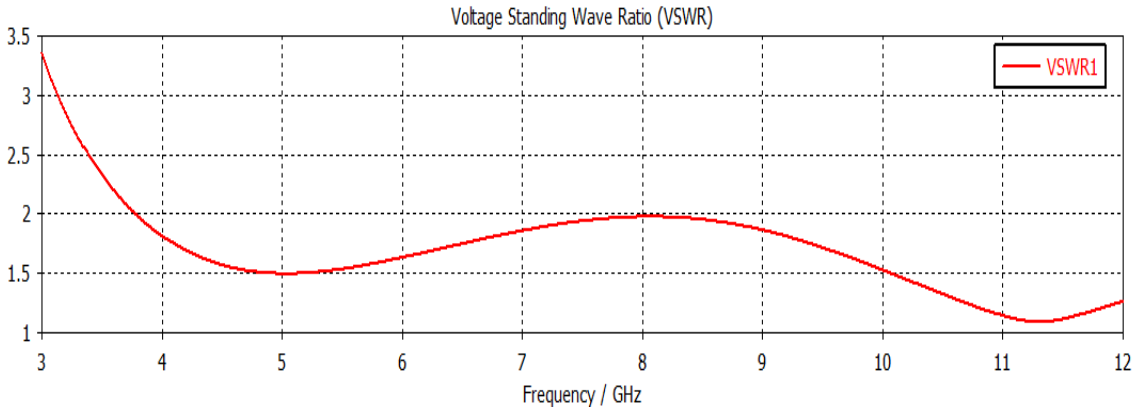

Figure 5.7: VSWR of rounded Bow Tie Antenna

From the results, it is apparent that the proposed rounded bow tie antenna behaves as a dual band like the classical bow tie antenna configuration (Figure 5.3). A

comparison of the two results (Figure 5.3 and Figure 5.6) reveals that the rounded bow tie antenna has larger bandwidth than the bow tie antenna.

The return loss of the rounded antenna (Figure 5.6) is compared with the bowtie antenna (Figure 5.4). If return loss of the classical bowtie antenna in Figure 5.3 is compared with return loss of the rounded bowtie antenna in Figure 5.7, a very small difference is observed. Strong evidence of the difference is found. This indicates that the curved edge, which is added into bowtie antenna, has little influence on bandwidth enhancement.

Bowtie antennas are kinds of frequency independent antennas.There are a lot of advantages of bow tie antennas. Main advantages of designing bowtie antenna are simple design and broadband impedance characteristic (Gonzales et al, 2005; Wiesbeck et al, 2009). Truncation principle- has been applied for practical purposes where the size of any physical object is obviously finite (Wiesbeck et al, 2009; Sarkar et al, 2010). To prove this idea, the proposed rounded bow tie antenna is truncated from its edges. Figure 5.8 presents the schematic diagram and dimensions of the truncated rounded bowtie.

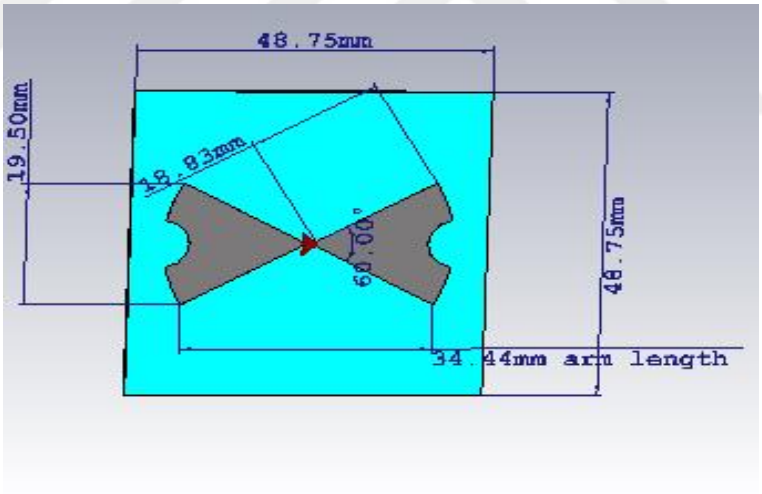

Figure 5.8: Schematic diagram and the size of Truncated Rounded BowTie Antenna

The graphs below illustrate two of main antenna parameters for truncated bow tie antenna. Figure 5.9 provides the simulated results via CST Microwave Studio. From the graph below, it is clear that proposed antenna's -10 dB bandwidth is 7.9706 GHz (from 4.0294 GHz to 12 GHz. Figure 5.10 illustrates VSWR of the truncated bow tie antenna. Similarly, the condition VSWR<2 is satisfied between 4.0294 and 12 GHz for the proposed structure. These two graphs reveal that both results are compatible in the 3,1-10,6 GHz frequency range. Thus, both VSWR and S_{11} graphs comply with the FCC restrictions (FCC, 2002).

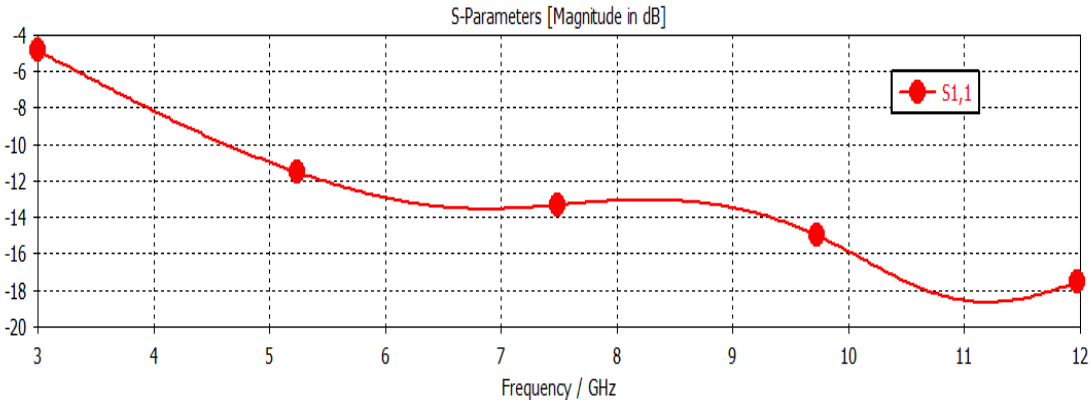

Figure 5.9: Return loss (S_{11}) of the Truncated Rounded Bowtie Antenna

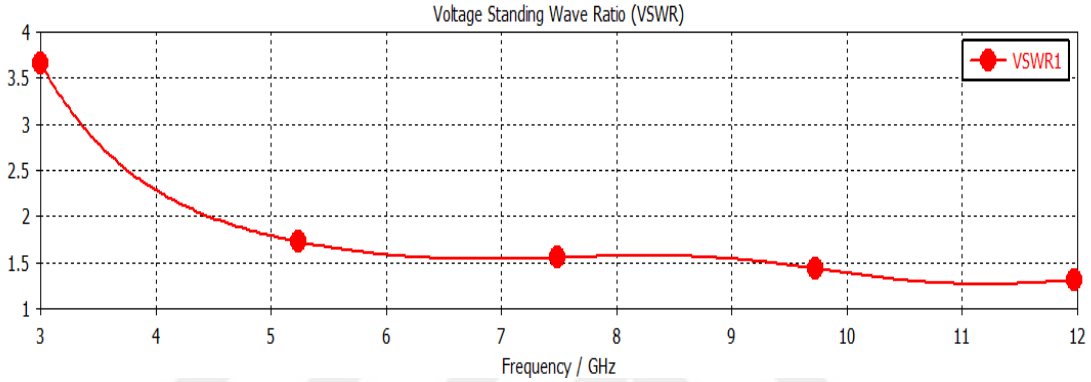

Figure 5.10: VSWR of the Truncated Rounded Bowtie Antenna

6. ROUNDED BOWTIE ANTENNA

In this chapter, a rounded bowtie antenna is designed and studied for Ultra-Wideband (UWB) frequency range for wireless communications applications. Antenna behavior is analyzed by observing Return Loss (S_{11}), Voltage Standing Wave Ratio and Radiation Pattern. Parameters affecting antenna structure such as the thickness of the substrate and relative permittivity are varied to clarify the antenna behavior in UWB systems.

6.1. Antenna Design

In this section, a rounded tie antenna is designed and investigated in the 3.1-10.6 GHz frequency range. The antenna configuration which is printed on a dielectric substrate is shown in Figure 6.1. The dielectric constant of the substrate is ε_r = 2 and the flare angle α = 60°. The dimensional parameters for the structure are given in Table 6.1. The excitation signal is Gaussian pulse.

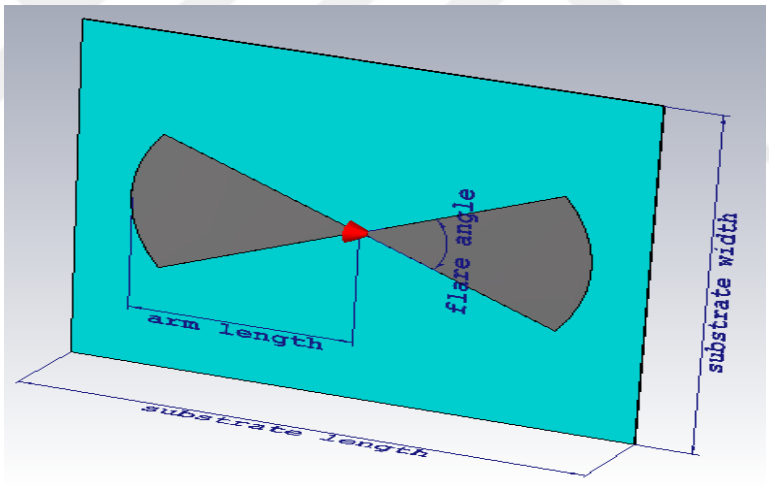

Figure 6.1: Rounded bow-tie antenna

Table 6.1: Rounded Bowtie Antenna Parameters

Parameter	Size
Arm length *(l_e)*	55 mm
Feed gap	0.67 mm
Feed width	0.67 mm
Metal thickness	0.044 mm
Substrate Thickness (*H*)	0.5 mm
Substrate length (*L*)	137.5 mm
Substrate width (*W*)	137.5 mm

Figures 6.2 and 6.3 illustrate the return loss (S_{11}) and VSWR characteristics of the proposed antenna respectively. In the figures, Return Loss is below -10dB and VSWR is below 2 within the frequency range of interest. Bandwidth is 7.31 GHz.

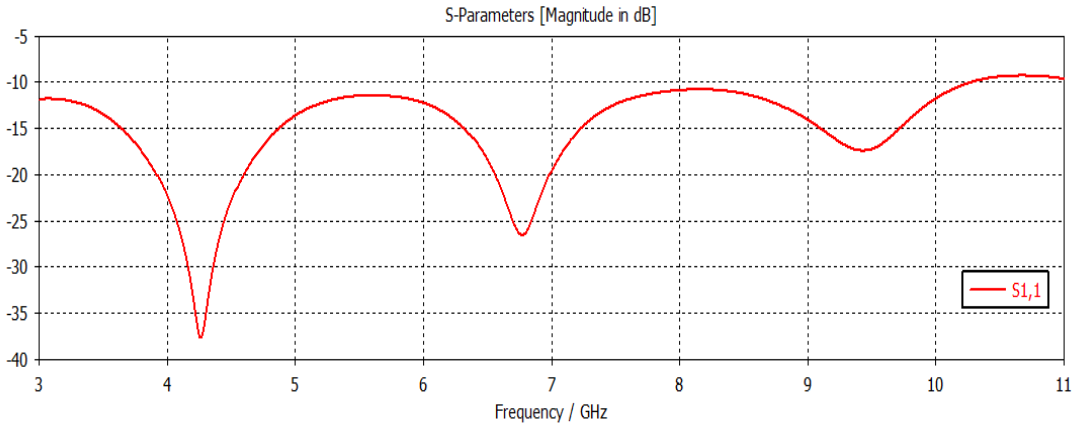

Figure 6.2: Return Loss of Rounded Bow Tie Antenna

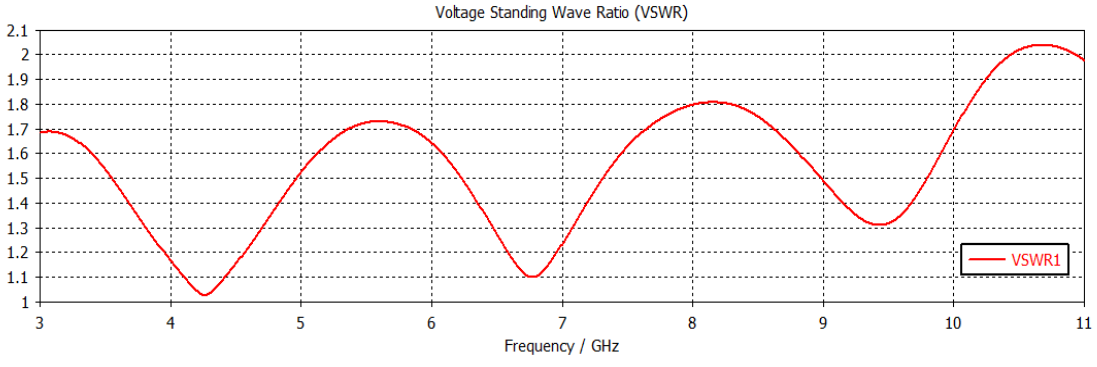

Figure 6.3: VSWR of Rounded Bow Tie Antenna

6.2. Impact of the Dielectric Substrate on the Antenna Performance

The effects of dielectric constant (ε_r) and substrate thickness (H) on radiation properties are investigated using CST MWS. Figures 6.4 and 6.5 show Return Loss and VSWR plots for different relative permittivity values. The antenna dimensions are the same as those given in Table 6.1. In the figures, as the dielectric constant increases, both Return Loss and VSWR graphs tend to get worse. The relative permittivity with ε_r= 2 gives the best results.

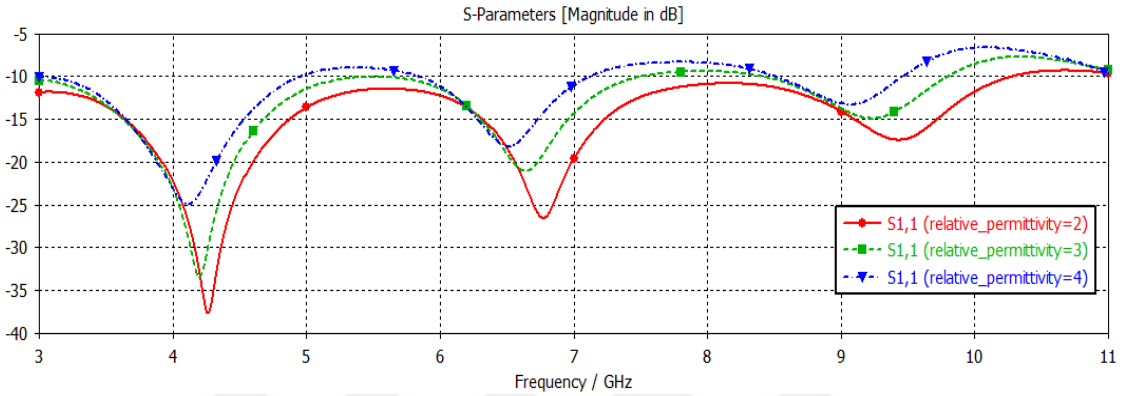

Figure 6.4: Return Loss of Rounded Bowtie Antenna at the three different ε_r values

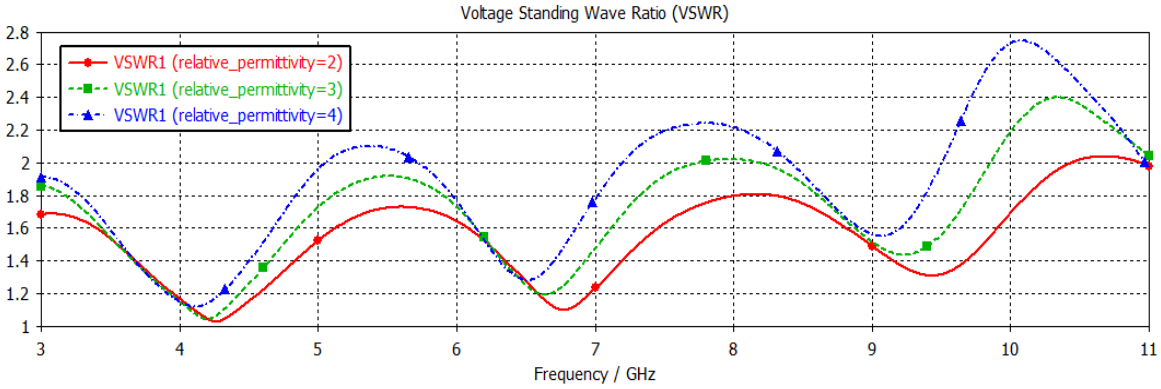

Figure 6.5: VSWR of Rounded Bowtie Antenna at the three different ε_r values

The best return loss and VSWR are given in Table 6.2 for relative permeability values. In table, it is clear that the smaller the dielectric constant is, the better the Return Loss and VSWR.

Table 6.2: Comparison of Return Loss and VSWR parameter at different ε_r

Relative Permittivity ε_r	Return Loss (dB)	VSWR
2	-37.66	1.03
3	-33.40	1.04
4	-24.90	1.12

Figures 6.6 and 6.7 illustrate the S_{11} Return Loss and VSWR graphs for different substrate thickness. Dielectric constant is chosen as ε_r= 2. In the figures, decrease when the substrate thickness decreases, S_{11} and VSWR are improved.

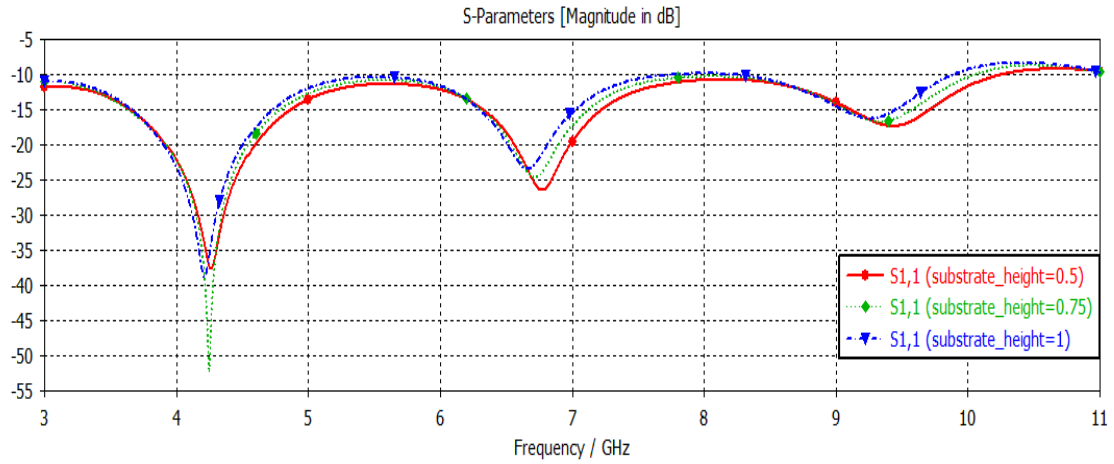

Figure 6.6: Return Loss of Rounded Bowtie Antenna at different substrate thickness (H) values

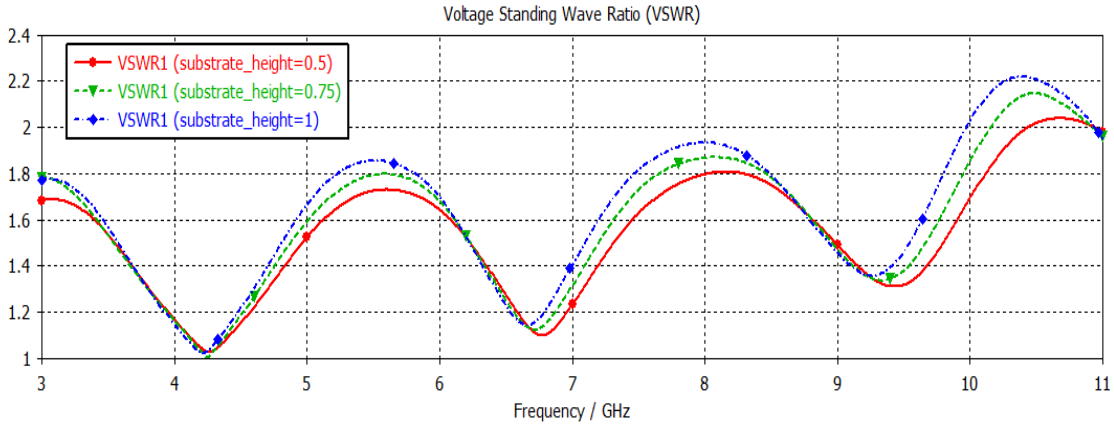

Figure 6.7: VSWR of Rounded Bowtie Antenna at different substrate thickness (H) values

The radiation pattern of the proposed antenna is illustrated in Figure 6.8. The figure includes the patterns for 3.1 GHz, 6.85 GHz, and 10.6 GHz frequencies. Dielectric constant and substrate thickness are selected as ε_r= 2 and H = 0.5 mm, respectively. As the frequency increases, some distortions are observable in the pattern characteristics.

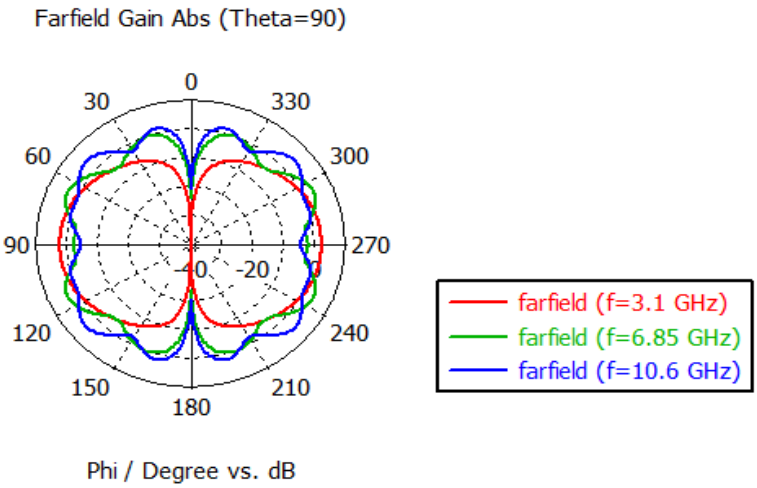

Figure 6.8: Radiation Pattern of Rounded Bowtie Antenna at three different frequencies 3.1GHz (red), 6.85GHz (green) and 10.6GHz (blue), respectively

In this chapter, a rounded bowtie antenna is investigated for UWB applications. The behaviour of the proposed antenna is analysed by modifying thickness and dielectric constant of the substrate. Then, VSWR, S_{11} and radiation pattern are interpreted in the 3.1-10.6 GHz frequency range. It is additionally observed that the proposed antenna performance can be improved by decreasing thickness and the dielectric constant of the substrate. When considering the radiation pattern for the designed structure, it is observed that the antenna has almost all directional radiation patterns in every selected frequency. Thus, the proposed rounded bowtie antenna is appropriate for UWB applications.

7. TRUNCATED ROUNDED BOWTIE ANTENNA

Truncated rounded bowtie antenna is proposed for UWB applications in this chapter. Beveling technique is employed to increase the bandwidth of the bowtie antenna. The corresponding bandwidth is from 3 to 11 GHz in order to observe the bandwidth enhancement in the frequency range of interest for UWB applications. The effective parameters of the antenna, including S_{11}, VSWR and radiation pattern are examined so as to analyze the enhancement techniques obviously. Besides, the relative permittivity and substrate thickness effects are examined to determine their role in bandwidth enhancement. The proposed antenna is worked on to provide an UWB behavior with return loss less than -10 dB and VSWR less than 2 during the enhancement process. The simulation results of the truncated rounded bowtie antenna are presented by using CST Microwave Studio.

The dimensions of the truncated rounded bow tie antenna are given in Table 7.1. As seen from the Table 7.1, truncated rounded bowtie antenna dimensions are chosen in order to compare simulation results properly according to former Section (Section 6). Additionaly, Figure 7.1 illustrates the dimensional labels of the proposed antenna.

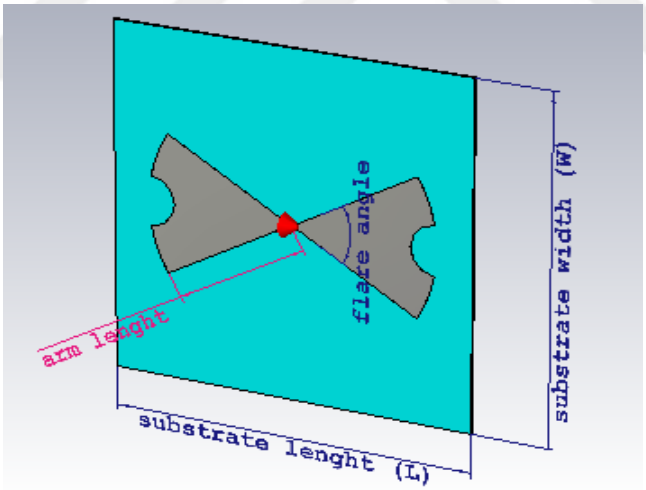

Figure 7.1: Truncated rounded bow-tie antenna

Table 7.1: Truncated Rounded Bowtie Antenna Parameter

Parameter	Size
Arm length (l_e)	55 mm
Feed gap	0.67 mm
Feed width	0.67 mm
Metal thickness	0.044 mm
Substrate thickness (H)	0.5 mm
Substrate length (L)	137.5 mm
Substrate width (W)	137.5 mm
Relative permittivity	2
Flare angle (α)	60^o
Frequency center (f_c)	6.85 GHz
Input resistance	250 Ω

The Return Loss characteristic of the truncated rounded bowtie antenna is displayed for the frequency range between 3 GHz and 11 GHz as in Figure 7.2. The simulated return loss bandwidth ranges from 3 to 11 GHz which covers the UWB frequency spectrum. In other words, a 116,78 % percentage bandwidth is obtained as shown in the S_{11} parameter curve in Figure 7.2. The worst case of the return loss within the simulated frequency range is -9.33 dB.

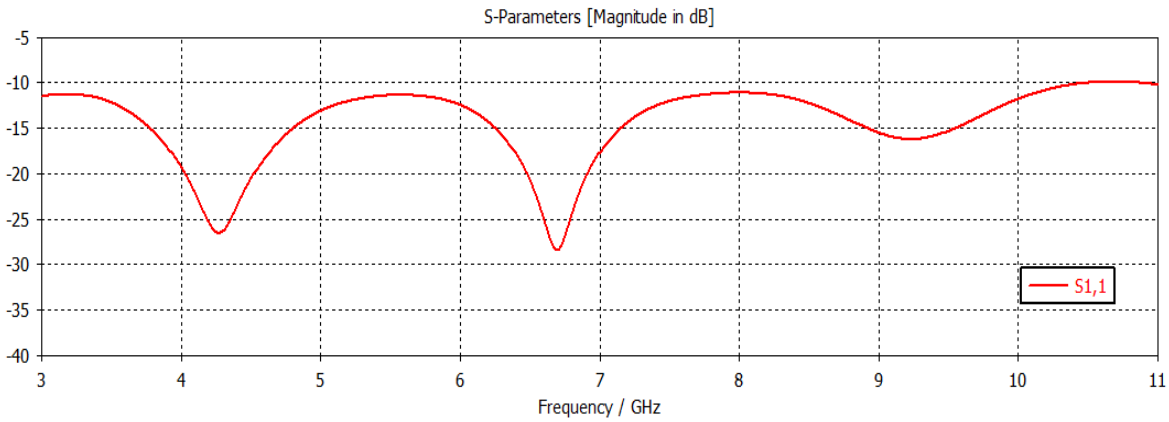

Figure 7.2: Return Loss of Truncated Rounded Bow Tie Antenna

Figure 7.3 shows the VSWR characteristic of the truncated rounded bowtie antenna. VSWR is smaller than 2 in the entire UWB frequency range. The lowest VSWR is obtained as 1.08 which is very close to unity at the frequency of 6.696 GHz.. The less VSWR is, the better match is. Therefore, VSWR is a reasonably significant compromise as shown in Figure 7.3.

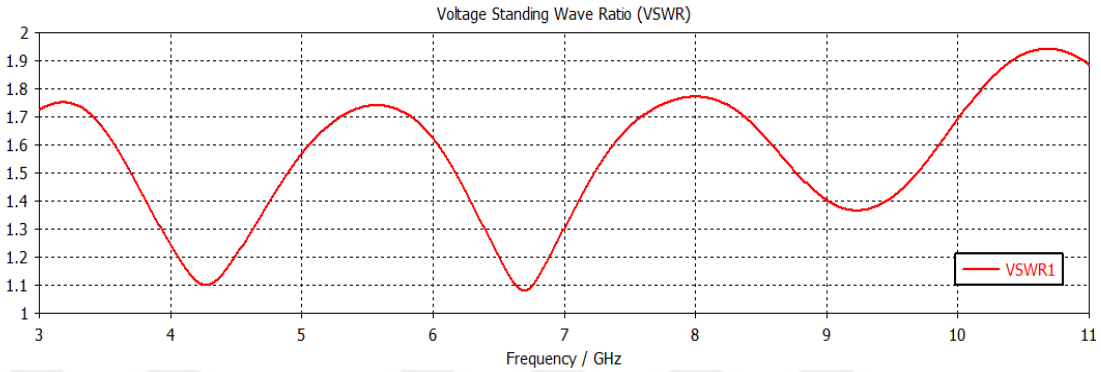

Figure 7.3: VSWR of Truncated Rounded Bow Tie Antenna

Figure 7.4 shows the radiation patterns of the truncated rounded bowtie antenna at the lower (3.1 GHz), middle (6.85 GHz) and upper (10.6 GHz) frequencies of the UWB frequency band of interest, respectively. From the simulation results, these antennas have almost omnidirectional radiation pattern with some distortions at three desired frequencies. Hence, it is acceptable for the mobile communication and great deal of UWB applications in order to provide efficient communication requirements.

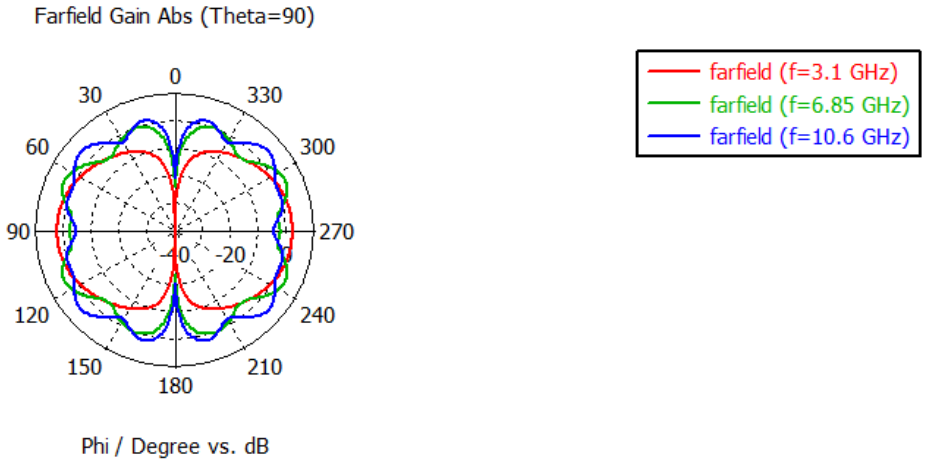

Figure 7.4: Radiation Patterns of Truncated Rounded Bow Tie Antenna at the three different frequencies 3.1GHz (red), 6.85GHz (green) and 10.6GHz (blue), respectively

Figure 7.5 illustrates the return loss characteristic of the proposed antenna by changing the relative permittivity. By observation of Figure 7.5, when the relative permittivity decreases, the proposed antenna tends to meet the UWB requirements. It can

additionally be observed from the figure that, the relative permittivity has remarkable effect on the antenna bandwidth.

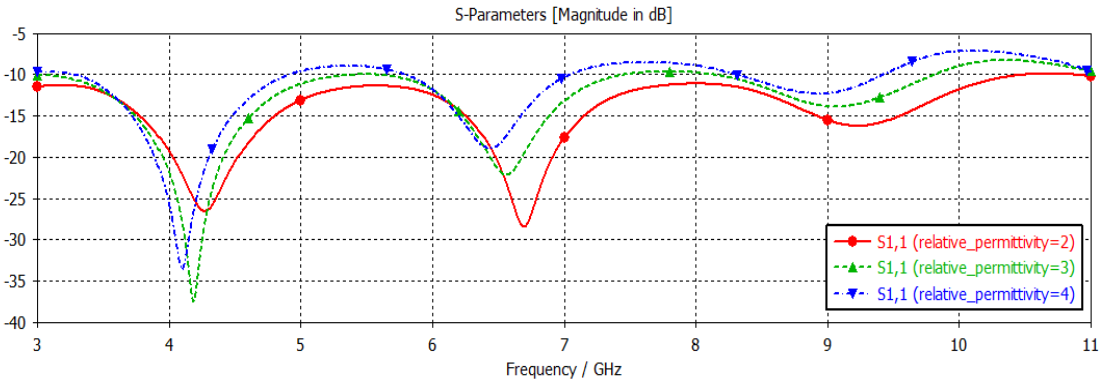

Figure 7.5: Return Loss of Truncated Rounded Bow Tie Antenna at the three different ε_r values

Figure 7.6 shows the effect of the relative permittivity on VSWR parameter. The remarkable value of the relative permittivity is observed as 2 where VSWR is less than 2 in the frequency range of 8 GHz (from 3 GHz to 11 GHz). Since, the relative permittivity, which is 2, provides better results as compared to the other relative permittivity values including the values of 3 and 4.

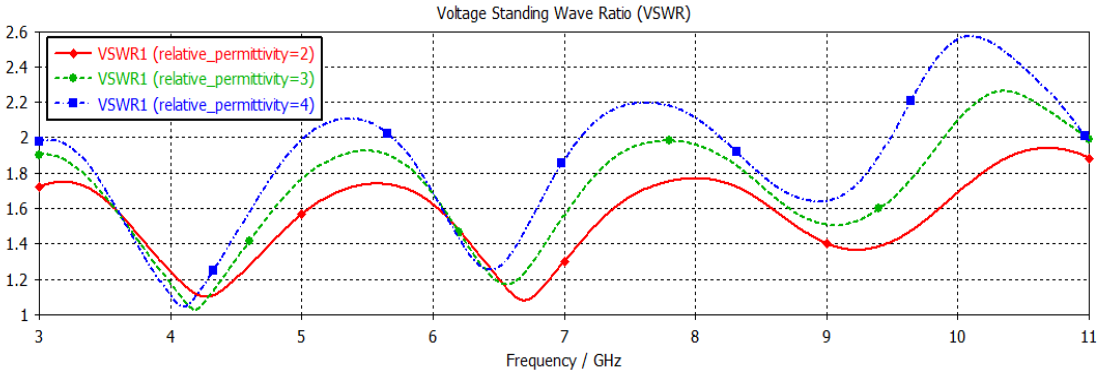

Figure 7.6: VSWR of Truncated Rounded Bow Tie Antenna at the three different ε_r values

After defining the best relative permittivity of antenna, substrate thickness effect (H) is illustrated in Figures 7.7 and 7.8. As the substrate thickness of the proposed antenna varies, the return loss and VSWR values also vary. Incrementing the substrate thickness doesn't provide acceptable value for antenna parameters as given in Figure 7.7 and Figure 7.8. It is observed that the suitable substrate thickness is 0.5 mm according to UWB requirements. Consequently, the optimum values for relative permittivity and substrate thickness are ε_r=2 and H=0.5 mm, respectively.

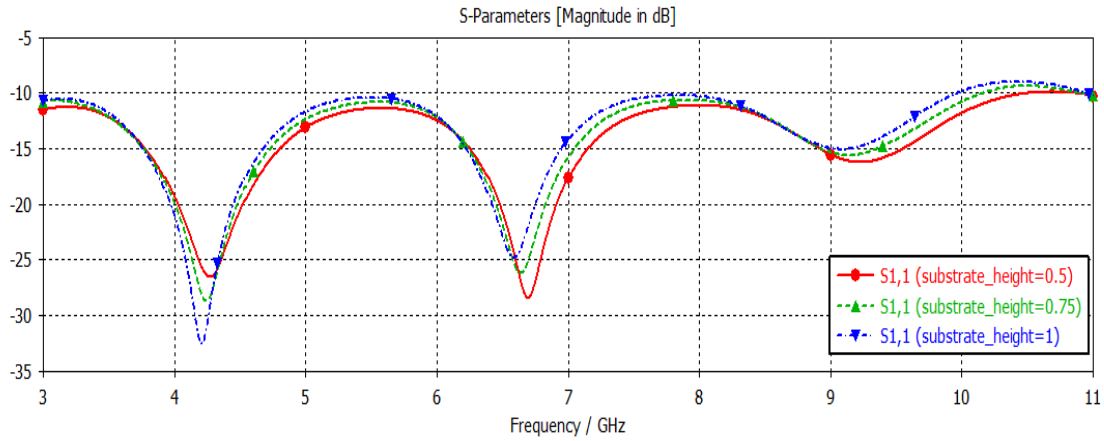

Figure 7.7: Return Loss of Truncated Rounded Bowtie Antenna at different substrate thickness (H) values

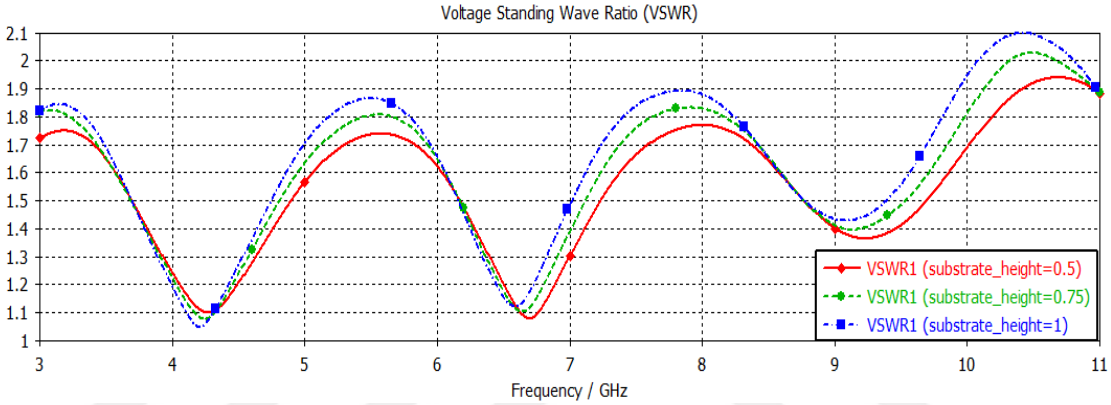

Figure 7.8: VSWR of Truncated Rounded Bowtie Antenna at different substrate thickness (H) values

Varying the flare angle (α) of a truncated rounded bowtie antenna also gives the possibility to obtain various return loss characteristics of the proposed antenna as shown in Figure 7.9. Flare angle (α) effects on the antenna parameters are examined and simulated by increasing the angle. As it can be seen from Figure 7.9, the return loss of truncated rounded bowtie antenna has different values at different flare angles (α). It is noticed that $\alpha=70^{o}$ implicates better return loss characteristic than the other angles, including $\alpha=30^{o}$, $\alpha=50^{o}$ and $\alpha=90^{o}$, respectively, according to the UWB requirements and FCC regulations. The arm length of the antenna is remaining the same at 55 mm during the flare angle parameter sweep process. The proposed antenna is overloaded when the flare angle is increased. Hence, $\alpha=70^{o}$ provides the acceptable value in order to obtain the desired antenna performance for UWB applications.

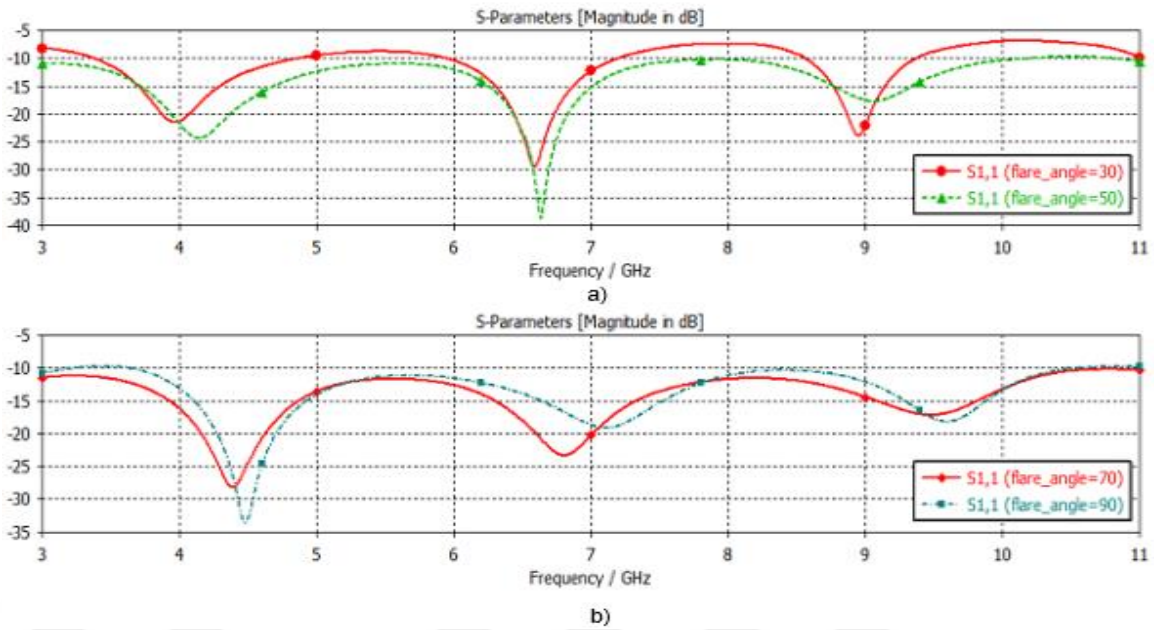

Figure 7.9: Return Loss of Truncated Rounded Bowtie Antenna at different flare angle (α) values

Figure 7.10 illustrates the return loss characteristic of the truncated rounded bowtie antenna which changes in accordance with arm length *(l_e)*, 40, 55, 70, 100 mm, respectively. l_e=*70* is acceptable value for this proposed antenna.

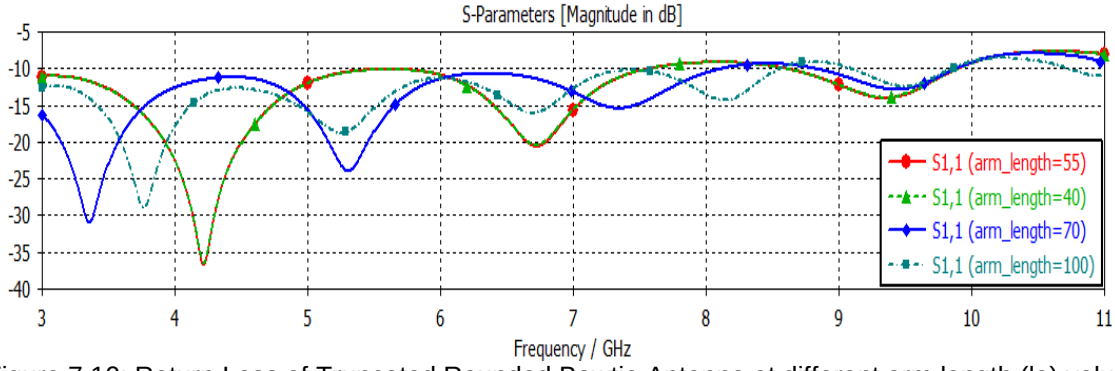

Figure 7.10: Return Loss of Truncated Rounded Bowtie Antenna at different arm length (le) values

8. BEVELED EDGE ROUNDED BOW-TIE ANTENNA

This section deals with another different shape of classical bowtie antenna, which is mentioned in former chapter 5, so as to enhance its performance including better return loss (S_{11}), lower VSWR, flatter input impedance and less distortion radiation pattern. Inasmuch as the other configurations of classical bowtie antenna are not yet ample to cover the all UWB frequency band (3.1-10.6 GHz), a different approach, namely beveling the arm corners is provided to overcome this drawback of antenna design.

A great deal of literature survey is available in journals, magazines and conference papers explaining miscellaneous bowtie antennas. The effect of beveled corner is examined by (Liu et al, 2008; Qu and Ruan, 2006; Kaur and Solanki, 2012). Liu et al. investigated the corner effect on the antenna performance by using three different prototypes. In these studies, impedance bandwidths, field distributions, radiation patterns are simulated via Ansoft HFSS and measured via Agilent N5230A. Qu et al. also focused on three bowtie antenna configurations including quadrate, rounded-edge and triangular shapes. The work of Qu et al. reveals that the existence of the round corners has significant effects on the classical bowtie antenna. Kaur et al. analyzed also three various shapes of bowtie antenna so as to improve the antenna performance by modifying the edges of the each arm. Simultaneously, the flare angle and rounded corner radius effects are examined whether trade-off condition occurs or not. Henceforth, the radius of the rounded corners isn't changed beyond certain value due to trade-off condition. In other words, increasing the radius value beyond certain value doesn't make the antenna parameters improve significantly.

In this section, beveling technique is applied for rounded bowtie antenna which has been already simulated and examined in Section 6. Transmission Line Method is applied while the effective antenna structure dimensions are preserved so as to compare with other examined bowtie antenna configurations by using CST Microwave Studio.

According to the transmission line model theory, there are several formulas for specifying antenna dimension and permittivity of the substrate. Thereby, some physical parameters ought to be calculated by using these equations. The proposed bow tie consists of several physical parameters, namely the ground plane, dielectric substrate and two metal arms. The proposed equations for dimensions are given as follows:

$$\varepsilon_{eff} = \frac{(\varepsilon_r + 1)}{2} + \left((\varepsilon_r - 1) x (1 + (10 x \frac{d}{w}))^{-1/2} \right) \quad (8.1)$$

$$L = \lambda_o x \left(\frac{1}{\sqrt{\varepsilon_{eff}}} \right) \quad (8.2)$$

Equations (8.1, 8.2) are essential formulas in order to determine the effective relative permittivity and arm length of the bow tie antenna. Equation (8.1) represents the calculation of the effective relative permittivity where *w* is bow-tie width and *d* is substrate thickness.

The bowtie antenna radiates in a nonhomogeneous medium, typically the substrate and air because of its structure. Therefore electric field lines occur in the substrate and air (Fringing effect) (Nahar and Sharma, 2014). As a result, this transmission line doesn't support transverse electric-magnetic (TEM) mode due to different phase velocities of air and substrate. The effective relative permittivity is crucial parameter which can also vary with different frequencies. After these considerations, effective relative permittivity is obtained by using Equation (8.1) as given in the following equation (8.3) where relative permittivity ε_r is 2.

$$\varepsilon_{eff} = \frac{2+1}{2} + \left((2-1)(1+10 x \frac{0.4}{64})^{-1/2} \right) = 1.992 \cong 2 \quad (8.3)$$

Equation (8.3) is consistent with the theory that the range of effective dielectric constant changes from $1 < \varepsilon_{eff} \leq \varepsilon_r$.

8.1. ANTENNA GEOMETRY

Figure 8.1 illustrates different views of the beveled edge rounded bowtie antenna structure which is designed via CST Microwave Studio. From Figure 8.1 and Table 8.1 it can be inferred that the geometry of the proposed antennas are determined by parameters including flare angle (α) which causes the bandwidth improvement and arm length (l_e) which complies with radiation characteristics.

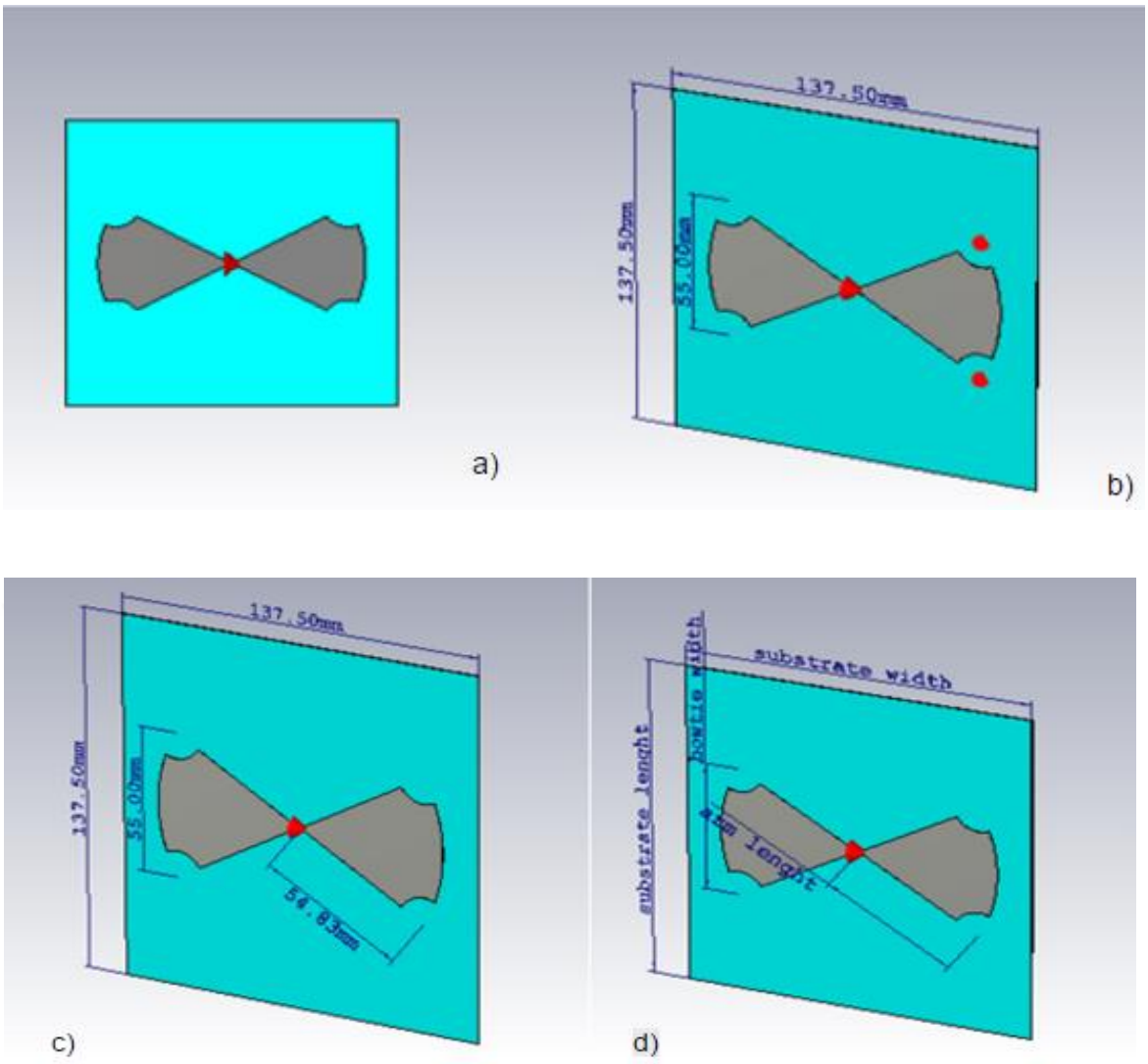

Figure 8.1: Different views of the bevelled edge rounded bowtie antenna a) front b-c) perspective with millimeter values d) perspective with dimension labels

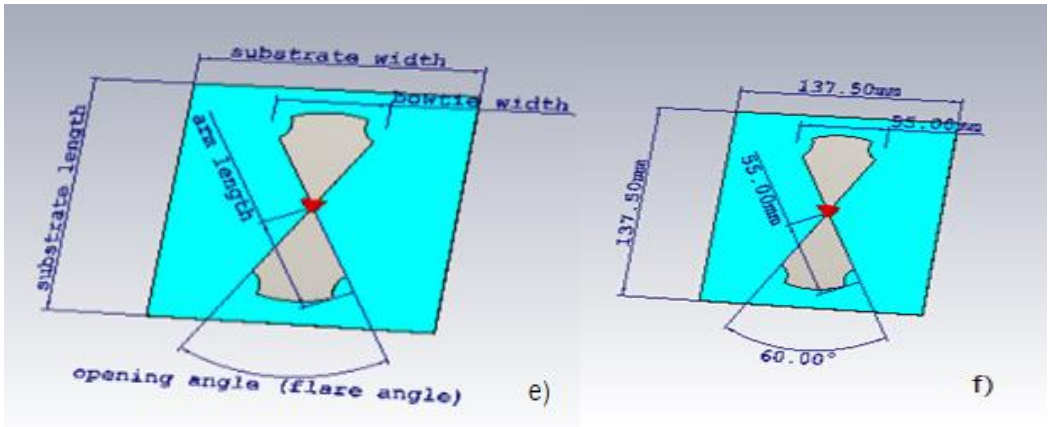

Figure 8.1: Different views of the bevelled edge rounded bowtie antenna e) top with dimension labels f) side view with millimetre values

Beveled Edge Rounded Bow Tie Antenna dimensions are chosen the same as the other proposed antenna dimensions in this thesis in order to observe the improvements in bandwidth and antenna parameters (Table 8.1). The Gaussian pulse is applied into the port as an excitation signal. The Fourier series and Fourier Transform of the Gaussian pulse are obtained by using template based post processing tool via CST MWS as shown in Figure 8.2 and Figure 8.3. The main reason of this application is that the antenna simulation results are sketched (obtained) with respect to the UWB frequency range as given in Figure 8.4, 8.5, 8.6, and 8.7.

Table 8.1: Four Different Rounded Bowtie Antenna Structure's Dimensions

Physical Parameters	**Rounded Bow Tie Antenna**	**Truncated Rounded Bow Tie Antenna**	**Classical Bow Tie Antenna**	**Beveled Edge Rounded Bow Tie Antenna**
Arm length *(l_e)*	55 mm	55 mm	55 mm	55 mm
Feed gap	0.67 mm	0.67 mm	0.67 mm	0.67 mm
Feed width	0.67 mm	0.67 mm	0.67 mm	0.67 mm
Metal thickness	0.044 mm	0.044 mm	0.044 mm	0.044 mm
Substrate Thickness (*H-d*)	0.5 mm	0.5 mm	0.5 mm	0.5 mm
Substrate length (*L*)	137.5 mm	137.5 mm	137.55 mm	137.55 mm
Substrate width (*W*)	137.5 mm	137.5 mm	110 mm	137.5 mm
Relative Permittivity	2	2	2	2
Flare angle (α)	60^o	60^o	60^o	60^o

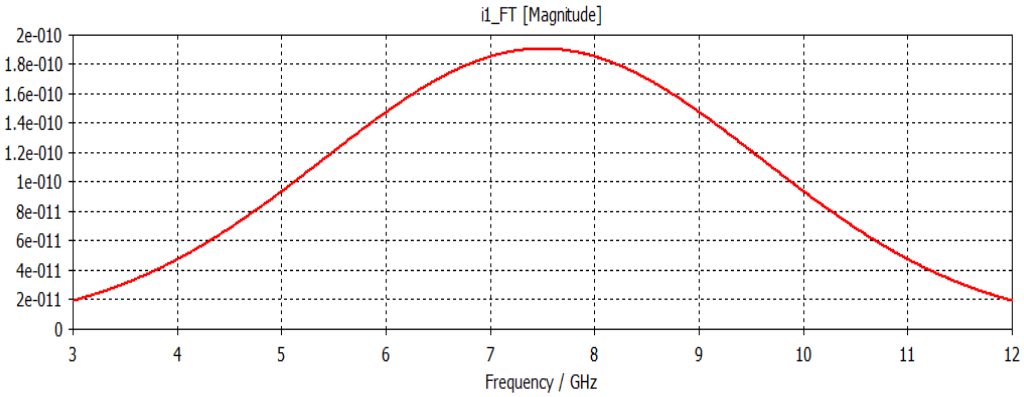

Figure 8.2: The Fourier transform of the excitation signal

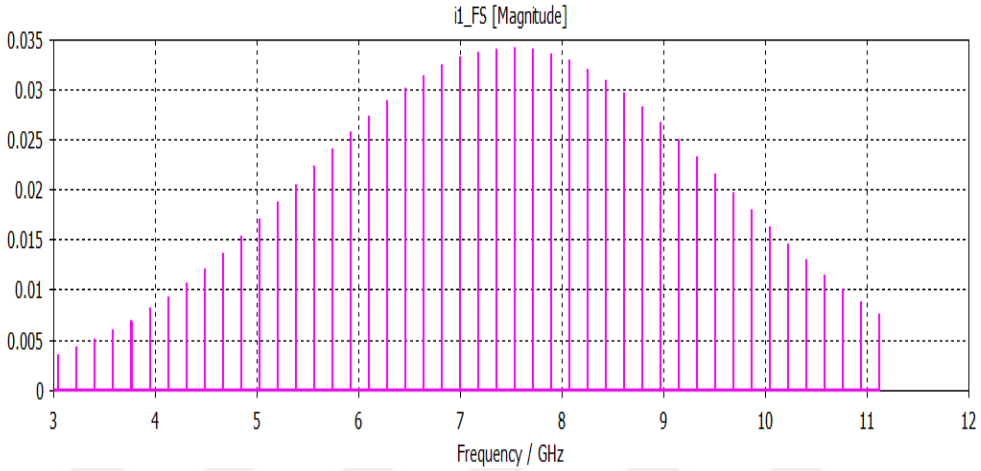

Figure 8.3: The Fourier series of the excitation signal

8.2. SIMULATION & RESULTS

The results obtained from the simulation program are presented in this section. As Figure 8.4 indicates that the return loss of the proposed antenna meets the UWB requirements defined by FCC. Figure 8.5 provides the minimum return loss value which occurs at 4.098 GHz. The numerical value of the minimum return loss value is -27.958 dB as shown in Figure 8.5. Additionally, Figure 8.6 indicates the minimum return loss value in linear scale. Figure 8.7 shows the VSWR characteristic of the proposed antenna.

Another parameter is Return Loss (R_L) so as to define the effect of VSWR parameter. Generally, the return loss is measured in dB scale as given in Figure 8.5. It is apparent from Figure 8.6 that the linear value of S_{11} is 0.04. Now, the S_{11} from the simulation result is substituted into Equation (2.9) to calculate the exact value of the VSWR and provide that the theory and simulation results are compatible with each other. Thus, this substitution yields Equation (8.4):

$$VSWR = \frac{1+0.04}{1-0.04} = 1.0833 \tag{8.4}$$

The VSWR characteristic of the proposed antenna is represented in the frequency range from 3 to 11 GHz in Figure 8.7. It is concluded that VSWR is lower than 2 in the whole UWB frequency range as required by FCC. From Figure 8.8, we can conclude that Equation (8.6)'s result is an acceptable value for the UWB applications and design procedure.

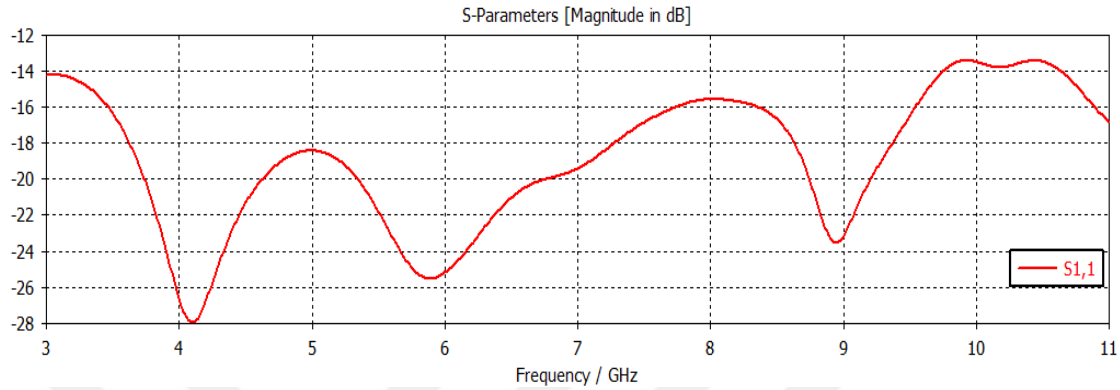

Figure 8.4: Return loss characteristic of the beveled edge rounded bow tie antenna

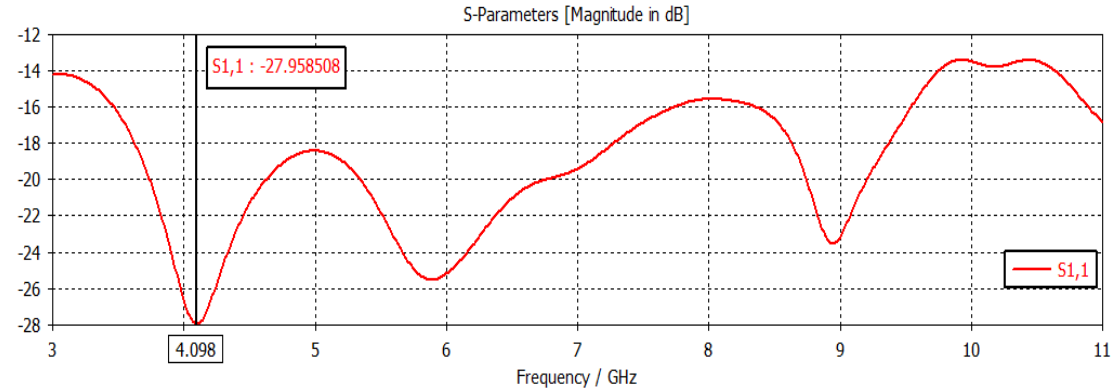

Figure 8.5: Minimum return loss value in dB scale of the proposed antenna in the UWB frequency range

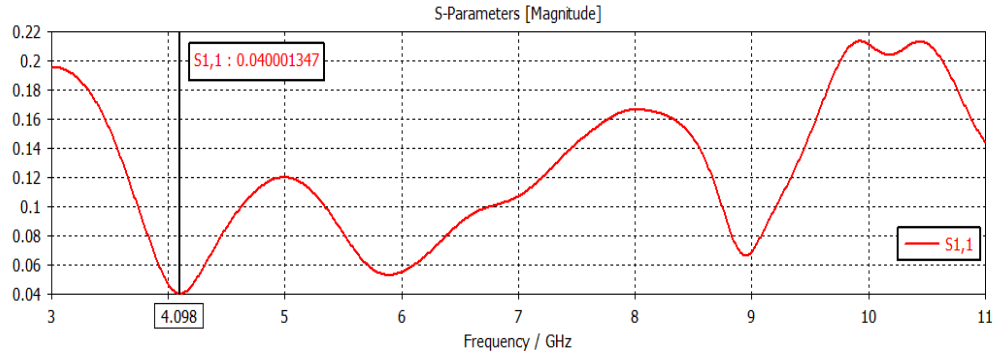

Figure 8.6: Minimum return loss value in linear scale of the proposed antenna in the UWB frequency range

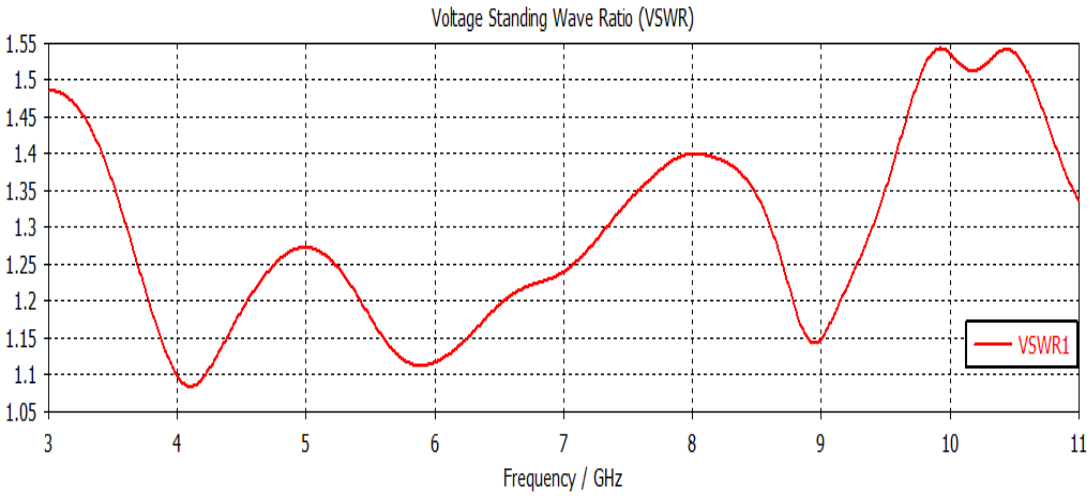

Figure 8.7: VSWR of the proposed antenna

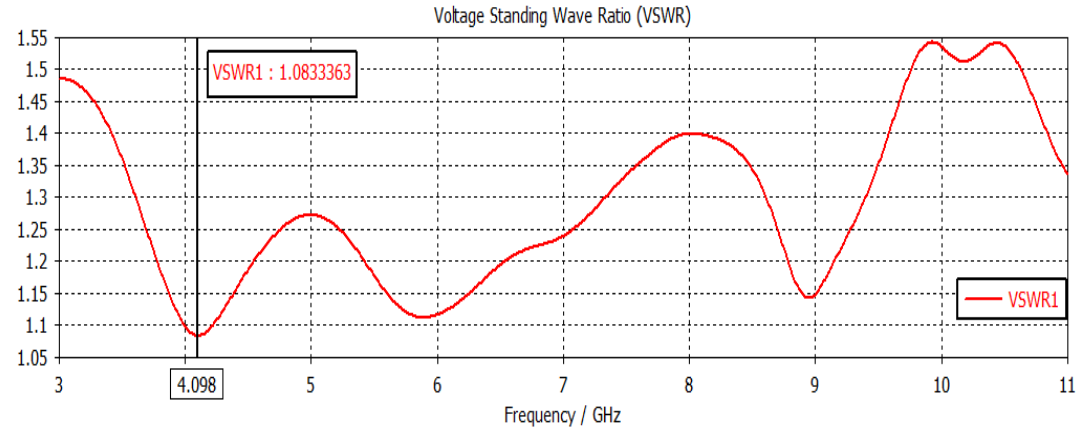

Figure 8.8: Minimum VSWR value of the proposed antenna

The real and imaginary parts of the proposed antenna impedance which are plotted by using CST MWS are shown is Figure 8.9. The purple line stands for the real part of the antenna impedance and the orange line stands for imaginary part of the antenna impedance. Both Imaginary part and Real Part don't fluctuate severely. Besides, it is apparent that the antenna resistance is almost stable and the antenna reactance is approximately zero in the UWB frequency range namely, 3.1-10.6 GHz. Even when it is not zero at some frequencies, it is considerably small and hence negligible as compared to the resistance. Consequently, the load impedance or transmission line impedance ought to be adjusted by using the antenna impedance shown in Figure 8.9 in order to achieve the perfectly match condition.

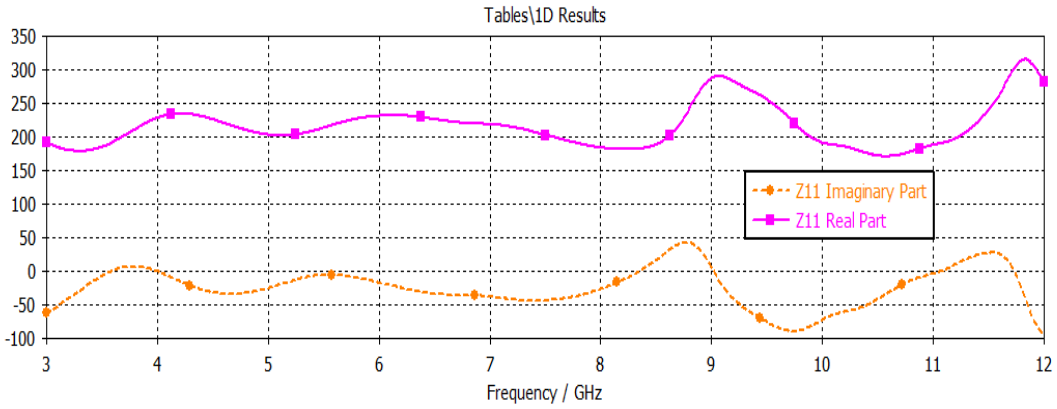

Figure 8.9: Real and Imaginary Part of the Antenna Impedance

Figure 8.10 represents the Cartesian representation of the proposed antenna's radiation pattern at the frequency of 6.85 GHz. Figure 8.11 shows the polar representation of the radiation pattern at the frequency of 6.85 GHz. Figures 10-11 reveal that the main direction of the radiation pattern occurs at ±90^{o}, main lobe magnitude is 2.2 dB and side lobe level is -1.7dB.

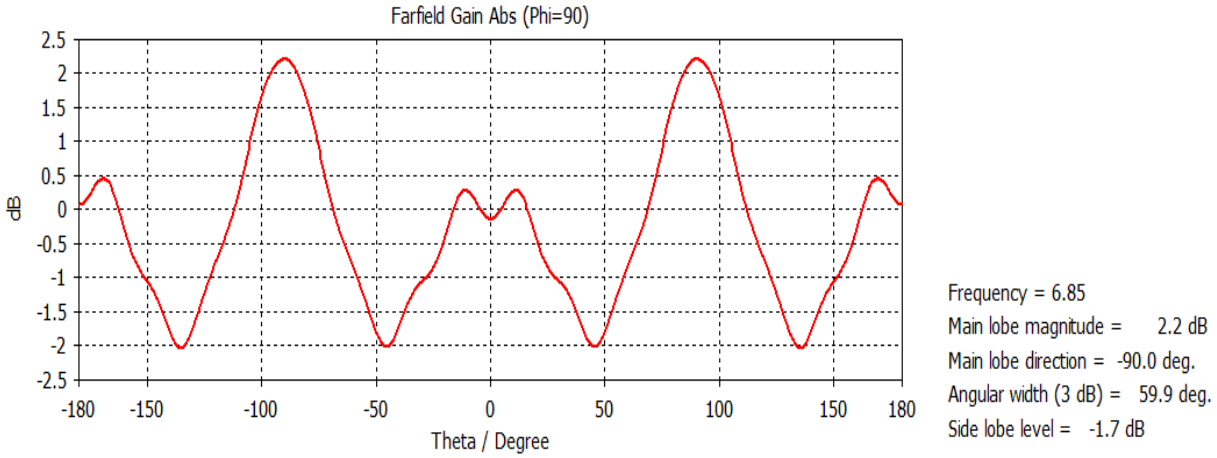

Figure 8.10: The Cartesian representation of the radiation pattern at 6.85 GHz

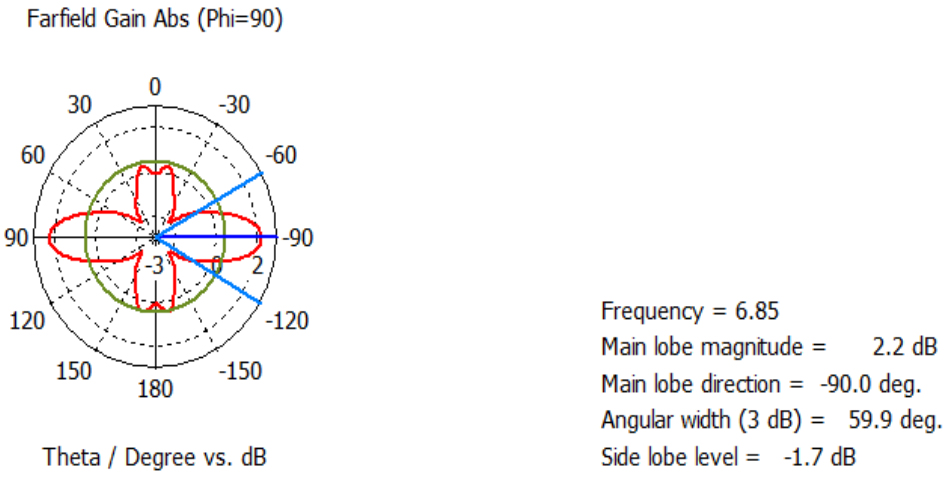

Figure 8.11: The Polar representation of the radiation pattern at 6.85 GHz

Figure 8.12 represents the Cartesian representation of the proposed antenna's radiation pattern at the frequency of 10.275 GHz. Figure 8.11 shows the polar representation of the radiation pattern at the frequency of 10.275 GHz. Figure 8.10 and Figure 8.11 reveal that the main direction of the radiation pattern occurs at ±90^{o}, main lobe magnitude is 6.55 dB and side lobe level is -7.2 dB. Figure 8.13 indicates that the radiation pattern characteristic is almost omnidirectional with less distortion which is suitable for UWB applications.

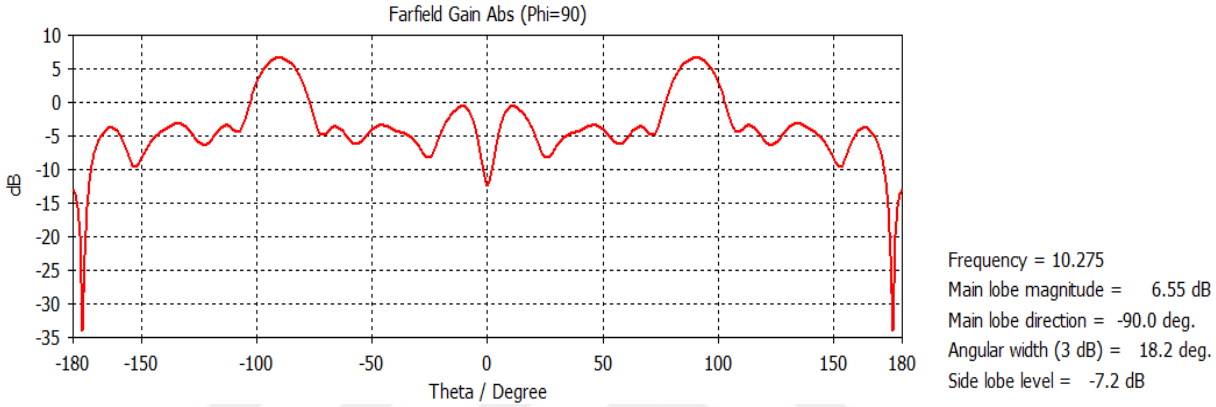

Figure 8.12: The Cartesian representation of the radiation pattern at 10.275 GHz

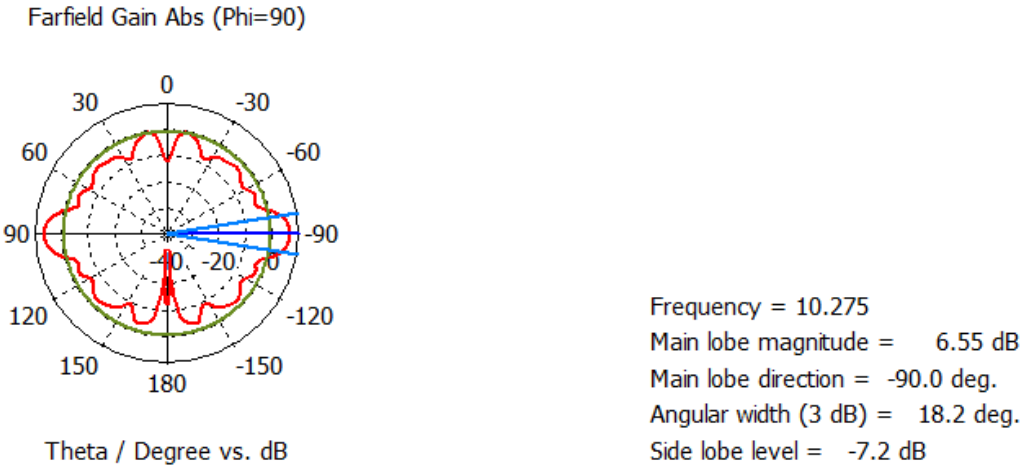

Figure 8.13: The Polar representation of the radiation pattern at 10.275 GHz.

Table 8.2: Comparison of the antenna parameters with respect to four different antenna structures

Antenna Types	VSWR	S_{11}	Bandwidth	Resonance Frequency
Classical Bow Tie Antenna	1.08	-27.994 dB	7.5 GHz (3.1-10.6 GHz)	6.15 GHz
Rounded Bow Tie Antenna	1.02	-39.033 dB	7.31 GHz (3-10.31 GHz)	4.206 GHz
Truncated Rounded Bow Tie Antenna	1.08	-27 dB	8 GHz (3-11 GHz)	6.696 GHz
Beveled Edge Rounded Bow Tie Antenna	1.08	-27.958 dB	8 GHz (3-11 GHz)	4.098 GHz

Up to now, four different bow tie antenna structures are investigated and examined. The CST MWS is used during the simulation process so as to obtain better and accurate antenna parameter results. Table 8.2 indicates that return loss and bandwidth are improved by designing different bowtie antenna configurations. VSWR decreases gradually from classical bow tie antenna to beveled edge rounded bowtie antenna. The minimum VSWR, which is almost unity (1.02), is observed for the rounded bowtie antenna. Further, the analysis shows that the bandwidth reaches 8GHz which exceeds UWB frequency range for truncated rounded bow tie antenna and beveled edge rounded bowtie antenna. The most significant improvement is found when the beveled edge rounded bowtie antenna is designed. Since, there is a significant positive correlation among S_{11}, VSWR and bandwidth for the proposed antenna.

The arm length effect on the antenna performance has been already highlighted at previous sections. The arm length effect on the beveled edge rounded bow tie antenna parameters can be examined since the most significant antenna structure is now defined as beveled edge one.

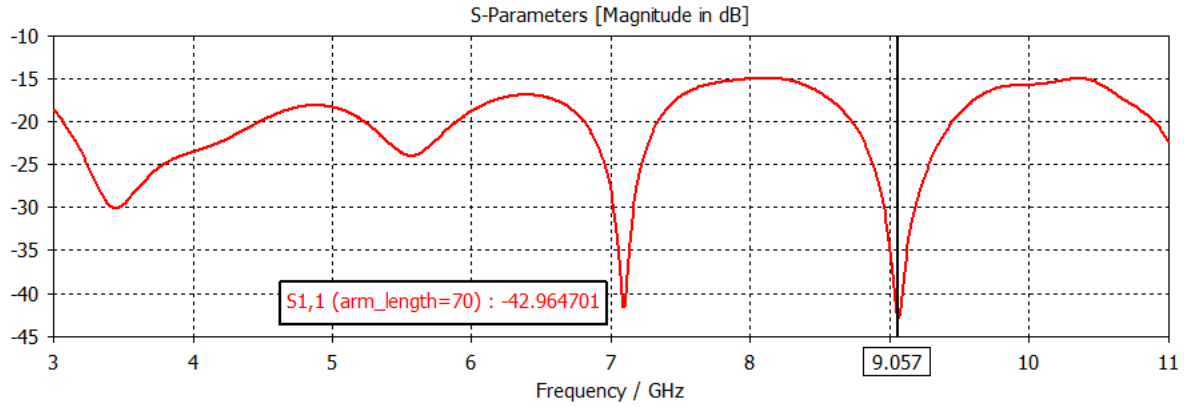

a)

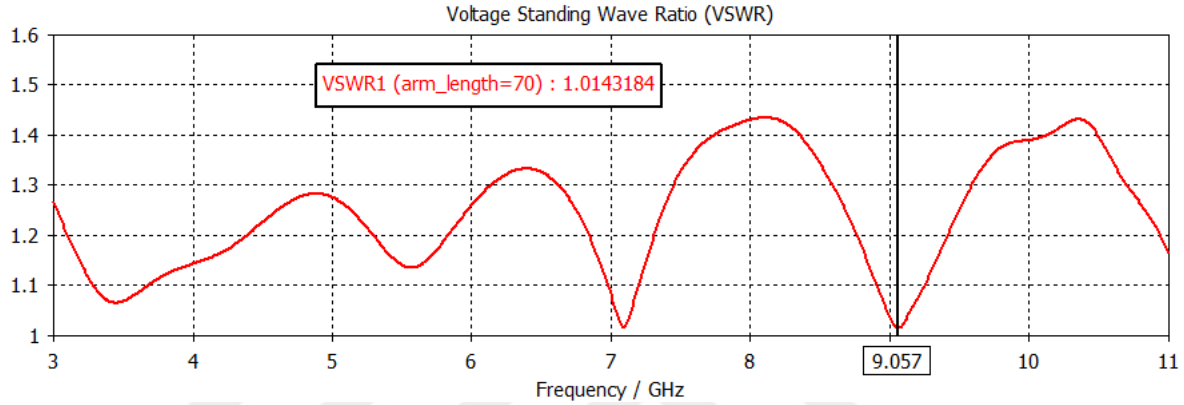

b)

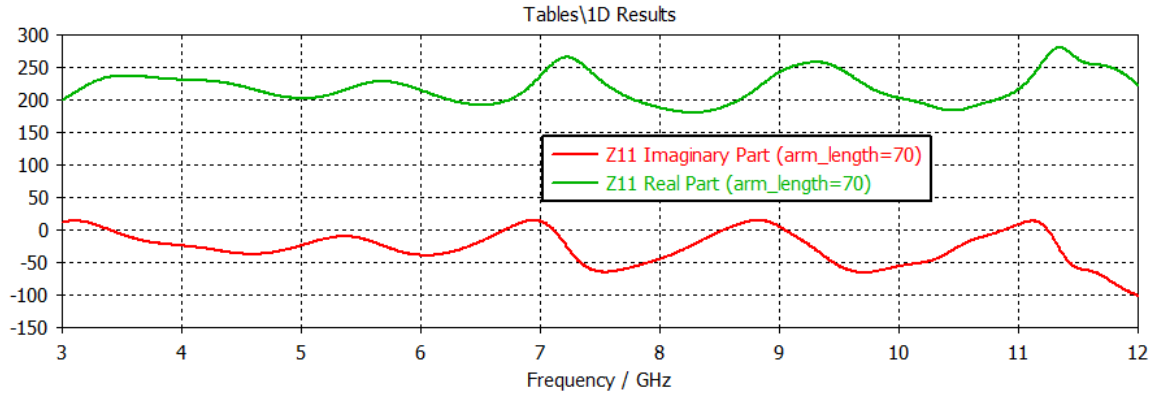

c)

Figure 8.14: a) The Return Loss b) VSWR and c) Impedance of the beveled edge rounded bowtie antenna when the arm length is 70 mm

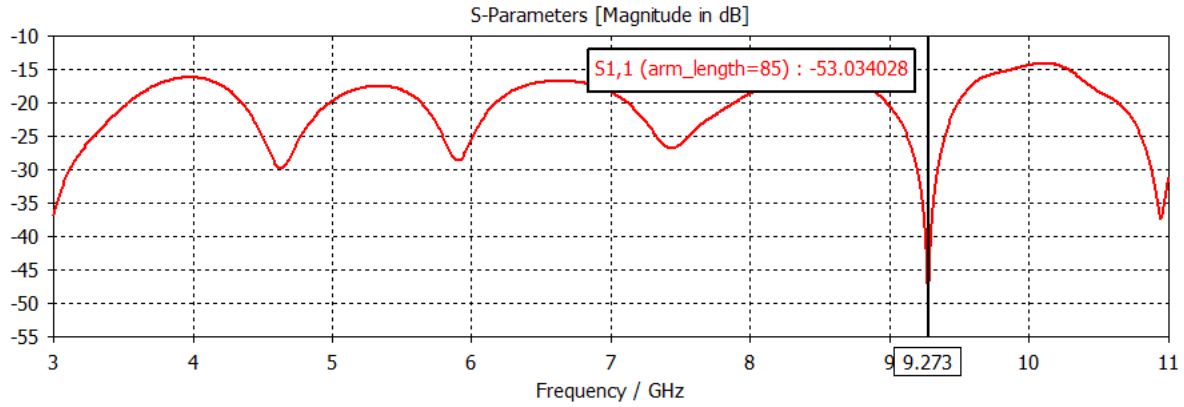

a)

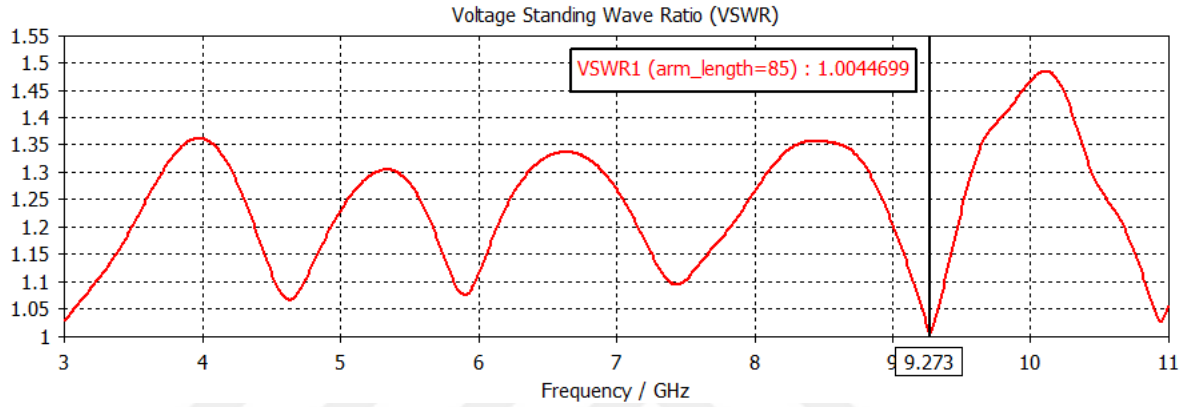

b)

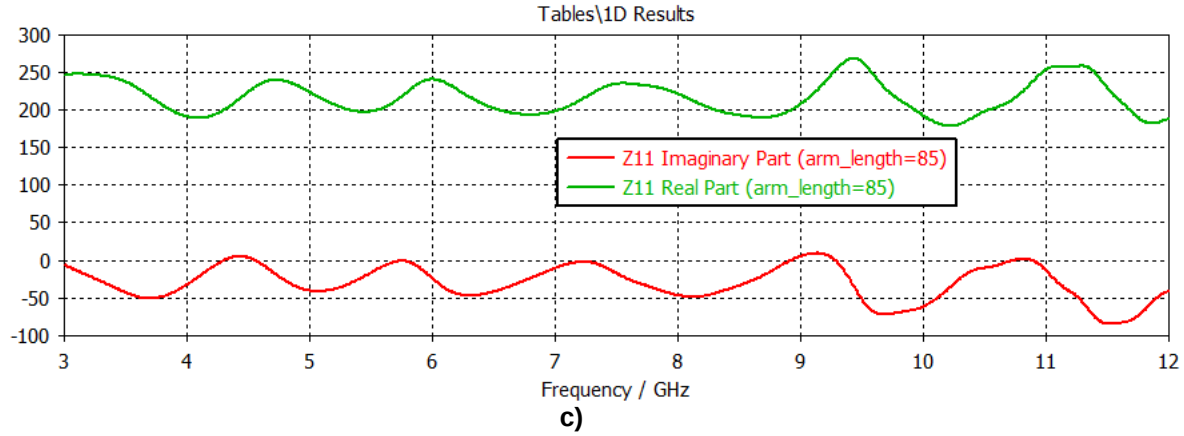

c)

Figure 8.15: a) The Return Loss b) VSWR and c) Impedance of the beveled edge rounded bowtie antenna when the arm length is 85 mm

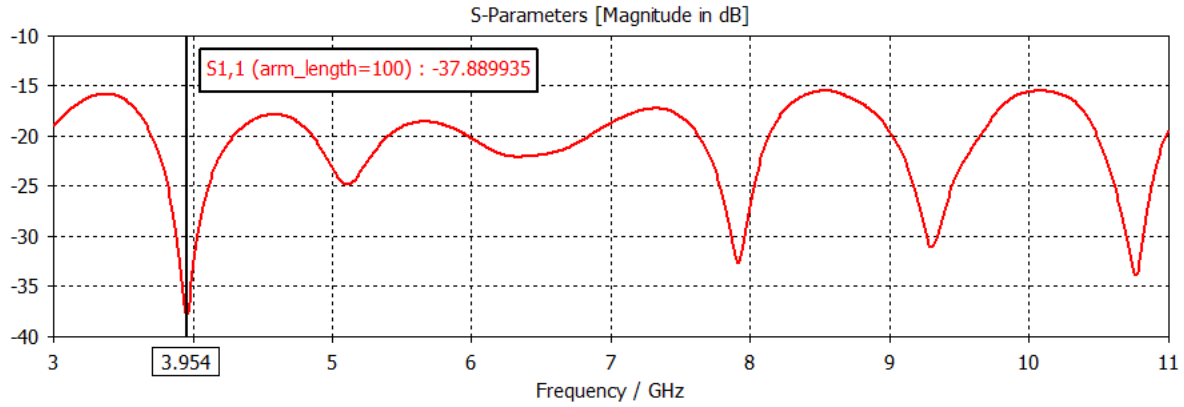

a)

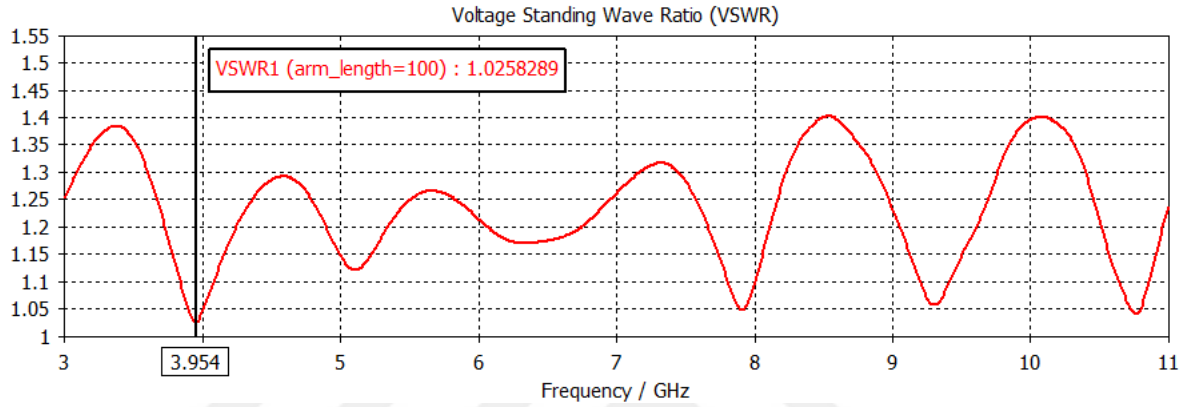

b)

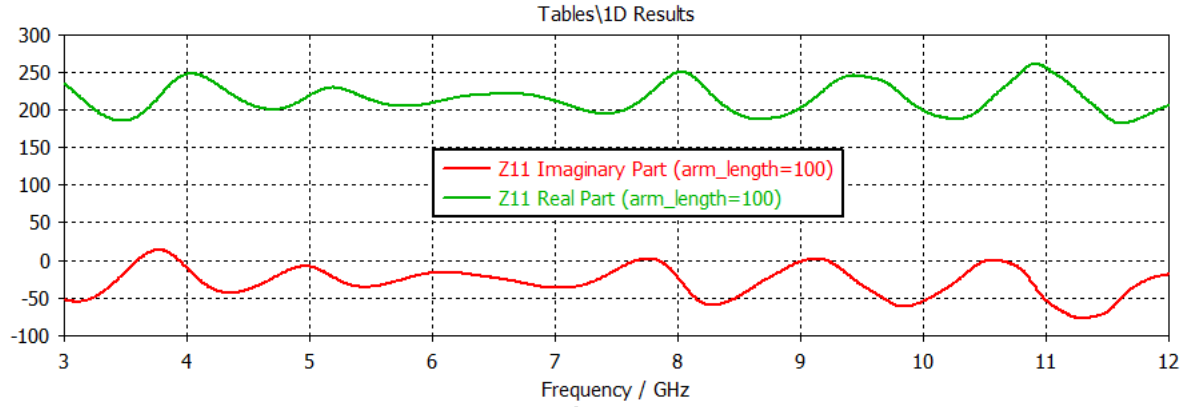

c)

Figure 8.16: a) The Return Loss b) VSWR and c) Impedance of the beveled edge rounded bowtie antenna when the arm length is 100 mm

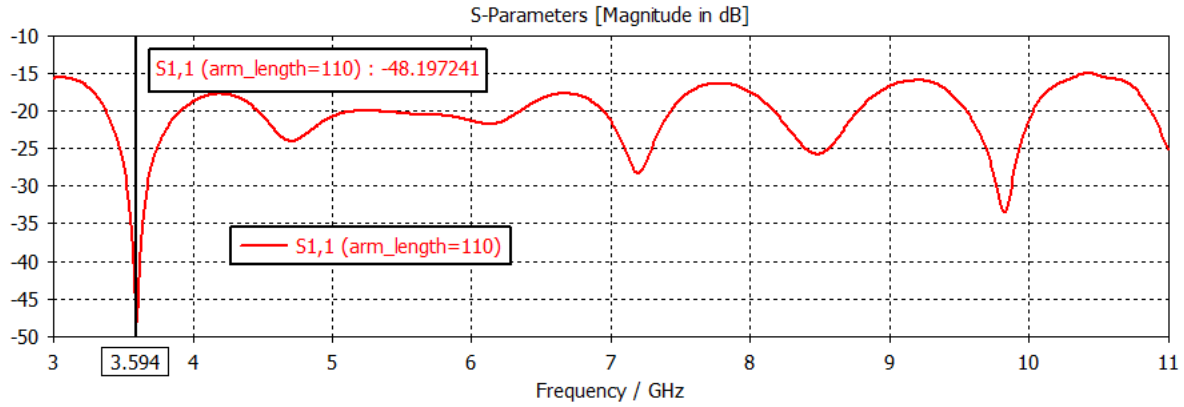

a)

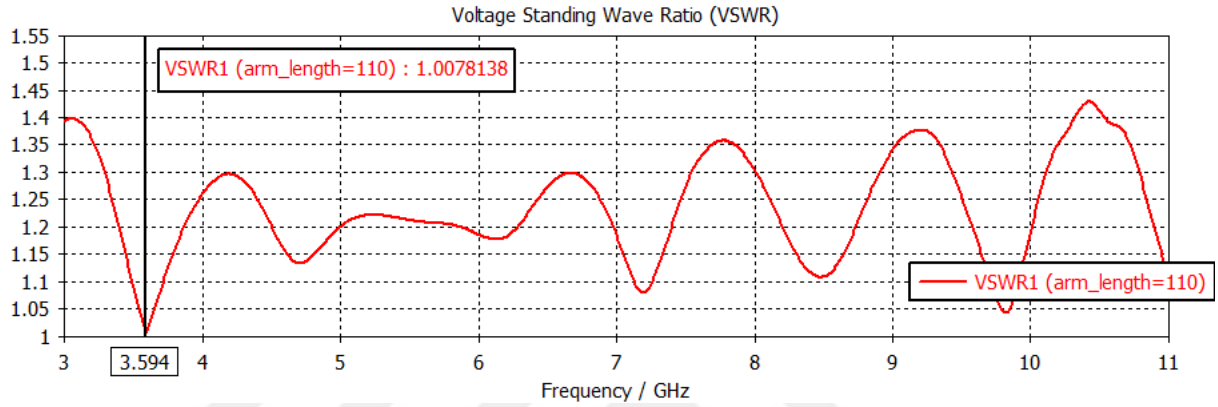

b)

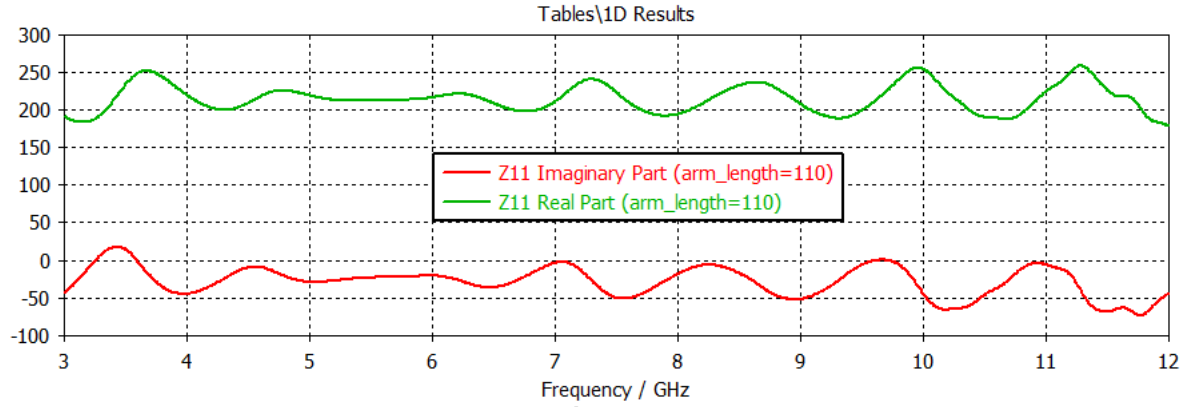

c)

Figure 8.17: a) The Return Loss b) VSWR and c) Impedance of the beveled edge rounded bowtie antenna when the arm length is 110 mm

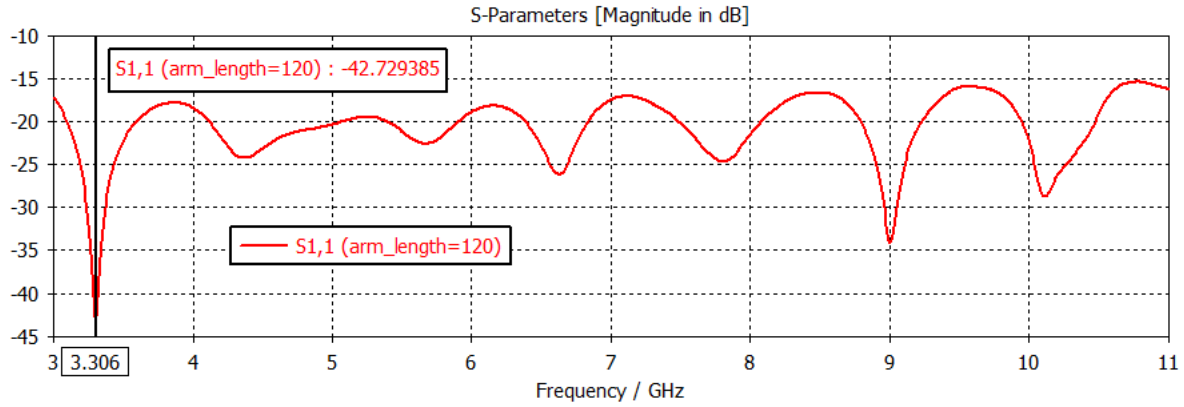

a)

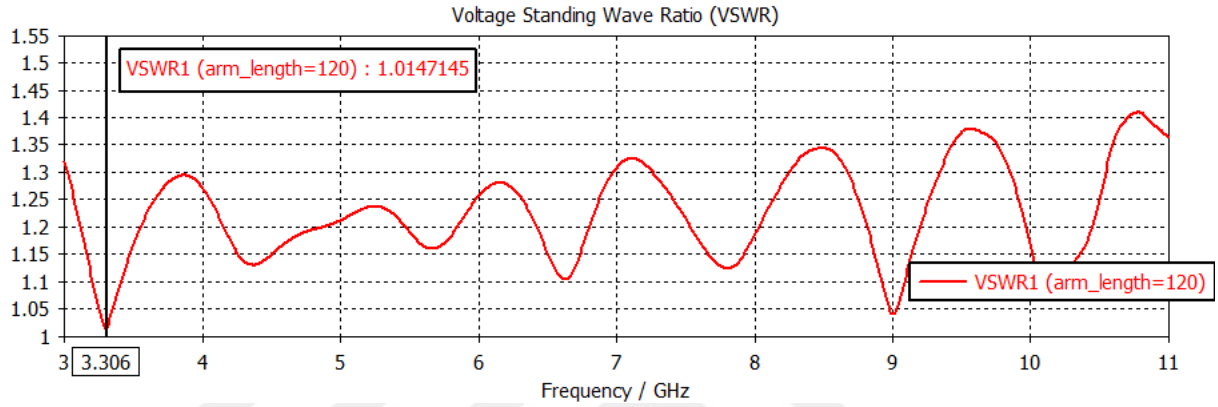

b)

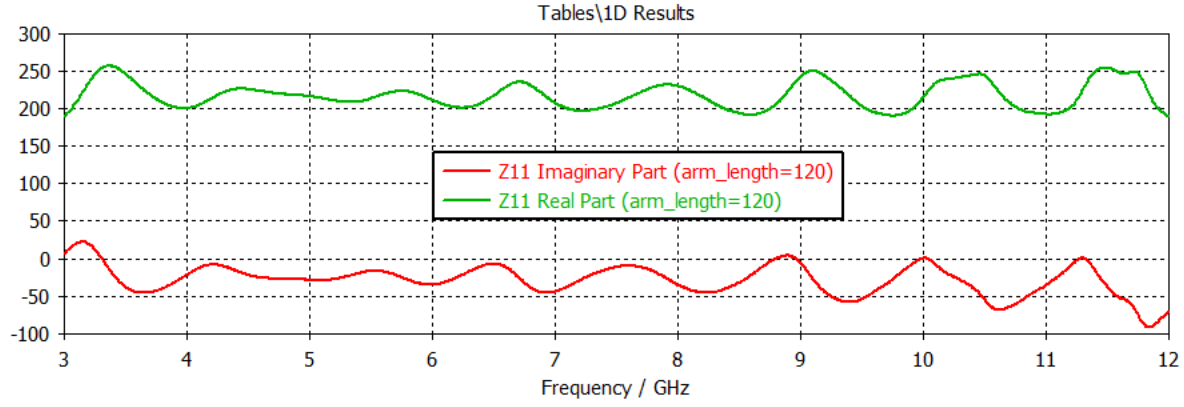

c)

Figure 8.18: a) The Return Loss b) VSWR and c) Impedance of the beveled edge rounded bowtie antenna when the arm length is 120 mm

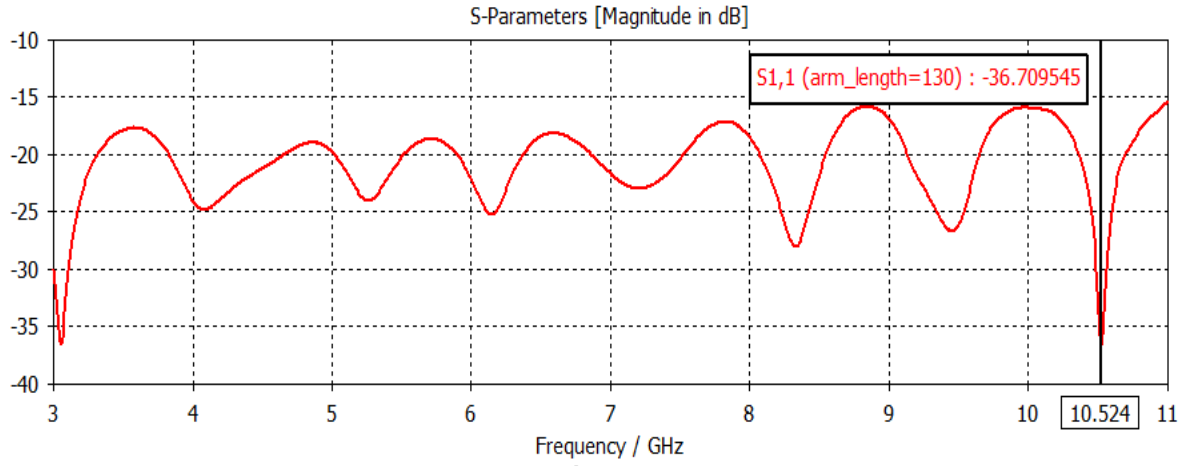

a)

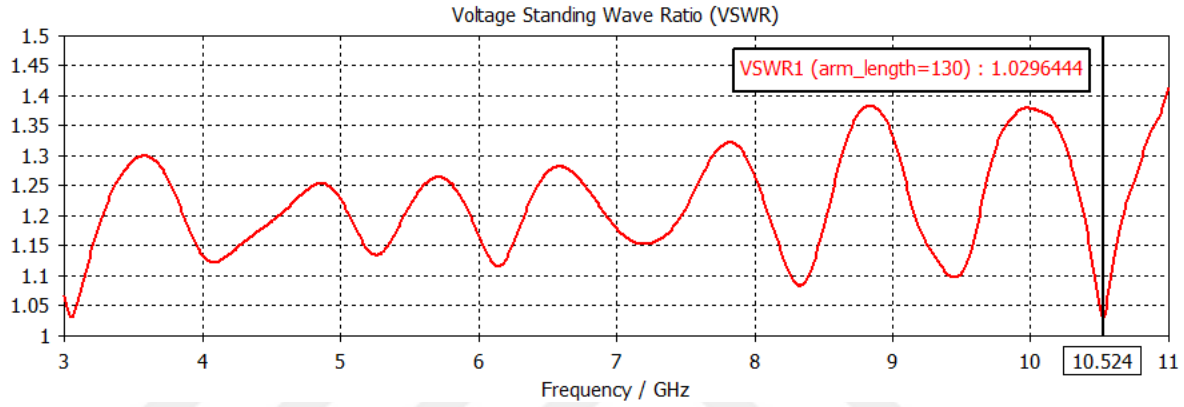

b)

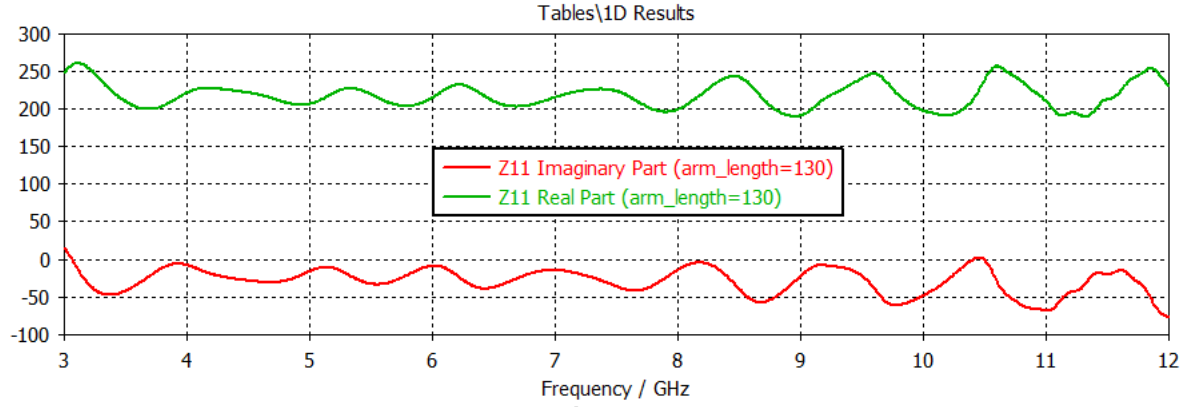

c)

Figure 8.19: a) The Return Loss b) VSWR and c) Impedance of the beveled edge rounded bowtie antenna when the arm length is 130 mm

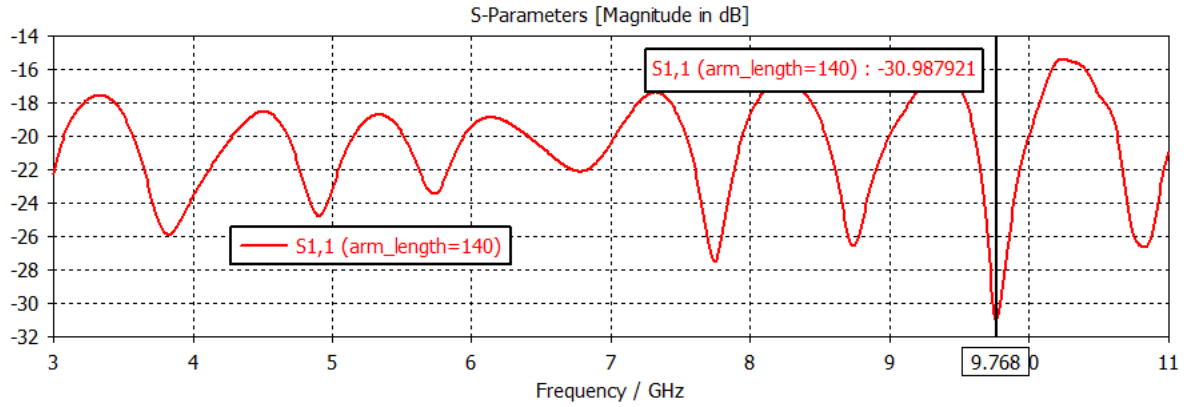

a)

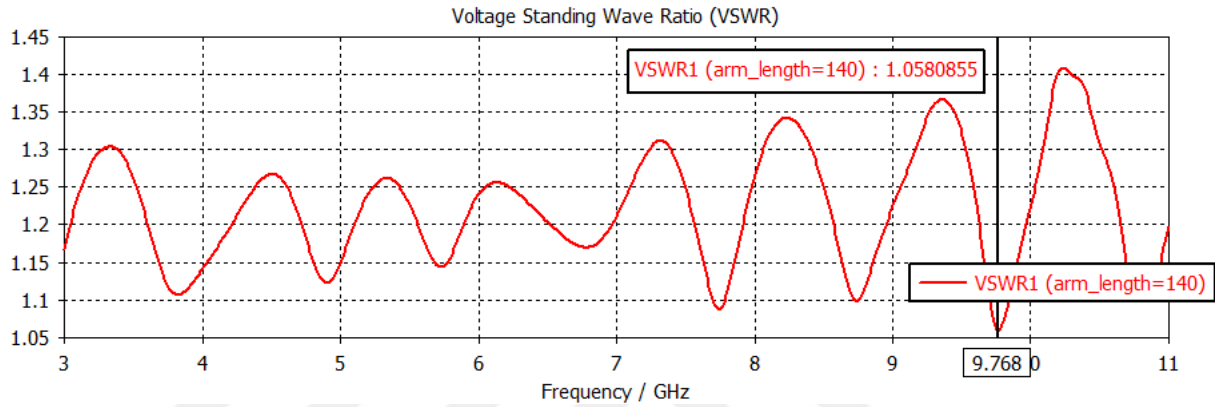

b)

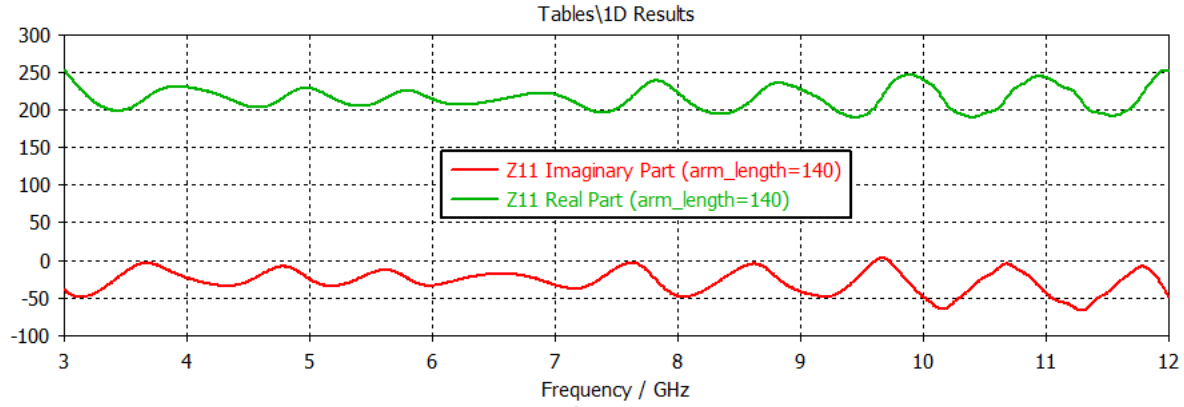

c)

Figure 8.20: a) The Return Loss b) VSWR and c) Impedance of the beveled edge rounded bowtie antenna when the arm length is 140 mm

Arm length is swept from 50 to 130 mm with an increment of 10 mm, 15 mm and 20 mm as tabulated in Table 8.3. Each antenna prototype is simulated with respect to the frequency in order to analyze antenna parameters including VSWR, S_{11} and Bandwidth. Figures from 8.14-to 8.20 illustrate radiation characteristics for the beveled edge rounded bowtie antenna with lengths 50, 70, 85, 100, 110, 120, 130, and 140 mm, respectively. Additionally, the data yielded by these figures are reported in Table 8.3. The proposed antenna's arm length of 85 and 110 mm provides convincing evidence that the antenna parameters are enhanced and complied with the FCC regulations & UWB requirements.

The beveled edge rounded bowtie antenna with 85 mm arm length has the lowest VSWR, the best return loss and the largest bandwidth which is acceptable for UWB applications.

Table 8.3: Beveled edge rounded bowtie antenna with different arm lengths over UWB frequency range (3-11 GHz)

Arm Length	VSWR	S_{11}	Bandwidth	Resonance Frequency
50 mm	1.0833	-27.958 dB	8 GHz (3-11 GHz)	4.098 GHz
70 mm	1.0143	-42.964 dB	8 GHz (3-11 GHz)	9.057 GHz
85 mm	1.0044	-53.034 dB	8 GHz (3-11 GHz)	9.273 GHz
100 mm	1.0258	-37.889 dB	8 GHz (3-11 GHz)	3.954 GHz
110 mm	1.0078	-48.1972 dB	8 GHz (3-11 GHz)	3.594 GHz
120 mm	1.0147	-42.7293 dB	8 GHz (3-11 GHz)	3.306 GHz
130 mm	1.0296	-36.709 dB	8 GHz (3-11 GHz)	10.524 GHz
140 mm	1.0582	-30.9879 dB	8 GHz (3-11 GHz)	9.768 GHz

9. MICROSTRIP ANTENNA

Microstrip antennas are commonly used structures for different application areas including microwave imaging, ground penetrating radar, UWB communication, handheld communication systems, remote sensing, radio frequency identification(RFID), global positioning system (GPS) applications, wireless application namely WiBro-WLAN; telemedicine application, RF energy harvesting due to its low profile, low cost, easy fabrication and mechanically robust etc. (Goudah and Yosef, 2012; Punitharaj and Kalamimani, 2013; Ghassemi et al, 2008; Shrestha, 2013; Agarwal et al, 2013; Kaushal and Tyagi, 2015). However, these types of antennas are lack of gain and impedance bandwidth. Various requirements must be taken into consideration such as physical structure, impedance matching, radiation pattern characteristics and efficiency of the antenna due to these drawbacks. Therefore, numerous types of microstrip antennas are designed and investigated in order to meet demand of the systems and improve the antenna parameters, namely, return loss, VSWR, radiation pattern and bandwidth (Fereidoony et al, 2012; Bugaj et al).

Microstrip antenna consists of radiating patch, dielectric substrate and ground plane. Radiating patch takes several different forms such as elliptic, square (Saidulu et al), circular (Prasad et al), rectangular (Prasad et al; Bernard and Izuchukwullah, 2013), circular ring, triangular (Johari et al), star shaped (Nasr et al, 2013) and semi-circle which vary with the system restrictions as shown in Figure 9.1. For instance, conventional microstrip antenna has narrower bandwidth than the circular or elliptical microstrip patch antenna (Ghassemi et al, 2008; Prasad et al). While choosing the effective patch shape, different techniques are utilized in order to obtain the best structures. Additionally, another crucial technique is also applied for feeding the antenna. In most recent studies, the antenna has been fed in four different ways, which determine the performance of the proposed antenna, including coaxial cable, microstrip line, aperture coupled feed and proximity coupled feed (Bernard and Izuchukwullah, 2013; Balanis, 2005). Furthermore, there are also several methods for analysing microstrip patch antenna e.g. transmission line model, cavity model and methods of moment (Bernard and Izuchukwullah, 2013; Banerjee and Bezboruah, 2015; Türker et al, 2007; Newman and Tulyathan, 1981; Karan and Ertürk, 2014). Three of the analysis methods are applied by using simulation programmes such as HFSS, CST MWS (CST, 2008) and COMSOL Multiphysics Modelling etc. as to analyse each antenna parameter. There is slight difference among the analysis techniques. Transmission Line Model is less accurate, less complicated than Cavity Model and lack of versatility. Moreover, the moment method is developed in order

to enhance the single antenna elements, finite/infinite arrays and arbitrary shaped patches, analyse the coupling effect of the antenna (Türker et al, 2007). In general, the moment method is the most accurate and the most versatile (Choukiker, 2009).

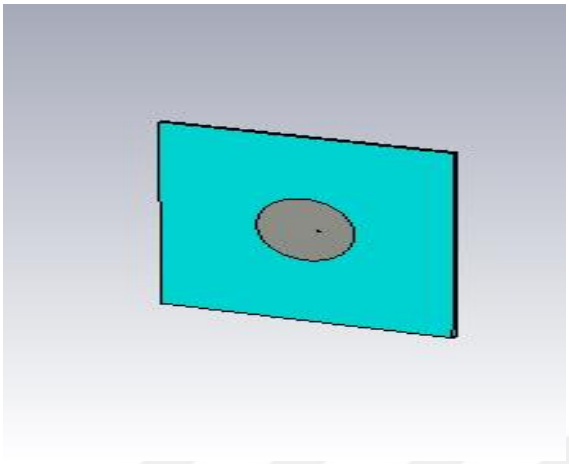

a)Circular Microstrip patch Antenna

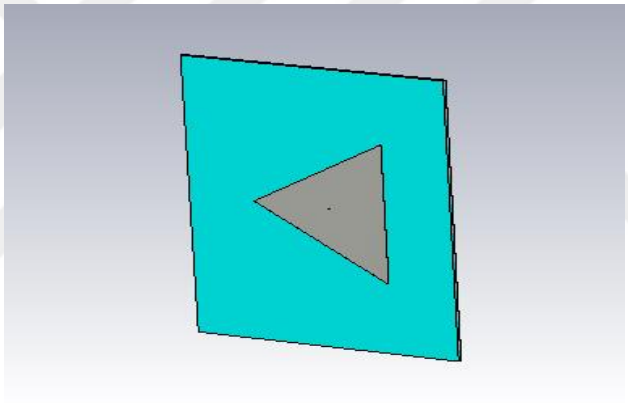

b)Triangular Pin Fed Patch Antenna

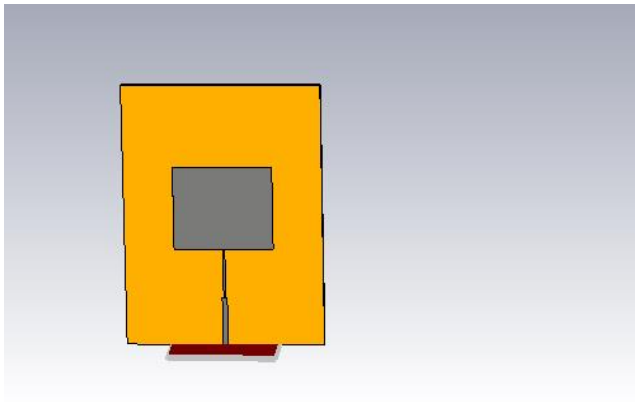

c)Rectangular Patch Microstrip Antenna

Figure 9.1: Different Microstrip Antenna Configurations a)Circular Patch Microstrip Antenna b)Triangular Pin Fed Patch Antenna c)Rectangular Patch Microstrip Antenna (CST, 2016)

There are essential physical parameters for microstrip antenna as to simulate and analyse the parameters. These parameters consist of the width of patch (W), the length of

patch (L), the width of the ground plane and substrate, the length of the ground plane and substrate, operating frequency (f_o), dielectric constant of substrate (ε_r), the thickness of dielectric substrate (H) and the thickness of conductor (t) as shown in Figure 9.2 and Figure 9.3. Table 9.1 illustrates the detailed antenna physical parameters' labels.

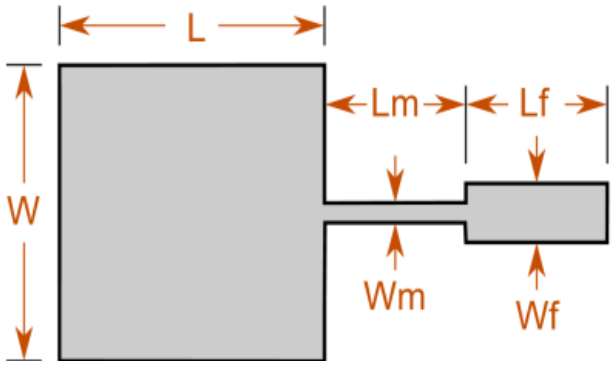

Figure 9.2: Microstip Antenna's physical parameters' labels from a) top view(Antenna Magus, 2016)

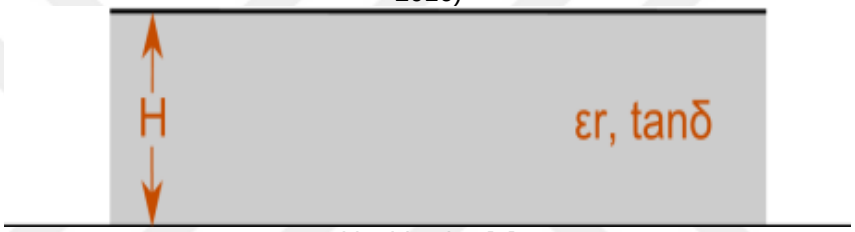

b) Side view[1]

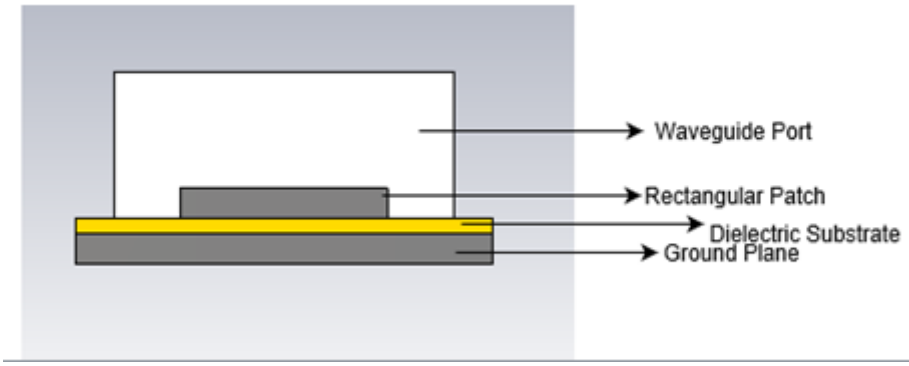

Figure 9.3: Front view of the microstrip antenna (Antenna Magus, 2016)

Table 9.1: Detailed Antenna Physical Parameters

Frequency centre	f_o
Patch Length	L
Patch Width	W
Matching Line Width	Wm
Matching Line Length	Lm
Feed Line Width	Wf
Feed Line Length	Lf
Substrate Thickness	H
Relative Permittivity	ε_r
Tan Delta	$\tan\delta$

9.1. TRANSMISSION LINE METHOD

A conducting strip is connected directly to the edge of microstrip patch (Bisht et al, 2014). This method has some merits and drawbacks depending on the application areas. The layout where the feed can be inserted into same substrate in order to provide sufficient structure, such as planar etc., is one of the advantages of the transmission line method (Choukiker, 2009) whereas fringing effect is the drawback of the transmission line model. Electromagnetic wave travels in non-homogenous medium because of the fringing field which is occurred by the fields at the edges of the patch. The amount of the fringing depends on the patch dimensions and thickness of the substrate. An effective dielectric constant (ε_{eff}) ought to be considered in case of fringing condition. The effective value of the dielectric constant (ε_{eff}) ranges from 1 to ε_r. Moreover, the value of the effective dielectric constant also depends on the frequency. The initial value of the effective dielectric constant is given as follows where W/h >1(Balanis, 2005):

$$\varepsilon_{eff} = \frac{(\varepsilon_r + 1)}{2} + \frac{(\varepsilon_r - 1)}{2\sqrt{1+12h/W}} \tag{9.1}$$

The extension of the length is introduced, i.e. electrically patch of the microstrip antenna looks greater than its physical dimensions. This extension is based on the width to height ratio (W/h) and the effective dielectric constant (ε_{eff}) as given in below:

$$\frac{\Delta L}{h} = 0.421 * \frac{\left((\varepsilon_{\text{eff}} + 0.3)(\frac{\text{W}}{\text{h}} + 0.264) \right)}{\left((\varepsilon_{\text{eff}} - 0.258)(\frac{\text{W}}{\text{h}} + 0.8) \right)} \quad (9.2)$$

The effective length of the patch due to fringing effect becomes as follows:

$$L_{eff} = L + 2\Delta L \quad (9.3)$$

9.1.1. Design Procedure:

- ✓ Specify the ε_{r}, operating frequency (f_{o}), and h.
- ✓ Determine the width of the patch by using below equation (9.4), ε_{r}, f_{o}, c and h where c is speed of the light
- ✓ Calculate the ε_{eff} by using Equation (9.1) and W
- ✓ Finally , calculate the actual length of the patch using below equation (9.5) (Yadav and Pahwa, 2014)

$$\text{W} = \frac{\text{c}}{2\,\text{f}_{o}\sqrt{\frac{(\varepsilon_{\text{r}} + 1)}{2}}} \quad (9.4)$$

$$\text{L} = \frac{\text{c}}{2\,\text{f}_{o}\sqrt{\varepsilon_{\text{eff}}}} - 2\Delta L \quad (9.5)$$

9.2. RECTANGULAR EDGE-FED PATCH ANTENNA

In this section, rectangular edge fed patch antenna is investigated and analysed with respect to antenna parameters including return loss, VSWR, radiation pattern and impedance of the antenna via CST MWS. The input signal of Gaussian pulse as shown in Figure 9.4 is used in order to compare time and frequency domain compatibility. Excitation of the proposed antenna is made through the waveguide port as shown in Figure 9.5. Different views of the proposed antenna are obtained via CST MWS as illustrated in Figures 9.6 (a-c). The physical parameters of the proposed antenna are definitely represented in Table 9.2. The proposed antenna is designed in accordance with Table 9.2 in order to have better results after some estimation. Another key point to consider is that mesh property is adjusted as Hexahedral TLM in favour of theoretical calculations.

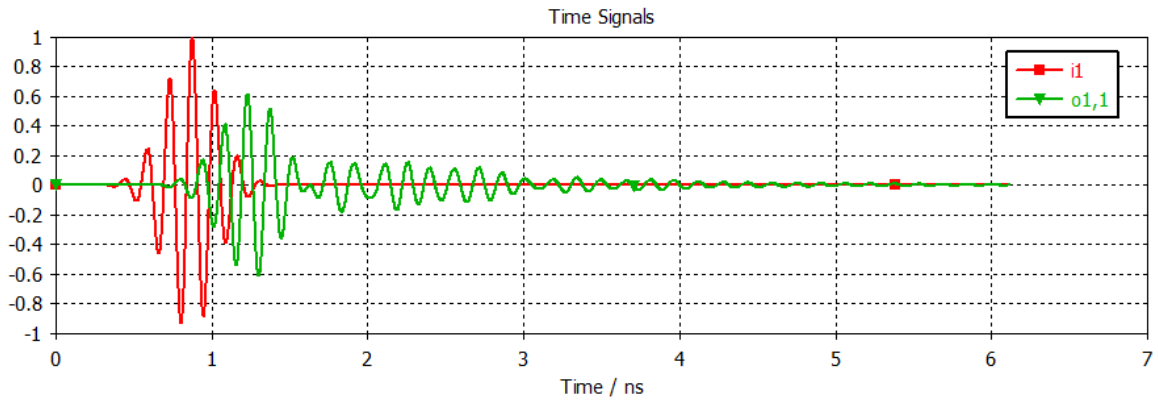

Figure 9.4: The Excitation Signal for input and output ports

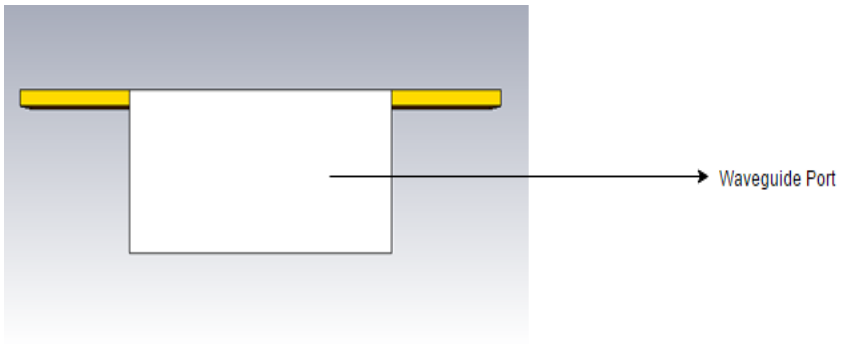

Figure 9.5: Waveguide Representation of the proposed antenna

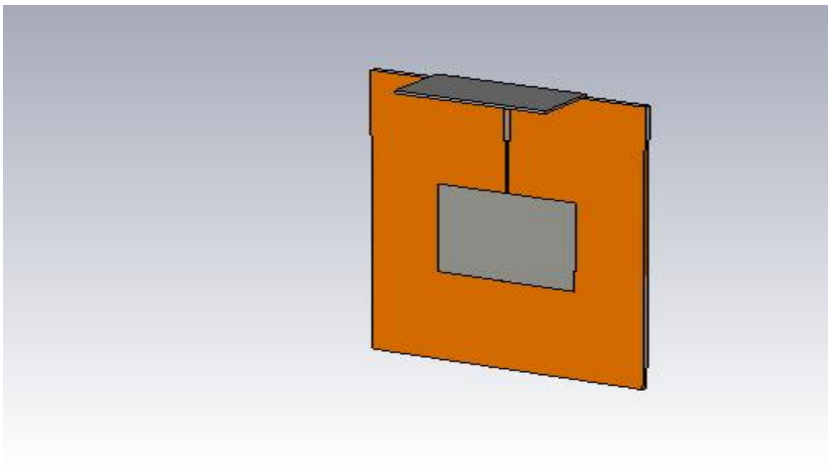

a) Perspective View of the proposed antenna

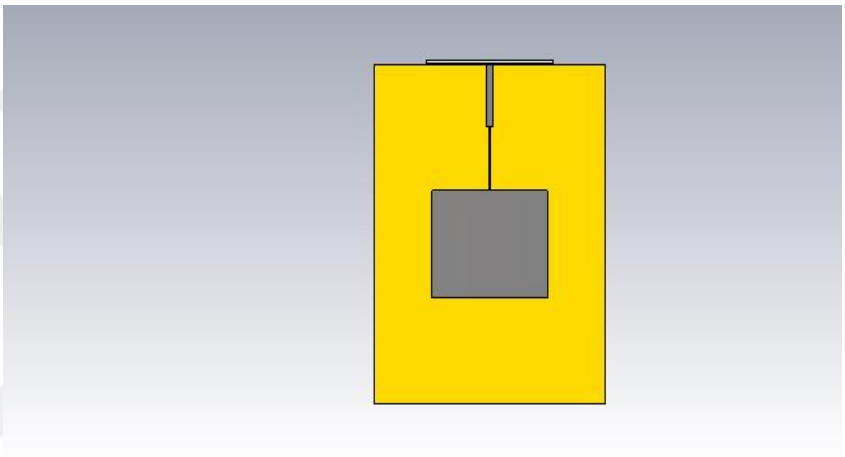

b) Front View of the proposed antenna

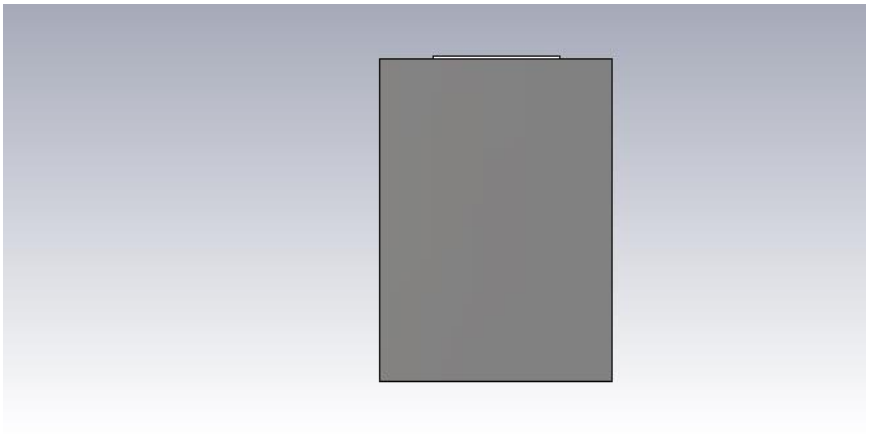

c) Back View of the proposed antenna

Figure 9.6: Different views of the proposed antenna obtained by CST MWS a) Perspective View b) Front View c) Back View

Table 9.2: The Rectangular Patch Microstip Proposed Antenna: Detailed Physical Parameters

Parameters	Values	Units
c	$3x10^8$	m/sec
Tan Delta	0	-
Matching Line Width	0.99	mm
Relative Permittivity	2	-
Feed Line Width	2.5269	mm
Substrate Thickness	2.6	mm
f_{center}	6.85	GHz
Ground Plane Feed Extension	7.162	mm
Feed Line Length	23.91	mm
Matching Line Length	24.28	mm
Patch Length	41.03	mm
Patch Width	49.95	mm
Ground Plane Width	99.91	mm
Ground Plane Length	123.078	mm
Metal Thickness	0.044	mm

9.2.1. SIMULATION & RESULTS

In this section, antenna parameters including return loss, group delay, radiation pattern, VSWR and efficiency are pointed out. The bandwidth can be evaluated by using return loss and VSWR of the proposed antenna. Thus, Return Loss and VSWR characteristics are illustrated in Figures 9.7 and 9.9. Figure 9.7 depicts return loss characteristic of the proposed antenna. Likewise, Figure 8 outlines the bandwidth by using measure lines via CST MWS. The resonant frequencies can also be determined in Figure 9.8.

It can be observed from the figures that two resonance frequencies occur and the proposed antenna shows dual band characteristics. As shown in Figure 9.8(a), the first resonance frequency is at 6.4365 GHz and -10 dB bandwidth of 100 MHz ranges from 6.3893 to 6.4898 GHz. Likewise, Figure 9.8 (b) depicts that second resonance frequency of the proposed antenna occurs at 8.4443 GHz and -10 dB bandwidth of 250 MHz ranges from 8.3441 to 8.5981 GHz. However, these two bandwidths are narrow for UWB applications. Adjunctly, the first resonance is at 6.4365 GHz with corresponding return

loss as -15.622 dB and the second resonance is at 8.4443 GHz with corresponding return loss as – 36.455 dB. In other words, corresponding return loss is -15.622 dB at the first resonance and – 36.455 dB at the second resonance.

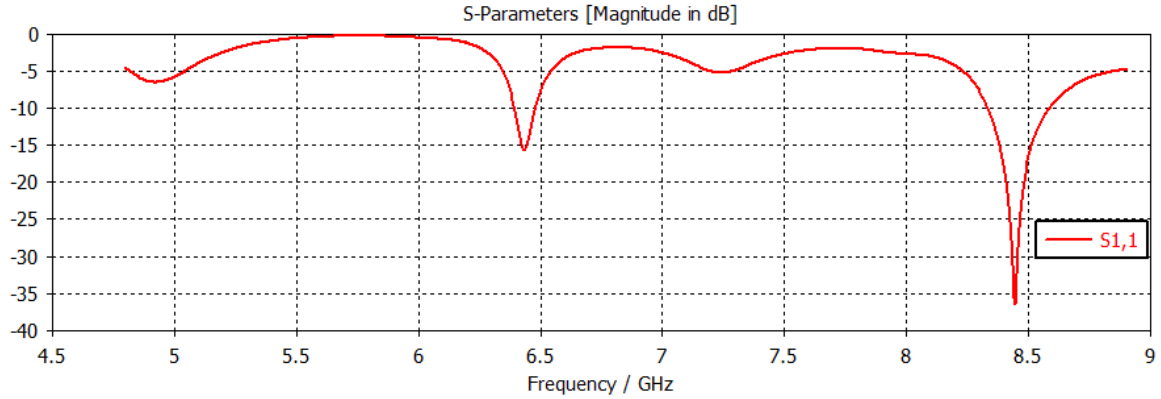

Figure 9.7: Return Loss Characteristic of the proposed rectangular patch microstrip antenna

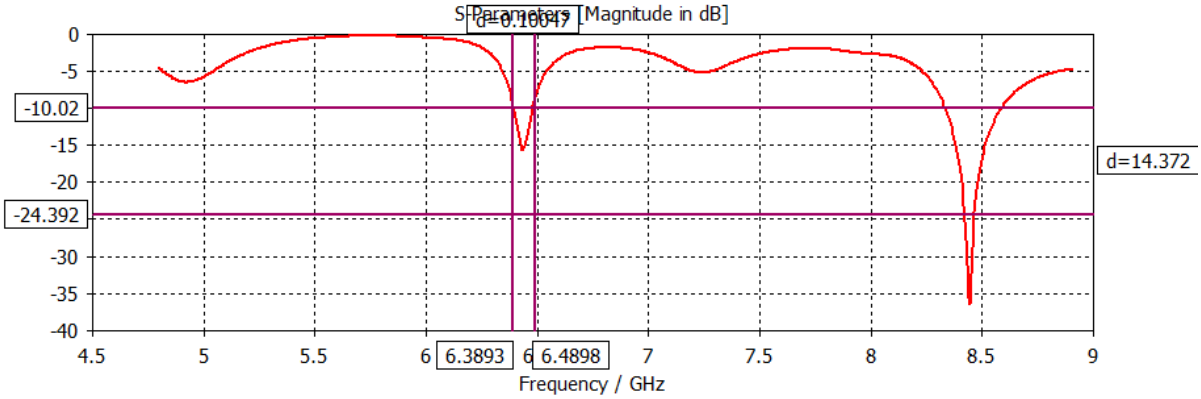

a)

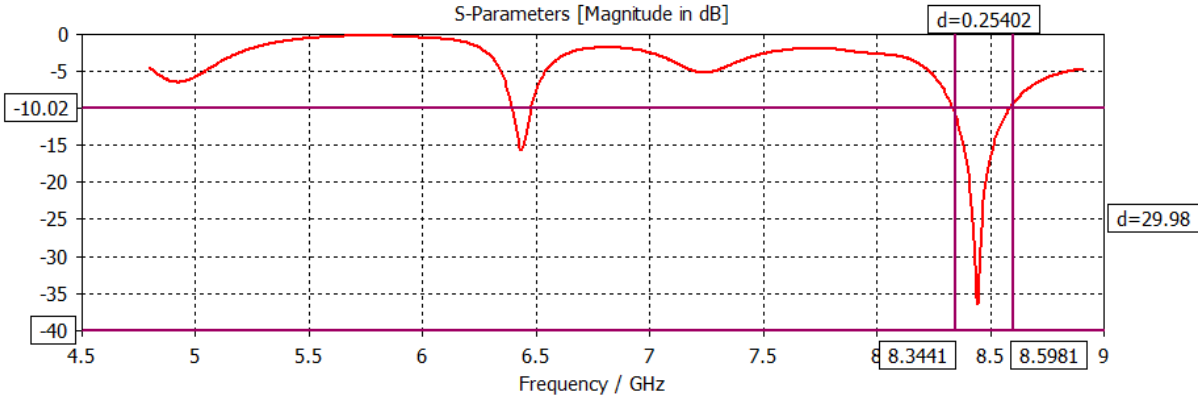

b)

Figure 9.8: Return Loss Characteristic of the proposed rectangular patch microstrip antenna with measure lines a) at first resonance b) at second resonance

Figures 9.9 and 9.10 illustrate VSWR characteristics of the proposed antenna. Figure 9.10 clearly depicts bandwidth of the proposed antenna in accordance with return loss characteristic as shown in Figures 9.8(a-b). The minimum VSWR occurs at second resonance frequency of 8.4443 GHz and is 1.03 which is almost unity. Figure 9.11 shows impedance characteristic of the proposed antenna including real (green) and imaginary parts (red). Imaginary part is almost zero over entire frequency band but there are some peak values which are not desired for perfectly match condition and causes power dissipation due to reactive power.

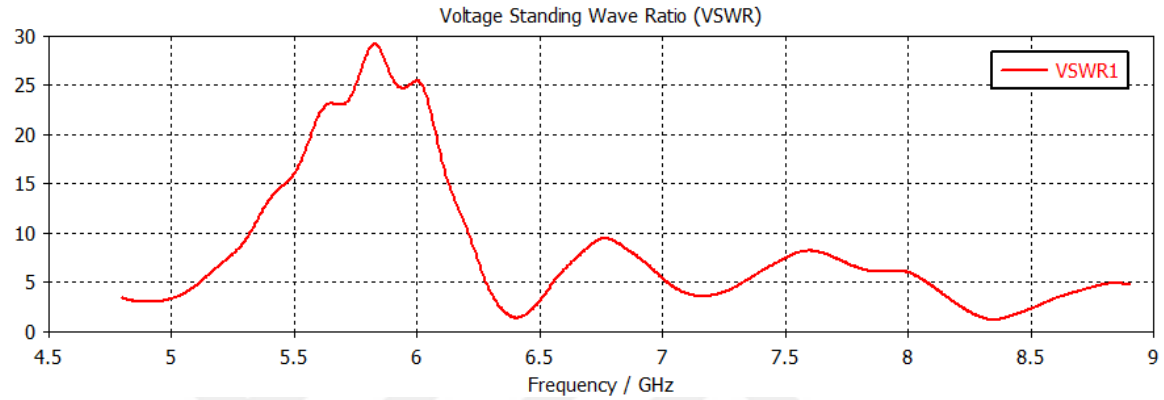

Figure 9.9: VSWR Characteristic of the proposed rectangular patch microstrip antenna

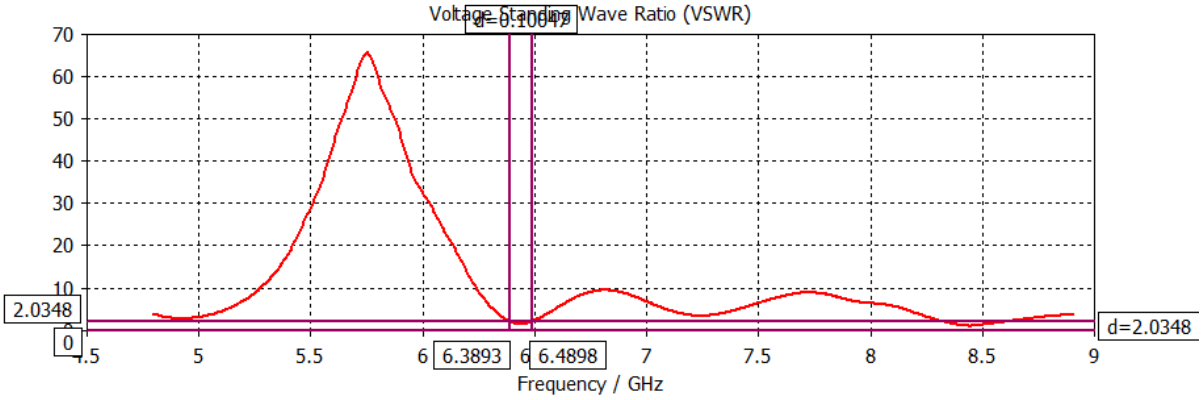

a)

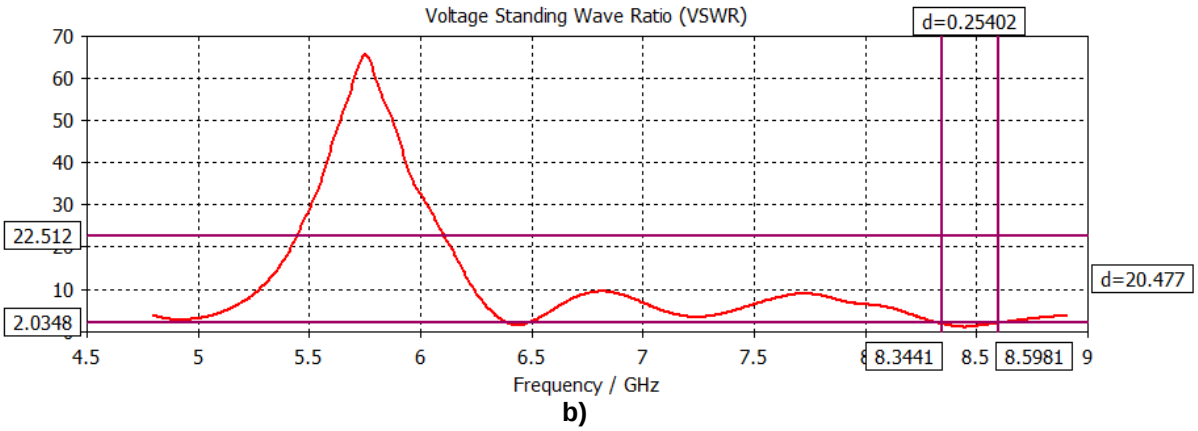

b)

Figure 9.10: VSWR Characteristic of the proposed rectangular patch microstrip antenna with measure lines a) at first resonance b) at second resonance

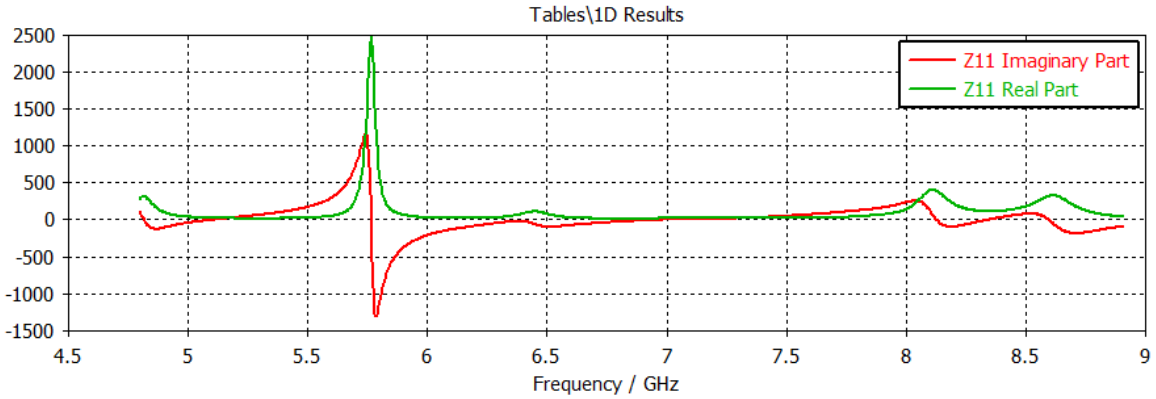

Figure 9.11: The impedance characteristic of the proposed antenna

Another significant parameter to analyse time domain characteristic of the proposed antenna is group delay. Group delay outlines not only phase information which is related with frequency but also non-dispersive characteristic of the proposed antenna (Mazhar et al, 2013). This parameter is illustrated in Figure 9.12 in order to define the antenna's time domain property and observe linear phase response i.e. constant group delay. Sharp fluctuations of group delay which are not negligible at the resonance frequencies are detected inasmuch as they break down the constant group delay requirements(Peng and Ruan, 2013).

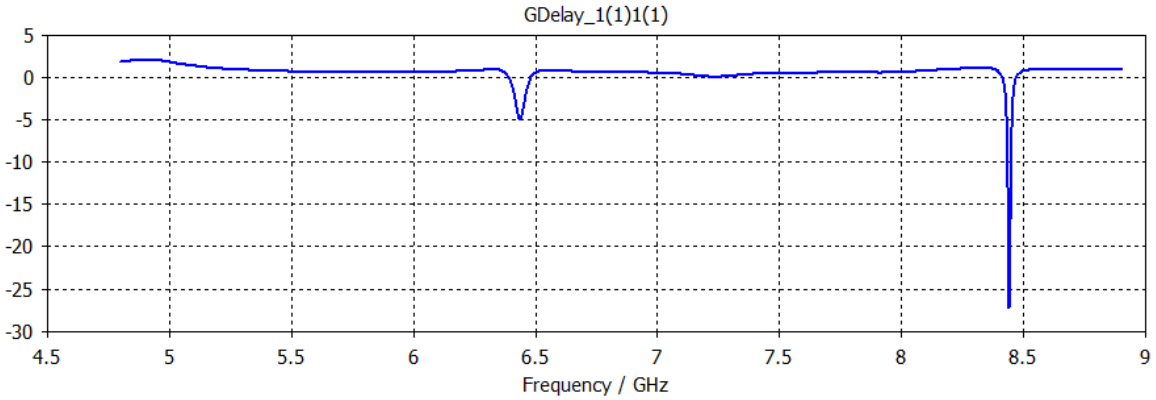

Figure 9.12: The group delay of the proposed antenna

Figure 9.13 illustrates the simulated radiation patterns for the proposed antenna when ϕ=90^o at three frequencies 6.165, 6.85 and 7.535 GHz respectively. The angular widths (3 dB) are 30.5^o , 36.4^o and 25.8^o with respect to three frequencies. The main lobe magnitude occurs at 6.165 GHz as given in Figure 9.13. Three of the radiation patterns are directional in the broadside directions. Additionally, minor lobes are observed by examinig each radiation pattern. Main lobe direction varies with respect to operating frequency as well. In conclusion, these type of radiation patterns are acceptable for some applications namely wireless commnications, GSM, WLAN and GPS etc. However they are not applicable for entire UWB frequency range applications because of antenna's

narrow bandwidth, directional radiation pattern which do not meet UWB application requirements.

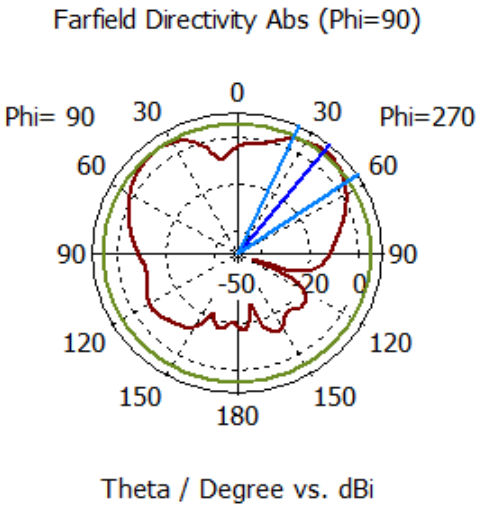

Frequency = 6.165
Main lobe magnitude = 6.62 dBi
Main lobe direction = 39.0 deg.
Angular width (3 dB) = 30.5 deg.
Side lobe level = -1.2 dB

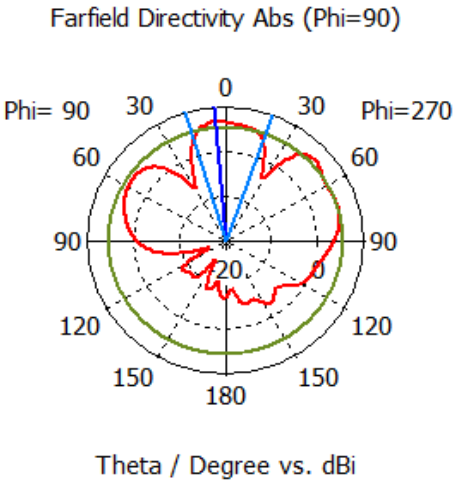

Frequency = 6.85
Main lobe magnitude = 6.84 dBi
Main lobe direction = 5.0 deg.
Angular width (3 dB) = 36.4 deg.
Side lobe level = -1.4 dB

b)

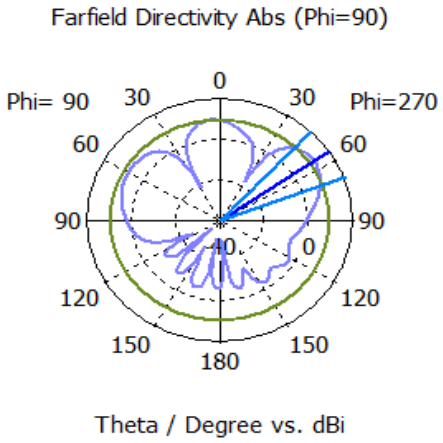

Frequency = 7.535
Main lobe magnitude = 11.3 dBi
Main lobe direction = 55.0 deg.
Angular width (3 dB) = 25.8 deg.
Side lobe level = -1.8 dB

c)

Figure 9.13: Radiation Pattern of proposed antenna at different frequencies a) 6.165 GHz b) 6.85 GHz and c) 7.535 GHz respectively

9.3. ELLIPTIC MICROSTRIP PATCH ANTENNA

In this section, the purpose of design the elliptic microstrip patch antenna is to provide better bandwidth. Additionally, antenna parameters are improved so as to compare the rectangular patch microstrip antenna which has been examined in previous section. Rectangular patch microstrip antenna has narrow bandwidth which does not meet UWB requirements and restriction of FCC. That's why another way to design is considered by changing the patch shape of the proposed antenna. Initially, the dimensions are chosen the same in order to observe merits and demerits of rectangular patch microstrip antenna.

Patch dimensions, namely patch width (W) and patch length (L) are calculated by using the transmission line model's characteristics equation which is given in previous section via Equation (8.4). Patch width, patch length and other crucial parameters are obtained in the following equations and all physical parameters of proposed antenna are tabulated in Table 9.3:

1) $$W = \frac{c}{2 f_o \sqrt{\frac{(\varepsilon_r + 1)}{2}}} = \frac{3x10^8}{2(6.85x10^9)\sqrt{\frac{3}{2}}} = 0.0179 \text{ m} = 17.9 \text{ mm} \cong 20mm$$

2) $$\varepsilon_{eff} = \frac{(\varepsilon_r + 1)}{2} + \frac{(\varepsilon_r - 1)}{2\sqrt{1 + 12h/W}} = \frac{(2+1)}{2} + \frac{(2-1)}{2\sqrt{1+12*1.5/20}} = 1.862$$

Where ε_r =2, h= 1.5 mm and W= 20 mm.

3) $$\frac{\Delta L}{h} = 0.421 * \frac{\left((\varepsilon_{eff} + 0.3)(\frac{W}{h} + 0.264)\right)}{\left((\varepsilon_{eff} - 0.258)(\frac{W}{h} + 0.8)\right)} = \frac{(1.862 + 0.3)(\frac{20}{1.5} + 0.264)}{(1.862 - 0.258)(\frac{20}{1.5} + 0.8)} = 0.546 \text{ mm}$$

Finally, ΔL becomes 0.819 mm.

4) $$L_{eff} = L + 2\Delta L = 17.9 + 2(0.819) = 19.53 \, mm$$

Which is almost 20 mm and identical with patch width.

Table 9.3: Physical Parameters of the rectangular patch and elliptic microstrip patch antenna

Parameters	Rectangular Patch Microstrip Antenna	Elliptic Microstrip patch Antenna	Units
c	$3x10^8$	$3x10^8$	m/s
Feed Line Length	20	20	mm
Feed Line Width	2,7	2,7	mm
Frequency Centre	6,85	6,85	GHz
Groundplane Length	60	20	mm
Groundplane Width	40	40	mm
Metal Thickness	2,83	2,83	mm
Patch Length(L)	20	20	mm
Patch Width(W)	20	20	mm
Relative Permittivity(ε)	2	2	-
Substrate Thickness(H)	1,5	1,5	mm
Tan Delta(δ)	0	0	-
Wavelength	43,77	43,77	mm

Figure 9.14 depicts two proposed microstrip antennas with different patch shapes. Figure 9.14(a) illustrates the rectangular patch antenna of 60 mm ground plane length and elliptic microstrip patch antenna of 20 mm ground plane length. The main point is to emphasize ground plane length effect on the antenna parameters. Henceforth, the ground plane lengths are chosen different from each other as given in Table 9.3 in order to observe changes. The ground plane length is increased by 20 mm up to 60 mm as to compare with rectangular patch efficiently.

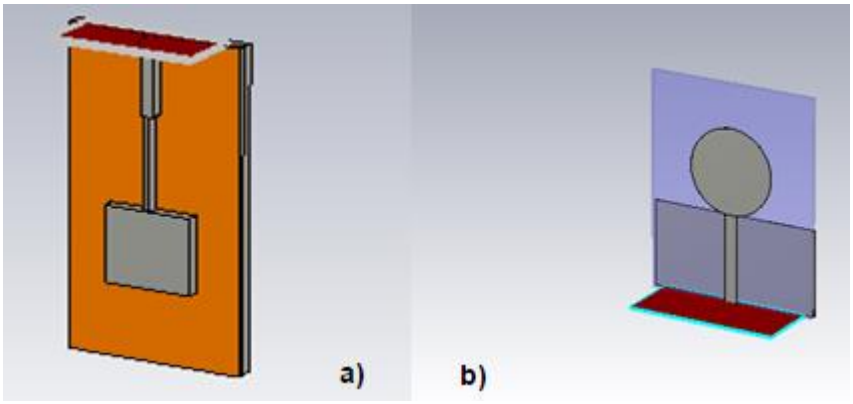

Figure 9.14: Perspective View of a) Rectangular Patch b) Elliptic Microstrip patch Antenna from CST MWS

9.3.1. SIMULATION & RESULTS

Figure 9.15 illustrates VSWR characteristics of the two proposed antennas with respect to the patch configurations. Rectangular patch antenna shows narrowband characteristic while elliptic microstrip patch antenna behaves as a broadband antenna characteristic but it does not still meet the entire UWB frequency range.

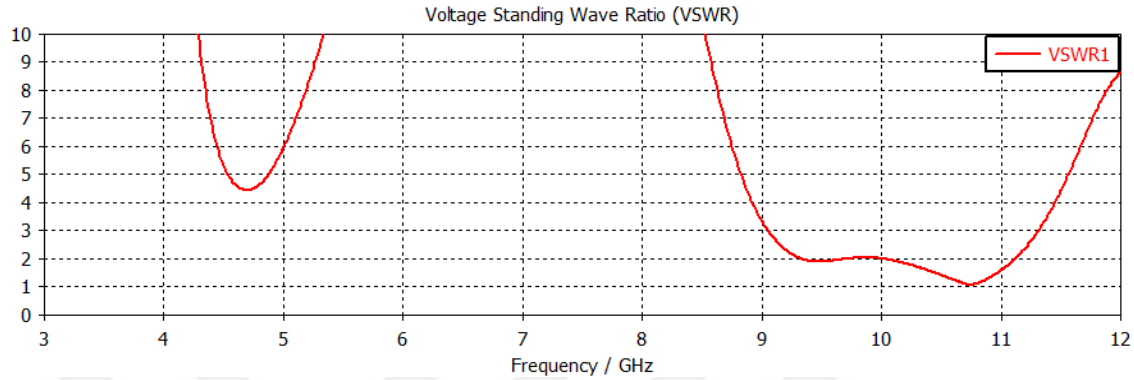

a) Rectangular patch microstrip antenna whence ground plane length is 60 mm

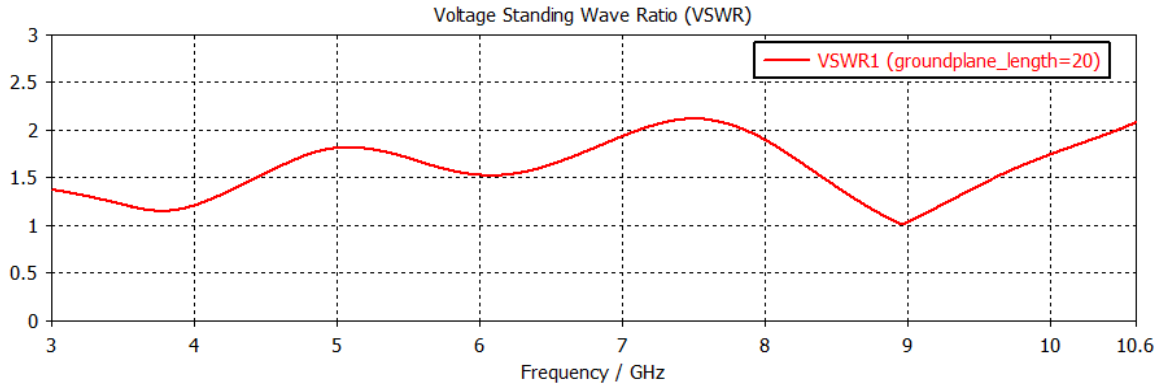

b) Elliptic microstrip patch antenna whence ground plane length is 20 mm

Figure 9.15: VSWR characteristic of the microstrip antenna a) rectangular patch b) elliptic patch when ground plane length is 20 mm

Figure 9.16 outlines return loss characteristics of the proposed antennas for rectangular patch in Figure 9.16(a) and elliptic patch in Figure 9.16(b). Additionally, Figures 9.17 and 9.18 illustrate the bandwidth characteristic of the two proposed antennas. As interpreted from Figure 9.17, the elliptic microstrip antenna has two -10 dB bandwidths of 4GHz which spans 3 GHz to 7GHz and of 2.4862 GHz which spans 7.99 GHz to 10.475 GHz. On the other hand, rectangular patch microstrip antenna has narrower bandwidth than elliptic microstrip patch antenna as shown in Figure 9.18. Actually, the bandwidth of the proposed rectangular patch antenna is enhanced by decreasing the ground plane length as compared to conventional antenna which is designed in the previous section and represented in Table 2. However, the impedance matching is still not perfect in order to deliver maximum power into the load. As a

conclusion, the rectangular patch microstrip antenna does not cover entire UWB frequencies yet.

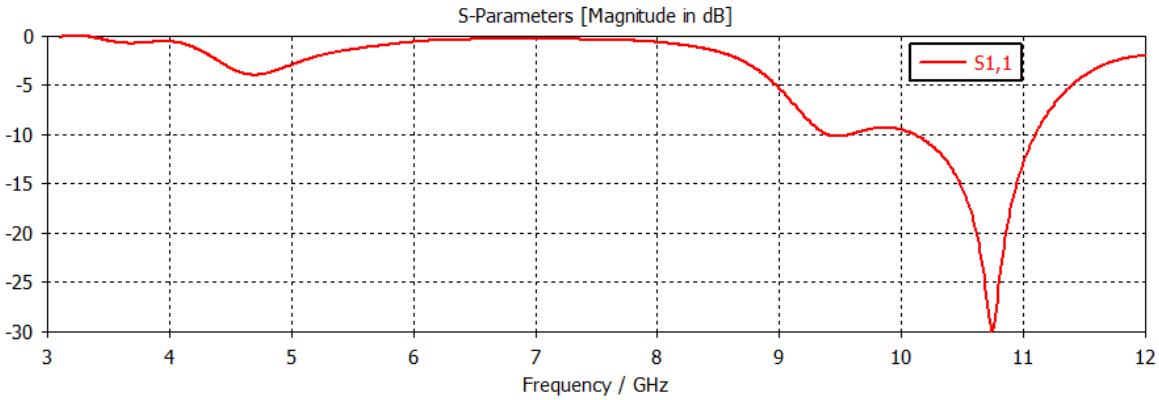

a) Rectangular patch microstrip antenna whence ground plane length is 60 mm

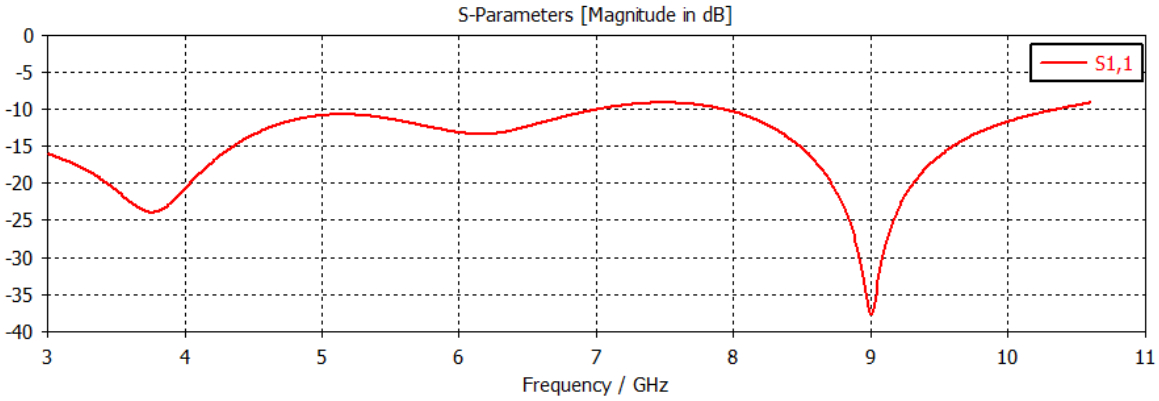

b) Elliptic microstrip patch antenna whence ground plane length is 20 mm

Figure 9.16: Return Loss characteristic of the microstrip antenna a) rectangular patch b) elliptic patch when ground plane length is 20 mm

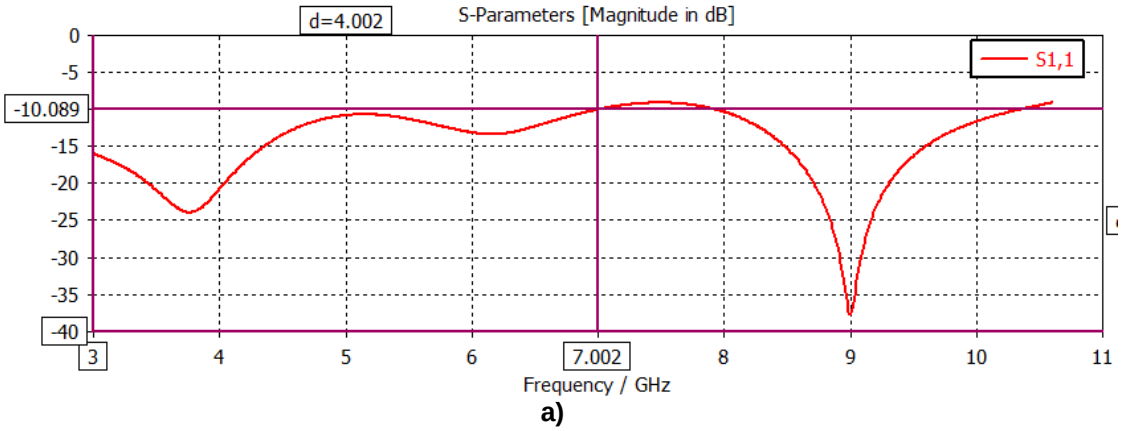

a)

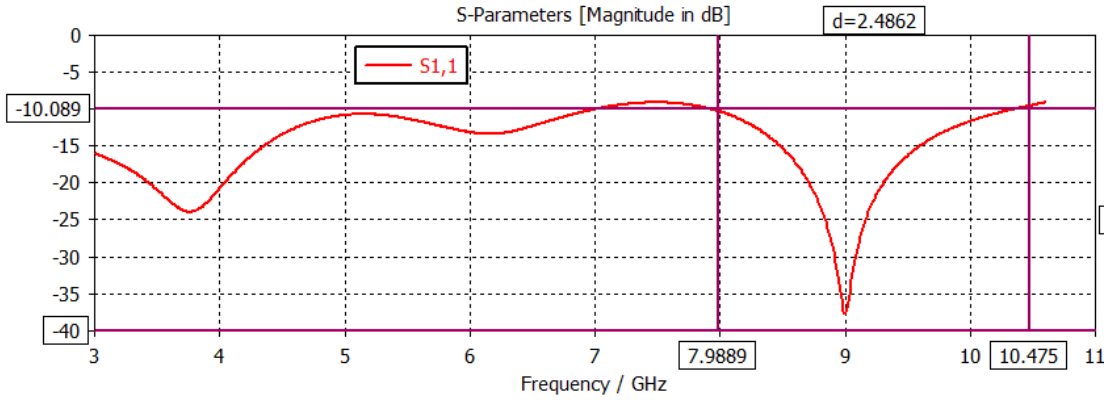

b)

Figure 9.17: Bandwidth characteristic of the proposed elliptic microstrip patch antenna

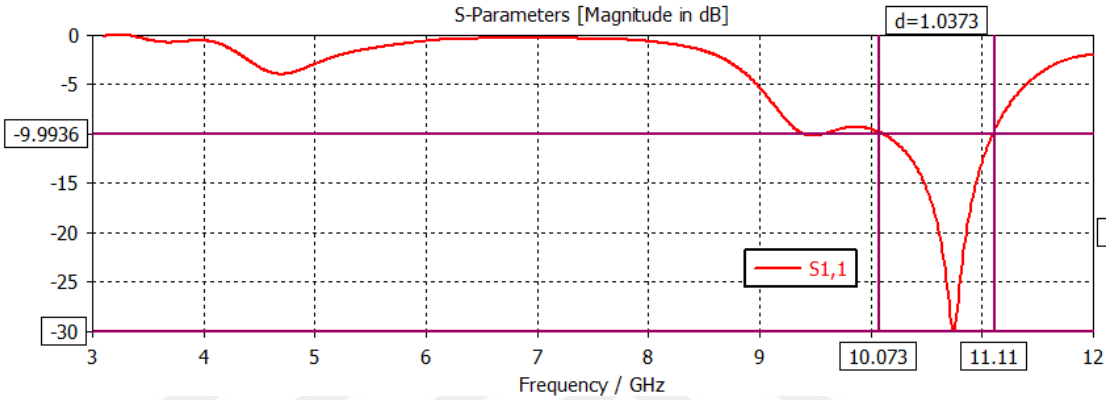

Figure 9.18: Bandwidth characteristic of the proposed rectangular patch microstrip antenna

9.3.1.1. Effect of the Ground Plane Length on Antenna Performance

In this section, only elliptic microstrip patch antenna will be improved through ground plane length. Figure 9.19 illustrates return loss characteristic of the proposed antenna with respect to various ground plane lengths. Initially, the ground plane is taken as 20 mm which is equal to patch length and then increased by 20 mm up to reach 60 mm so as to compare with the proposed rectangular patch antenna easily. There are some distortions in Figure 9.19(a) and Figure 9.19 (b) which reject signals from 7GHz to 8GHz. However, Figure 9.19(c) illustrates that the proposed antenna achieves wider impedance bandwidth as compared to Figure 9.19(a)-(b). Figure 9.20 also represents three values of ground plane length so that bandwidth improvement can be observed clearly.

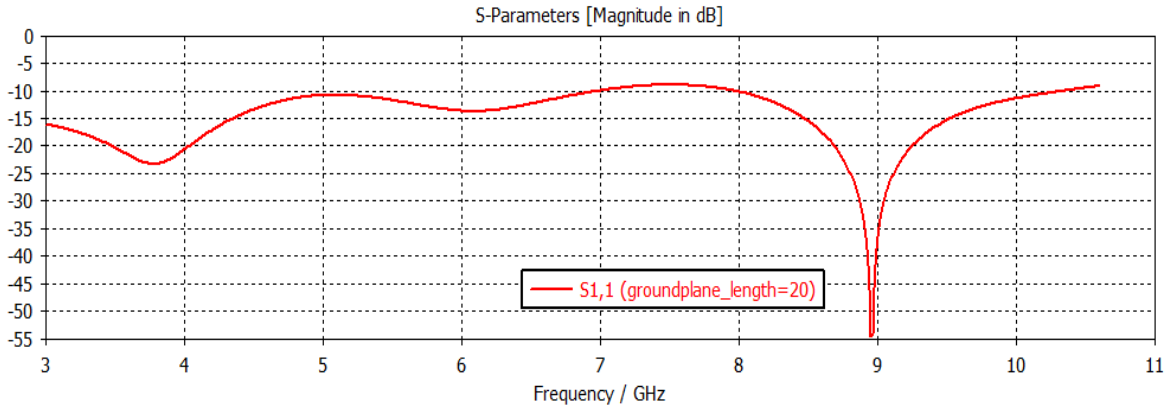

a) Return Loss characteristic of the proposed antenna with ground plane 20 mm

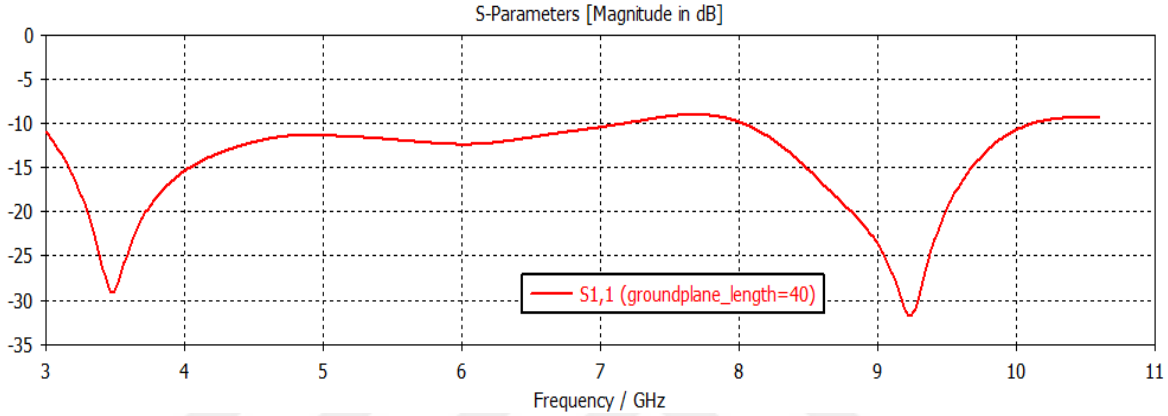

b) Return Loss characteristic of the proposed antenna with ground plane 40 mm

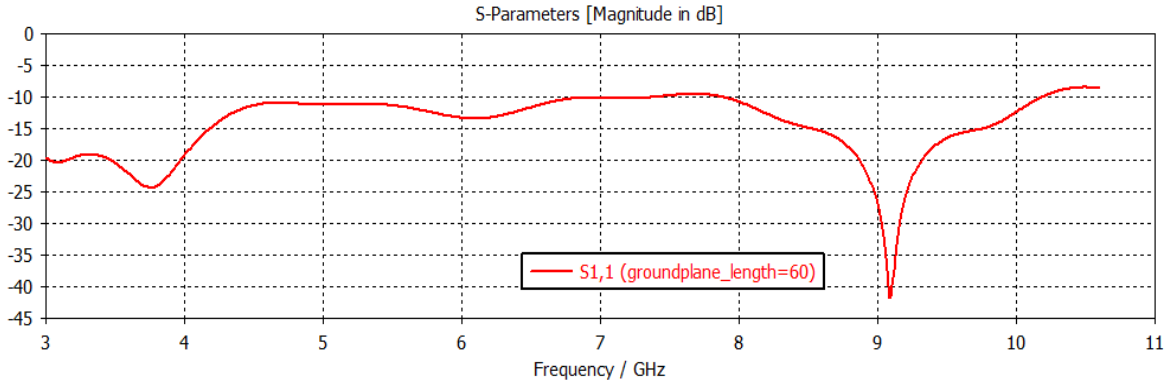

c) Return Loss characteristic of the proposed antenna with ground plane 60 mm

Figure 9.19: Various ground plane lengths effect on return loss parameter when a) 20mm b) 40mm c) 60mm, respectively

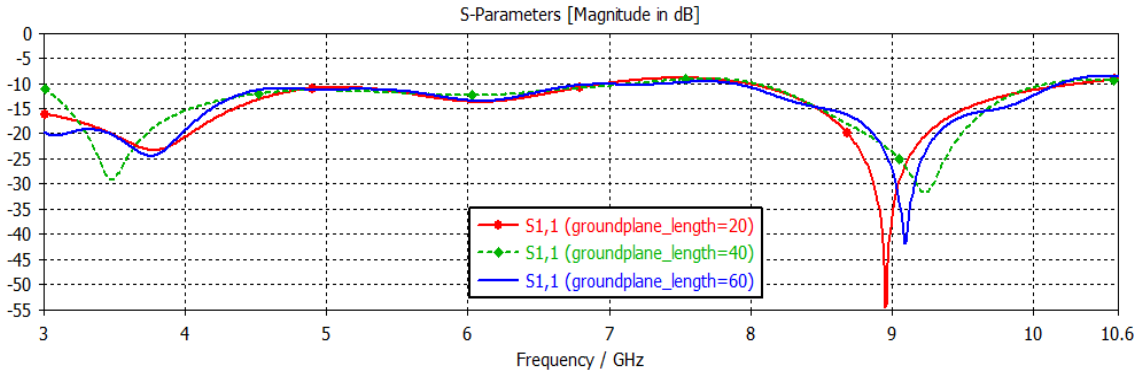

Figure 9.20: All figures plotted in Figure 19 a, b and c, respectively

VSWR characteristic as another crucial parameter is represented in Figure 9.21. When each VSWR characteristic is examined, proposed antenna radiates in the all UWB frequency range only when ground plane length is 60 mm in Figure 9.21(c). Furthermore, the proposed antenna with ground plane length 60mm delivers maximum power to the load or transmission line, i.e. perfectly match condition. To sum up, ground plane length essentially affects the return loss, impedance matching and bandwidth of the antenna. The simulated elliptic microstrip patch antenna indicates that the desired conditions over the entire UWB are achieved by reconfiguring the patch configuration and ground plane length. Table 9.4 outlines the final dimension values of the proposed elliptic patch antenna.

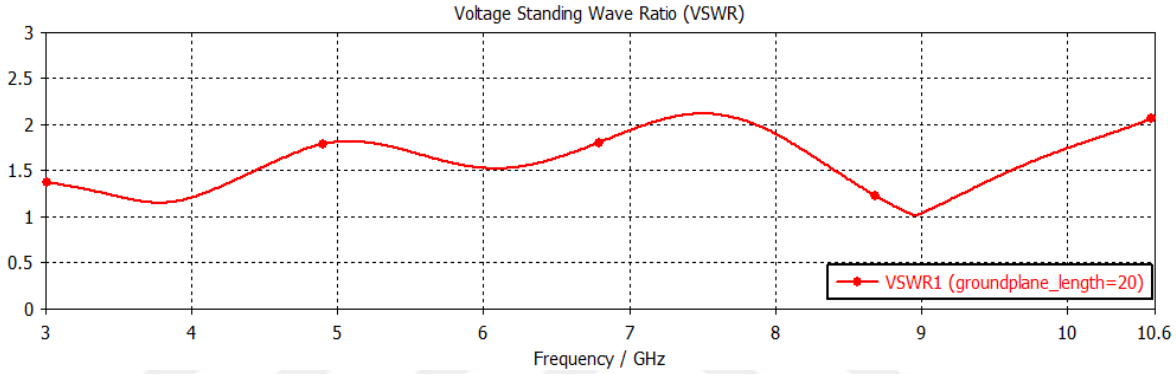

a) VSWR characteristic of the proposed antenna with ground plane 20 mm

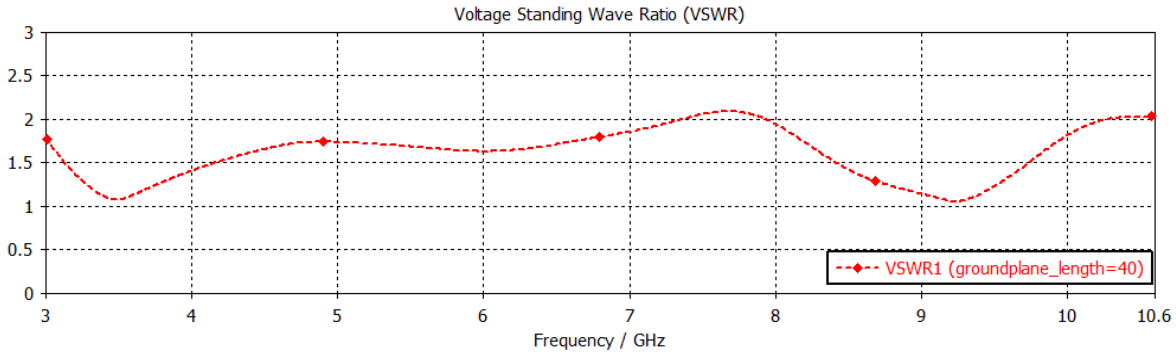

b) VSWR characteristic of the proposed antenna with ground plane 40 mm

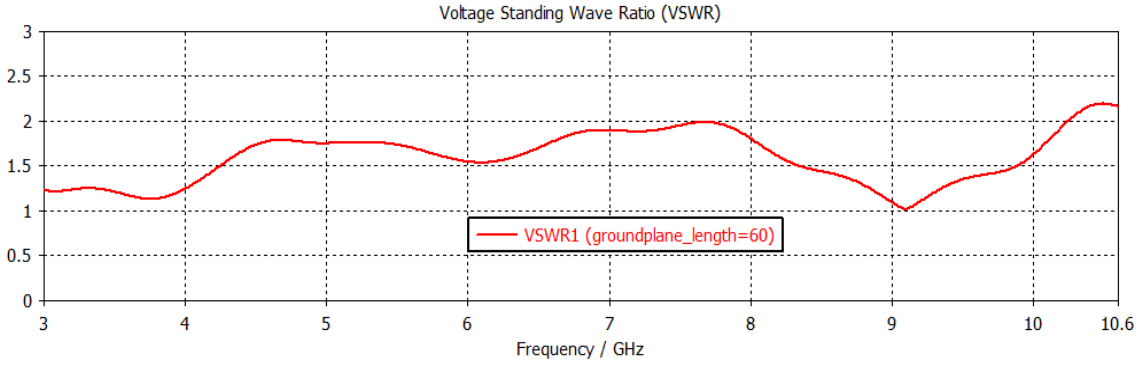

c) VSWR characteristic of the proposed antenna with ground plane 60 mm

Figure 9.21: VSWR characteristic when ground plane length is a) 20mm b) 40mm c) 60mm, respectively

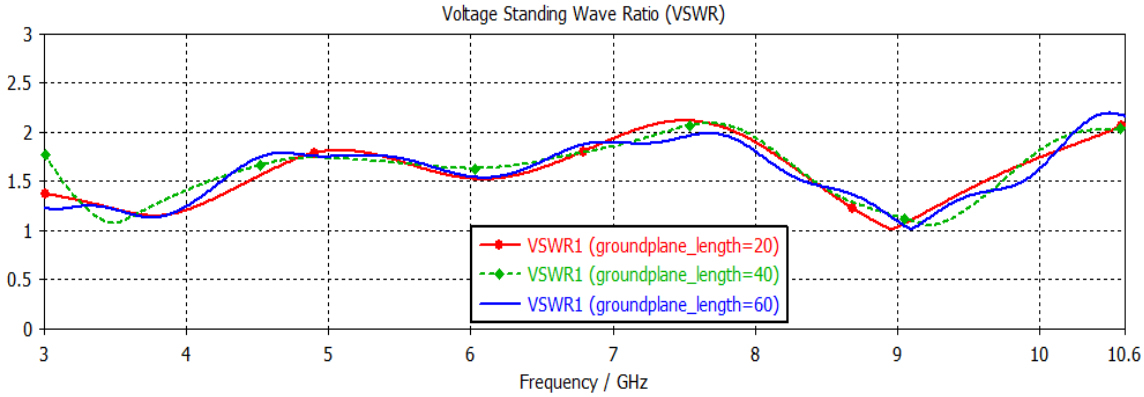

Figure 9.22: All figures plotted in Figure 21 a, b and c, respectively

Table 9.4: Final dimensions of the proposed antenna after simulation results

Parameters	Elliptic Microstrip patch Antenna	Units
c	$3x10^8$	m/s
Feed Line Length	20	mm
Feed Line Width	2,7	mm
Frequency Centre	6,85	GHz
Groundplane Length	20	mm
Groundplane Width	40	mm
Metal Thickness	2,8282	mm
Patch Length(L)	20	mm
Patch Width(W)	20	mm
Relative Permittivity(ε)	2	-
Substrate Thickness(H)	1,5	mm
Tan Delta(δ)	0	-
Wavelength	43,765	mm

10. OPTIMIZATION OF THE ANTENNA STRUCTURES

The purpose of this section is to optimize the different UWB antennas in order to observe best desired antenna parameters or physical parameter of aforementioned antenna structure throughout previous sections. The result of the optimized antenna ought to satisfy all constraints defined by FCC and UWB requirements. That's why the parameters which are optimized should be obviously defined.

There are tremendous methods for optimization of the antennas. Conventionally, parameters are optimized by using trial and error methods. However, trial and error methods are not efficient due to time consuming manner. A number of researches and investigations are found out to prevent these demerits of trial and error optimization techniques. So, some metaheuristic techniques are introduced by several researchers to find optimal or near optimal solutions in relatively short time such as Genetic Algorithm, Particle Swarm Optimization, Ant Colony Optimization, Bee Colony Optimization and Bacterial Colony Optimization inspired by natural events (Kennedy and Eberhart, 1995; Holland, 1984; Blum, 2005; Teodorovic et al, 2006; Niu and Wang,2012). These algorithms have gained utmost popularity in various research areas which are related with different engineering fields.

Particle swarm optimization was originally introduced by Eberthart and Kennedy (Kennedy and Eberhart, 1995). The main aim of the particle swarm optimization is to find out optimal or near optimal parameters for different optimization problems. In this thesis, particle swarm optimization is preferred in order to obtain the most appropriate antennas that work successfully and efficiently according to FCC regulation and UWB requirements. There are a number of merits such as accuracy, robustness, low cost and ease of implementation etc. Another comprehensive study of optimization technique is Genetic Algorithm which was proposed by Holland (Holland, 1984). These two challenging techniques have influence on the electromagnetic, antenna and communication community due to its merits including capability of solving high ordered non-linear systems, ease of implementation, robustness. Furthermore, these proposed two techniques are stochastic based search techniques as compared to evaluation algorithms and other conventional optimization methods (Islam et al, 2009; Asghar et al, 2013; Jayasinghe and Uduwawala, 2013; Saxena et al, 2011; Chouksey and Ghadle, 2012; Rani and Dawre; Harisharan and Kumar; Zubair and Moinuddin, 2013; John and Ammann, 2007).

In this section, genetic algorithm and particle swarm optimization methods are applied to design the UWB antenna structures which have been already examined in previous sections. The optimized parameters will be substrate thickness and relative permittivity. The genetic algorithm and particle swarm optimization methods handle the bandwidth with respect to the substrate thickness and relative permittivity of the antennas. The bandwidths of the proposed antennas are analysed after each optimization program is completed. Truncated rounded bowtie antenna and elliptic microstrip antenna structures are handled to improve the antennas' bandwidths.

10.1. ENHANCEMENT OF TRUNCATED ROUNDED BOWTIE ANTENNA via GENETIC ALGORTIHM TECHNIQUE

The aim of truncated rounded bowtie antenna optimization is to analyse the bandwidth by changing substrate relative permittivity. Firstly, genetic algorithm is used as an optimizer for relative permittivity decision. Population size is set as 8 chromosomes in all designs, the mutation rate is 5%, maximum generation (iteration) number is considered as 5, and maximum number of solver evaluation is set to 25). Uniform random distribution is chosen as an initial point set as shown in Figure 10.1. Numbers of generation and solver evaluation are taken as small as possible so as to keep the requirements at minimum level. Otherwise, various processes would be solved in 2 or 3 three days depending on optimizer variables and hardware specification. The run with 25 iterations of CST MWS optimizer toolbox takes almost 17 minutes on a single computer, Intel Core i7-5500U at 2.40 GHz. These variables are implemented by CST Optimization toolbox.

The simulation, which is run via genetic algorithm, runs over iterations until the expected value of the goal function is reached. Figure 10.2 shows the adjustment of the relative permittivity in order to observe the optimization technique clearly. Table 10.1 represents relative permittivity values from minimum to maximum value which will be obtained from iteration results. Figure 10.2 and Table 10.1 are compatible with each other.

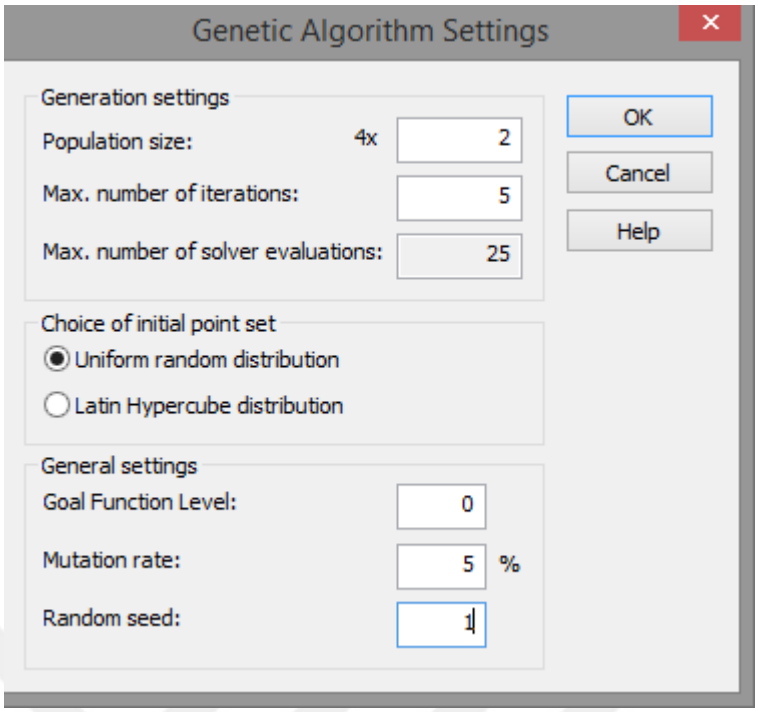

Figure 10.1: Genetic Algorithm settings

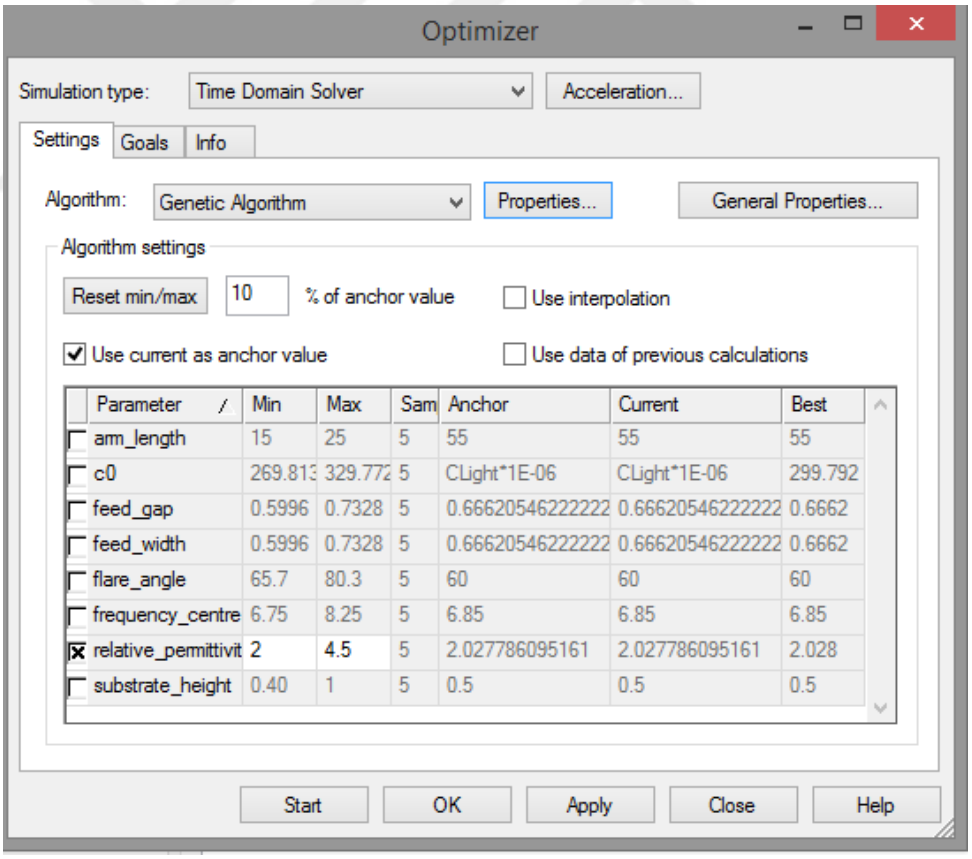

Figure 10.2: The optimization method's input parameter, relative permittivity setting from CST MWS

Table 10.1- Parameters used for optimization by using genetic algorithm

Name	Minimum	Maximum	Anchor
Relative permittivity	2.0	4.5	2.01749

Equation (10.1) is set up as goal function namely S_{11} and VSWR which provide UWB requirements defined by FCC. Figure 10.3 illustrates the goal function setting screen from CST MWS and weight is set up as 1.0. Goal functions which are used for optimization process is written in Equations (10.1) and (10.2):

$$\text{Goal} = \sum (S_{11} \leq -10\ dB) \tag{10.1}$$

$$\text{Goal} = \sum (VSWR \leq 2) \tag{10.2}$$

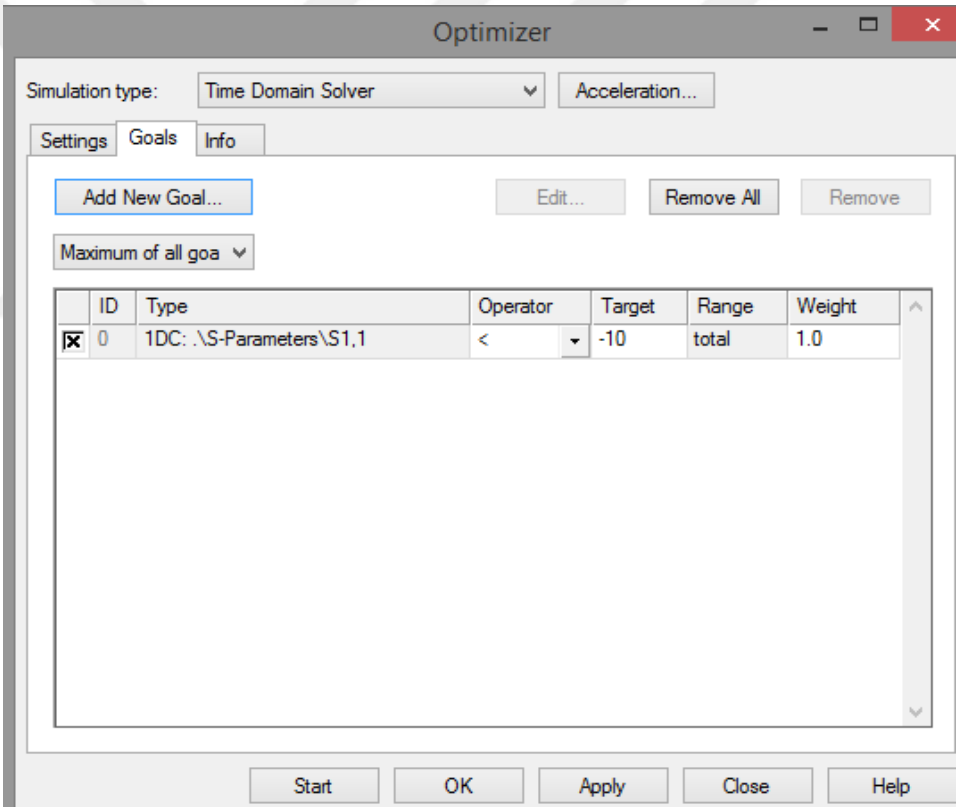

Figure 10.3: The goal function setting from CST MWS

Table 10.2 lists the relative permittivity values of each iteration results.

Table 10.2- Resulted relative permittivity values after each iteration

Number of iteration	Relative permittivity value after each iteration
1	4.18357
2	2.02779
3	4.42135
4	2.59860
5	4.17299
6	2.94379
7	3.32714
8	4.04115
9	2.21114
10	2.56455
11	2.81513
12	3.16574
13	2.28172
14	2.15056
15	2.22681
16	2.57351
17	2.17178
18	2.13270
19	2.57605
20	2.57287
21	2.41143
22	2.06880
23	2.14184
24	2.33027
25	2.02799

After 25th iteration, the best relative permittivity is obtained as 2.02779 at 2nd and 25th iteration. Figure 10.4 illustrates relative permittivity values of the proposed antenna with respect to iteration. The graph displays the change in the relative permittivity value of the proposed antenna. Clearly, it can be seen from Figure 10.4 that the best result of the relative permittivity is 2.02779.

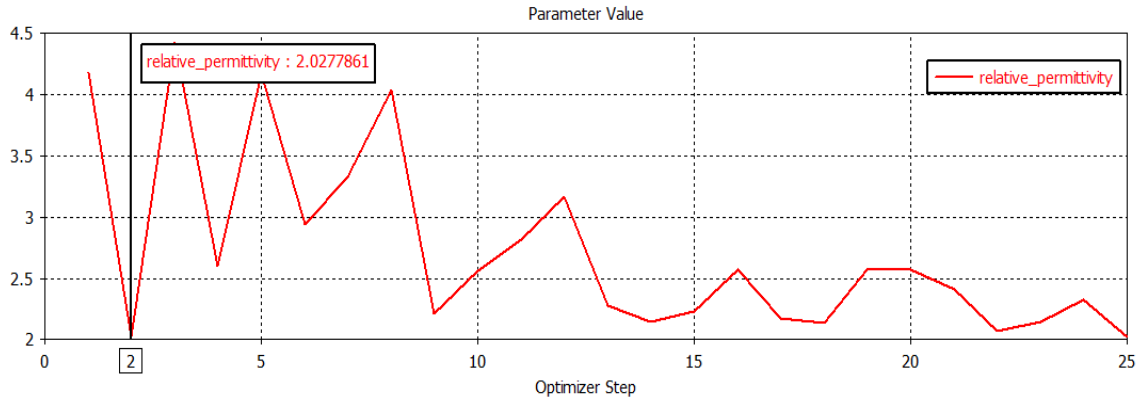

Figure 10.4: Relative permittivity values of each iteration

Figure 10.5 indicates return loss characteristic, which is already defined as a goal function via optimizer in terms of first iteration. It can be also inferred that it does not the meet the UWB requirements i.e, has not broadband characteristic at first iteration.

Additionally, optimized return loss characteristic of the proposed antenna is depicted in Figure 10.6. Bandwidth of the proposed truncated rounded bowtie antenna is increased slightly as compared to initial return loss characteristic as shown in Figure 10.5. Minimum return loss characteristics of the proposed antenna are represented in Figure 10.7 and 10.8. Figure 10.7 depicts the minimum return loss characteristic of the proposed antenna at first iteration. The best return loss of -28.97303 dB occurs at 4.053 GHz frequency. The optimization technique improves the return loss by an amount approximately -4.5 dB which is quite acceptable. Consequently, the best return loss characteristic is represented in Figure 10.8. The best value is -33.526573 dB at 4.206 resonance frequency. It can be also inferred that the resonance frequency is increased gradually by optimization techniques.

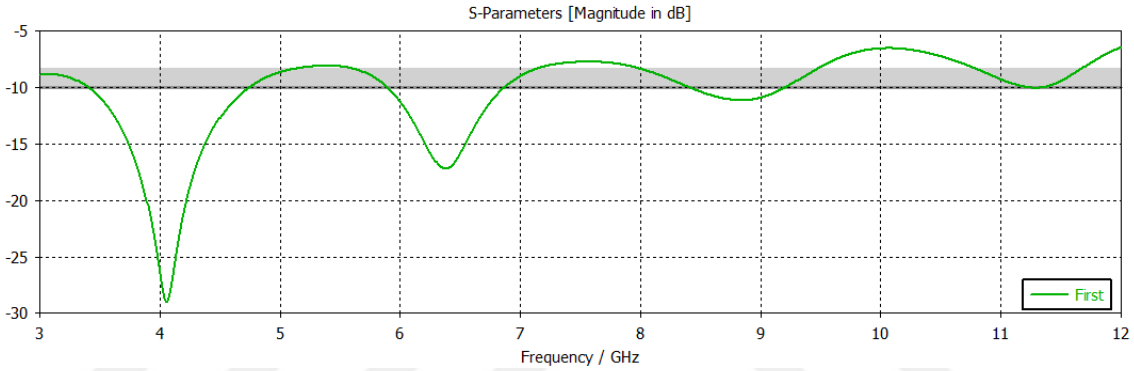

Figure 10.5: Return loss characteristic of the aforementioned truncated rounded bowtie antenna at fist iteration

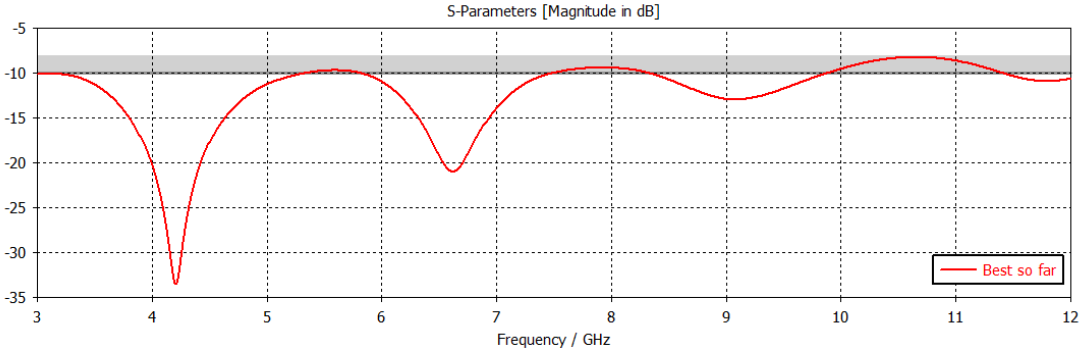

Figure 10.6: Optimized return loss characteristic of the aforementioned truncated rounded bowtie antenna

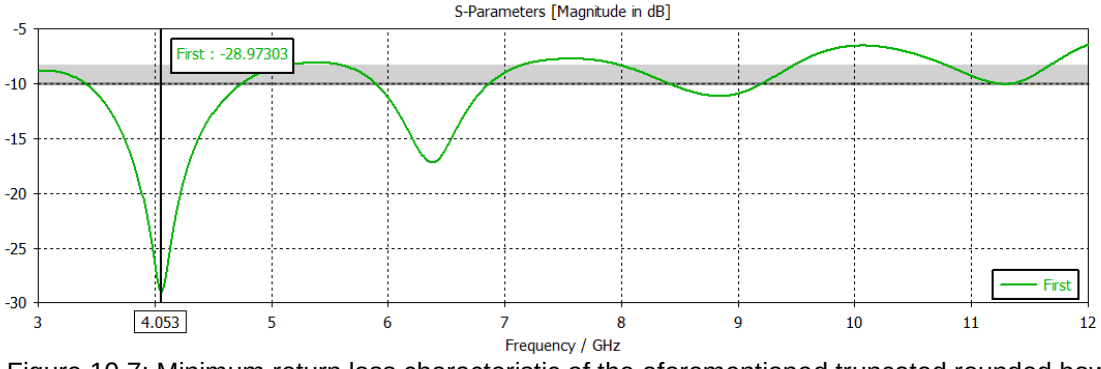

Figure 10.7: Minimum return loss characteristic of the aforementioned truncated rounded bowtie antenna at first iteration

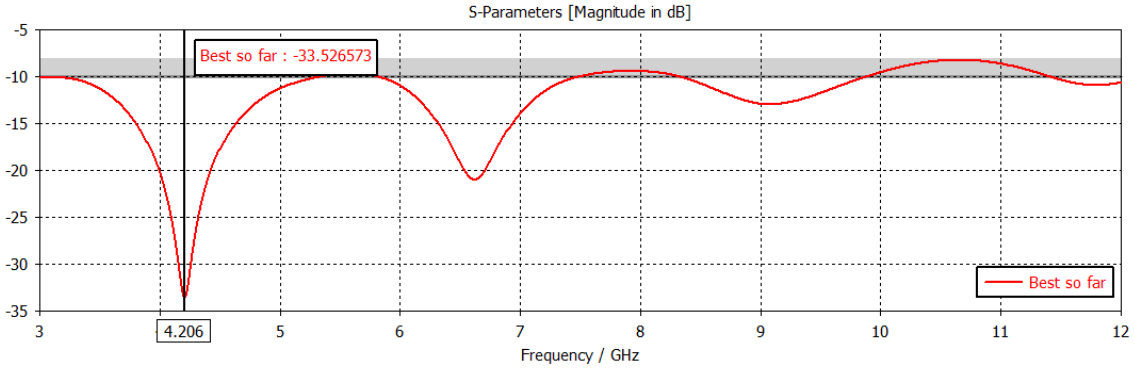

Figure 10.8: Optimized minimum return loss characteristic of the aforementioned truncated rounded bowtie antenna

The proposed truncated rounded bowtie antenna is also optimized via Genetic Algorithm with 265 iterations in order to confirm that the minimum iteration value such as 25 is quite acceptable range for determining the best value of relative permittivity in the UWB frequency range. Figure 10.9 depicts the relative permittivity values with respect to iteration numbers. According to the Genetic Algorithm optimized relative permittivity results with 265 iterations, the best relative permittivity is observed as 2.0174903 at 1st iteration. Furthermore, Figure 10.10 outlines the best return loss value which is obtained after 265 iterations. Corresponding minimum return loss value is obtained as -33.409361 dB which is very close to the value of best return loss value obtained via Genetic Algorithm with 25 iterations. The proposed two figures also explains that the iteration numbers might be selected as 25 in order to define the best relative permittivity value in the UWB frequency ranges from 3.1 to 10.6 GHz.

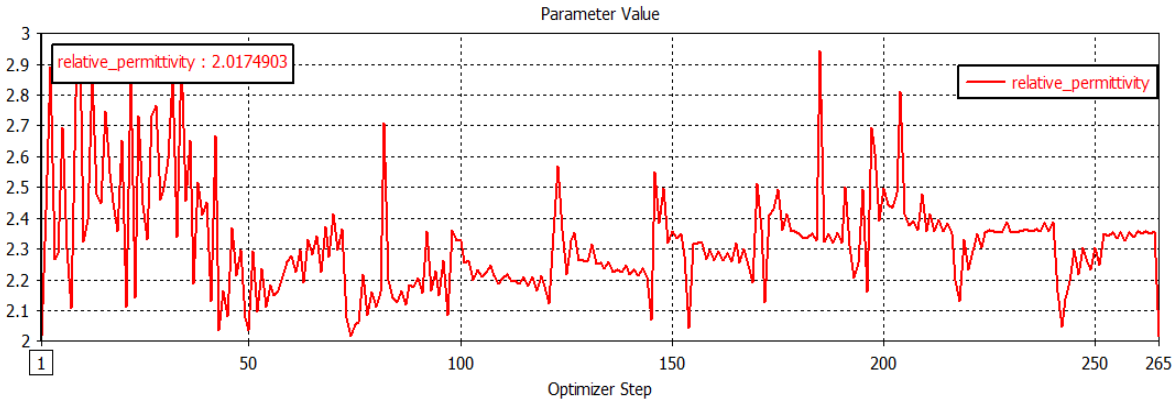

Figure 10.9: Relative permittivity values with 265 iterations

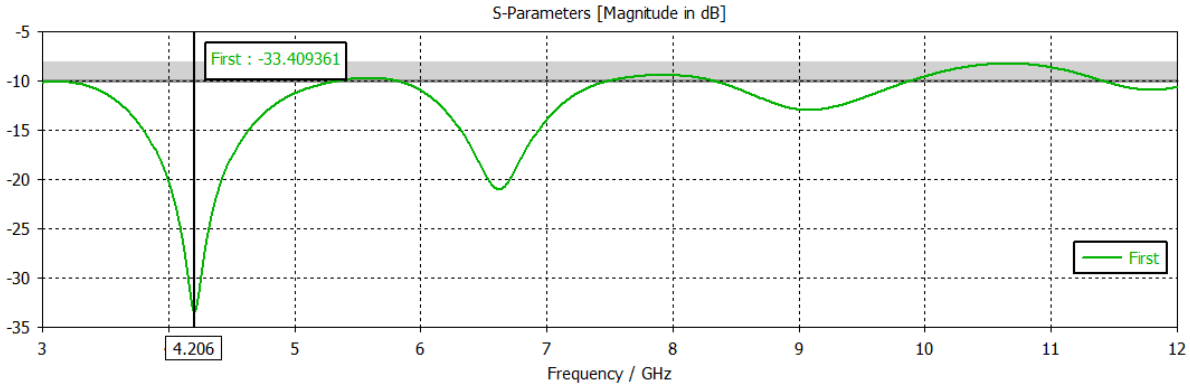

Figure 10.10: Minimum return loss characteristic of the truncated rounded bowtie obtained after 265 iterations

10.2. ENHANCEMENT OF TRUNCATED ROUNDED BOWTIE ANTENNA via PARTICLE SWARM OPTIMIZATION TECHNIQUE

The purpose of this section is to compare particle swarm optimization with genetic algorithm in order to obtain optimal relative permittivity values. There are similarities and dissimilarities between genetic algorithm and particle swarm optimization. However, there is no accurate restriction as to define which optimization technique is more efficient. For instance, both genetic algorithm and particle swarm optimization have initial population generated randomly and fitness (goal) function so as to assess the population. On the contrary, particle swarm optimization has no evaluation operator namely crossover and mutation while genetic algorithm evolves the optimization through selection, crossover and mutation. Furthermore, genetic algorithm is inherently discrete while particle swarm optimization is inherently continuous. That's why; genetic algorithm and particle swarm optimization ought to be adjusted so as to handle in terms of application areas. Classical particle swarm optimization method will be applied to electromagnetic problems including antenna parameter improvement and compared with other evolutionary algorithm techniques namely genetic algorithm.

Table 10.3 illustrates the lower bound and the upper bound of relative permittivity in order to improve bandwidth and return loss characteristic of the proposed antenna. Using CST MWS optimization toolbox, minimum frequency and maximum frequency are set up as 3.1 GHz and 10.6 GHz, respectively while relative permittivity is varied so as to observe the enhancement of the parameters. Simultaneously, return loss will be optimized regardless of other physical or antenna parameters. The fitness (goal) function which is preferred by optimizer is outlined by Equations (10.1) and (10.2):

Table 10.3- Parameters used for optimization by using genetic algorithm:

Name	Minimum	Maximum	Anchor
Relative permittivity	2.0	4.5	3.36808

$$\text{Goal} = \sum (S_{11} \leq -10\ dB) \tag{11.1}$$

$$\text{Goal} = \sum (VSWR \leq 2) \tag{11.2}$$

Table 10.4- Resulted relative permittivity values after each iteration:

Number of iteration	Relative permittivity value after each iteration
1	4.41757
2	4.25155
3	3.36808
4	2.43174
5	3.59257
6	4.43112
7	2.67011
8	2.41298
9	2.76757
10	3.60612
11	2.15489
12	2.39423
13	2
14	2.78112
15	2.97989
16	2.20621
17	2.81604
18	2.04388
19	2.16724
20	2.09945
21	2.00896
22	2.80700
23	2.66071
24	2.24061
25	2

Figure 10.11 depict the initial settings of particle swarm optimization. Swarm size is set as 4. Maximum number of iterations and solver evaluations are set as 6 and 25, respectively. The maximum number of solver evaluations is same with genetic algorithm settings so as to compare each other fairly. Figure 10.12 depict relative permittivity settings as mentioned in Table 10.3. The main aim is to assign return loss value which varies below -10 dB in the entire UWB frequency range. Table 10.4 outlines the optimized relative permittivity value in terms of iteration. After 25th iteration, the optimal relative permittivity is obtained as 2 at 13rd iteration. Figure 10.14 illustrates relative permittivity values of the proposed antenna with respect to iteration. The graph displays the change in the relative permittivity value of the proposed antenna. Clearly, it can be seen from Figure

10.14 that the optimal result of the relative permittivity is 2 which is almost identical with genetic algorithm result (2.0277861) obtained in previous section.

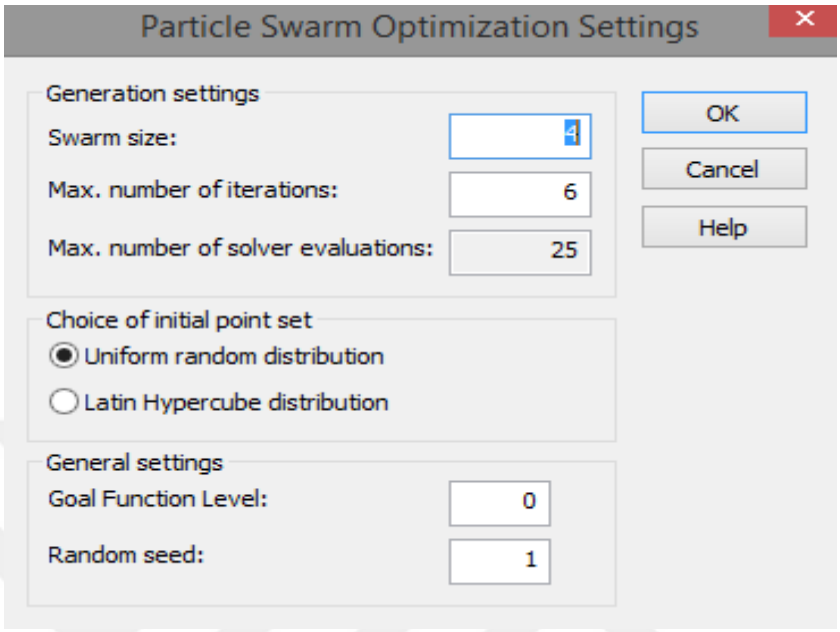

Figure 10.11: Particle Swarm Optimization settings

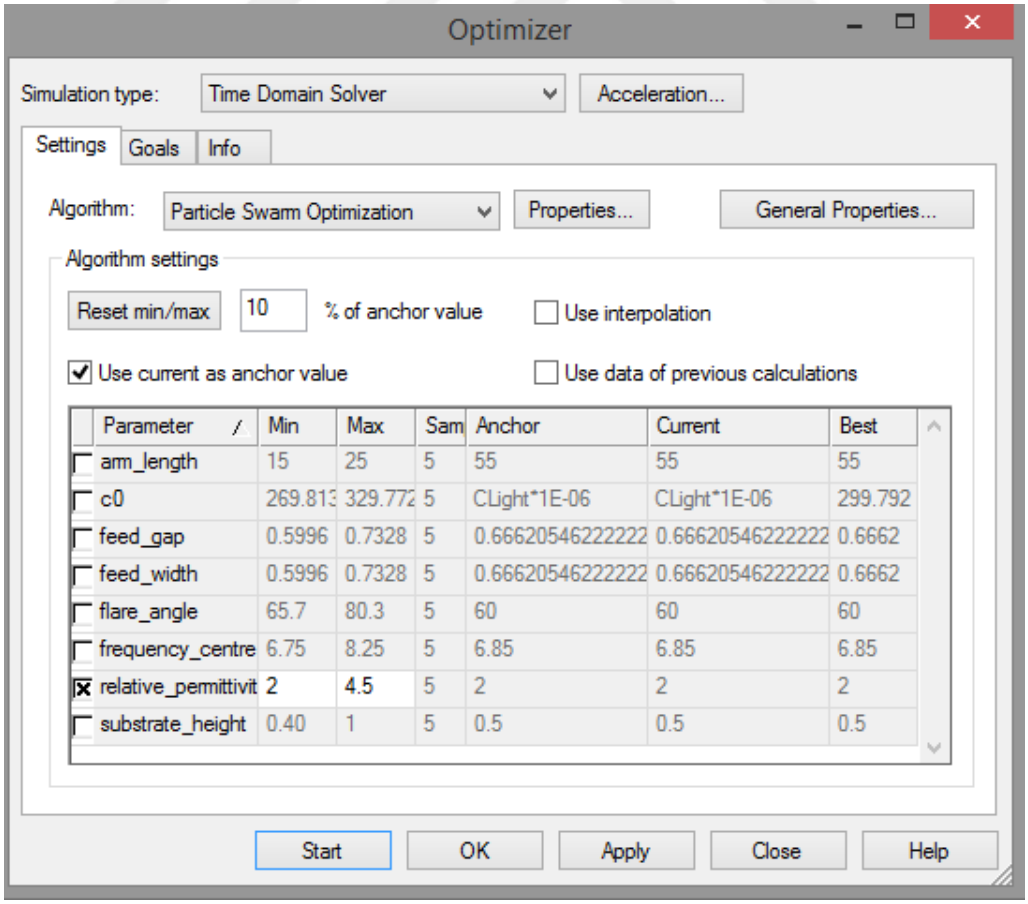

Figure 10.12: The optimization method's input parameter, relative permittivity setting from CST MWS

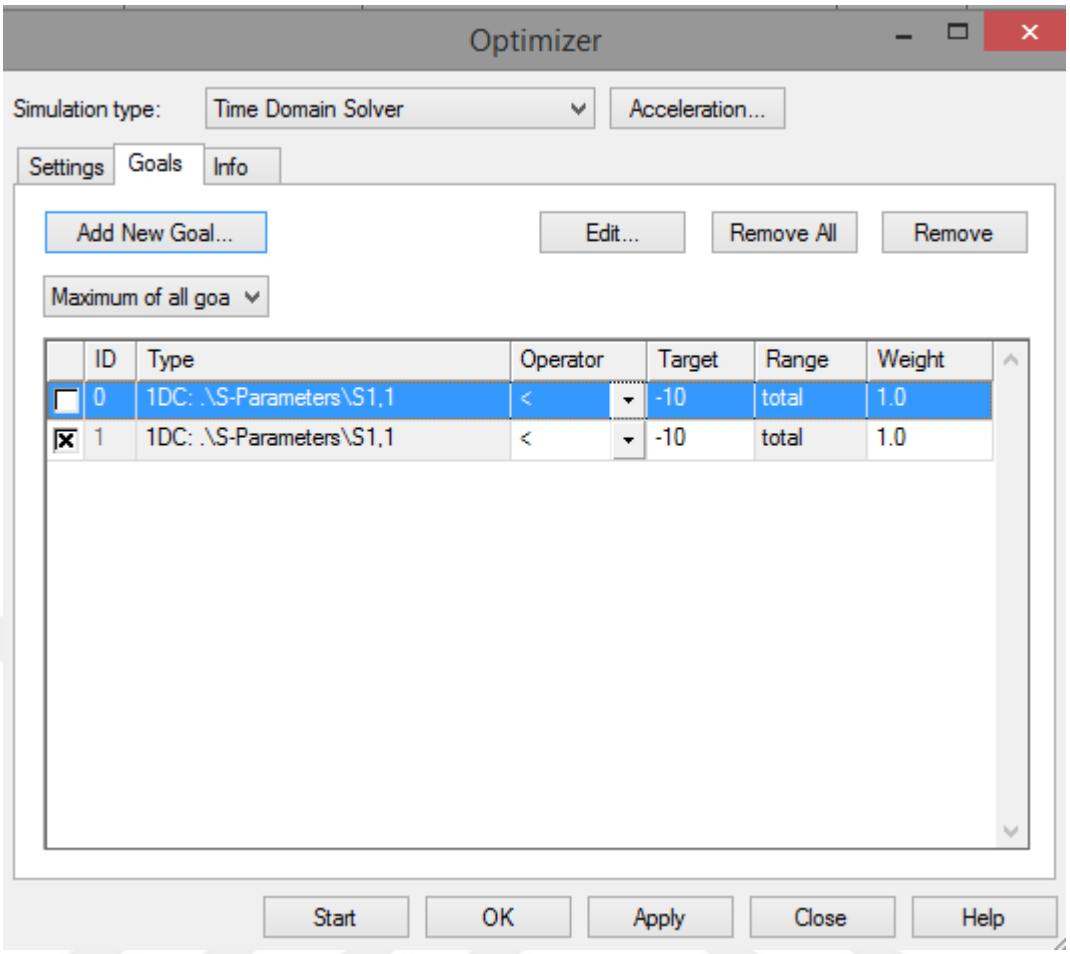

Figure 10.13: The goal function setting from CST MWS

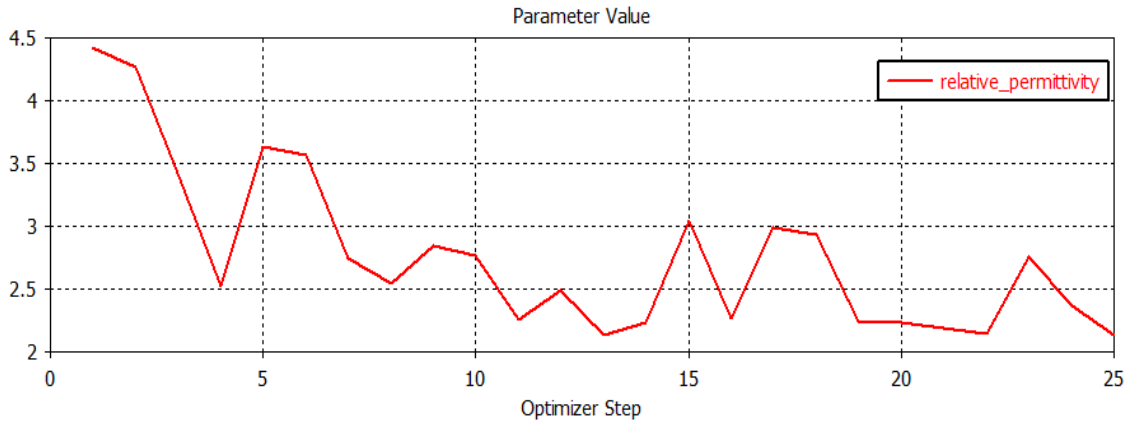

Figure 10.14: Relative permittivity values of each iteration

Figure 10.15 and 10.16 illustrate return loss characteristics of the proposed truncated rounded bowtie antenna at first iteration and optimized relative permittivity value, respectively. It can be concluded from Figure 10.15, the proposed truncated rounded bowtie antenna has not inherently wider bandwidth regardless of other dimensions of the antenna. Figure 10.16 depict the optimized return loss characteristic of the aforementioned truncated rounded bowtie antenna. Furthermore, the minimum values of return loss are displayed in Figure 10.17 and 10.18. These two values are the very close to the genetic algorithm results which are presented in previous section. Finally, all the results obtained from genetic algorithm and particle swarm optimization methods clarify that there is no big difference for best truncated rounded bowtie antenna relative permittivity determination through optimization techniques. That's why the evolutionary algorithm including genetic algorithm and particle swarm optimization are capable of solving the electromagnetic problems such as antenna parameters optimization effectively.

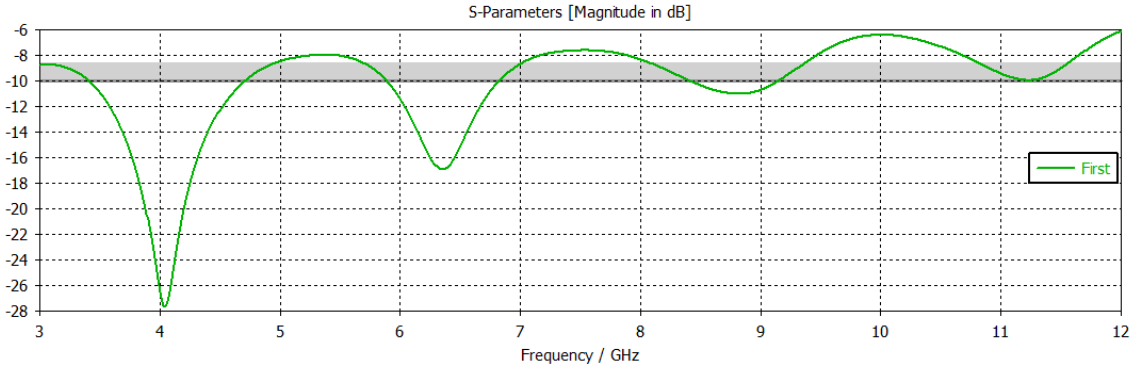

Figure 10.15: Return loss characteristic of the aforementioned truncated rounded bowtie antenna at fist iteration

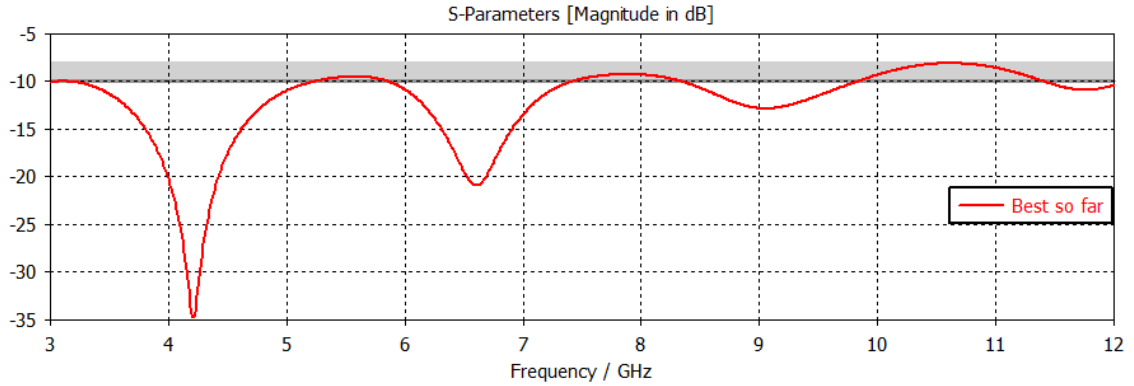

Figure 10.16: Optimized return loss characteristic of the aforementioned truncated rounded bowtie antenna

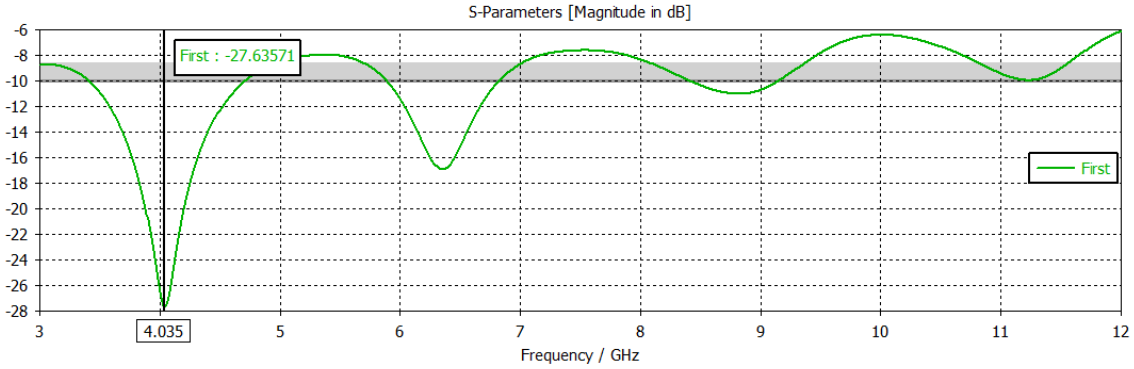

Figure 10.17: Minimum return loss characteristic of the aforementioned truncated rounded bowtie antenna at first iteration

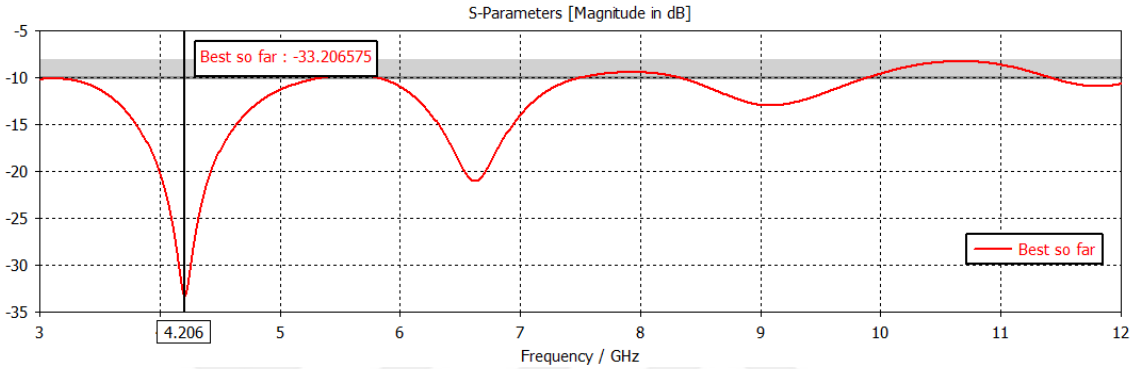

Figure 10.18: Optimized minimum return loss characteristic of the aforementioned truncated rounded bowtie antenna

Taking everything into account, the maximum number of iterations of particle swarm optimization is also considered as 265 to confirm that the iteration number of PSO might be selected as 25 in order to prevent the waste of time during the simulation procedure. The optimization results show that the best relative permittivity values is also obtained as 2 at 114th iterations and the best return loss value of -33.206575 dB at 4.206 GHz. These two results prove that the maximum numbers of iterations are 25 and 265 gives the same significant relative permittivity and return loss values. Figure 10.19 and 10.20 outline this idea with visualizations.

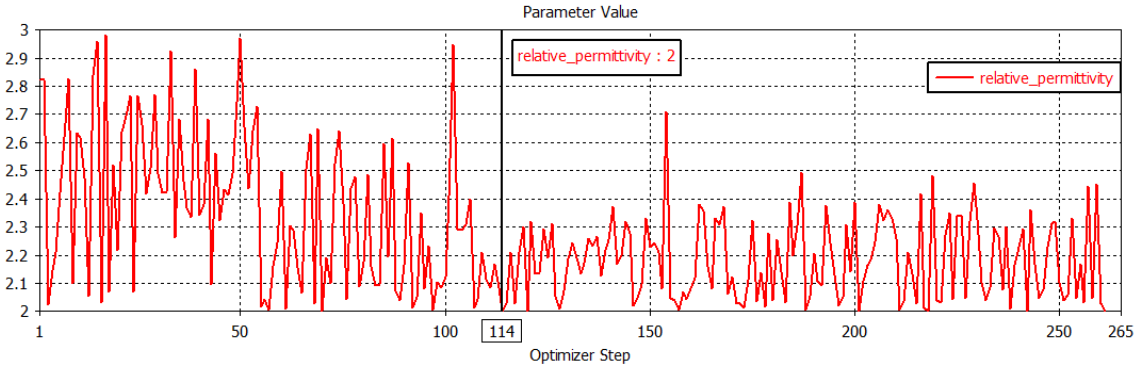

Figure 10.19: Relative permittivity values with 265 iterations

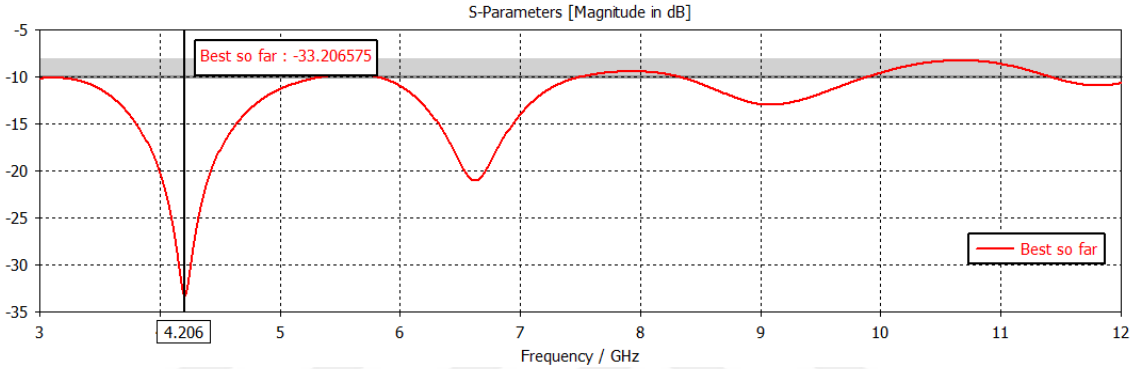

Figure 10.20: Minimum return loss characteristic of the truncated rounded bowtie obtained after 265 iterations

10.3. ENHANCEMENT OF ELLIPTIC MİCROSTRİP PATCH ANTENNA via GENETIC ALGORITHM

Table 10.5 represents the relative permittivity values between 3 and 5 in order to obtain explicitly UWB antenna characteristic. Furthermore, Table 10.6 shows the each relative permittivity values after iteration. The number of iteration is set up as 25 so as to elucidate the differences between particle swarm optimization and genetic algorithm. After 25th iteration, recover data for best relative permittivity is observed at 6th iteration. Additionally, the optimal relative permittivity is recorded as 3.125.

Table 10.5- Parameter used for optimization by using particle swarm optimization:

Name	Minimum	Maximum	Anchor
Relative permittivity	3	5	4.51763

Table 10.6- Resulted relative permittivity values after each iteration

Number of iteration	Relative permittivity value after each iteration
1	3.375
2	3.875
3	4.875
4	4.375
5	3.625
6	3.125
7	4.125
8	4.625
9	3.26611
10	3.36009
11	3.53182
12	3.91448
13	3.23622
14	3.21949
15	3.27028
16	3.31583
17	3.36401
18	3.25721
19	3.24807
20	3.36512
21	3.36373
22	3.31998
23	3.23066
24	3.25176
25	3.27500

Figure 10.21 depicts the initial settings of genetic algorithm. Population size is set as 2. Maximum number of iterations and solver evaluations are set as 5 and 25, respectively. The maximum number of solver evaluations will be same with particle swarm optimization so as to elucidate fairly. Figure 10.22 depicts relative permittivity settings as

mentioned in Table 10.5. The main aim is to assign return loss value which varies below -10 dB in the entire UWB frequency range. Table 10.6 outlines the optimized relative permittivity value in terms of iteration. Figure 10.23 shows goal function of the elliptic microstrip patch antenna as given in Equation 10.1.

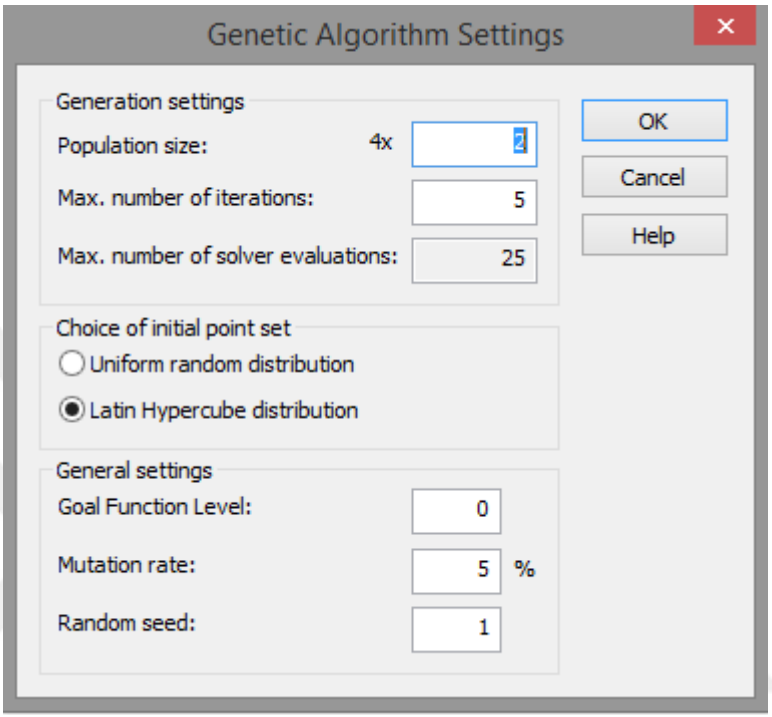

Figure 10.21: Genetic Algorithm settings

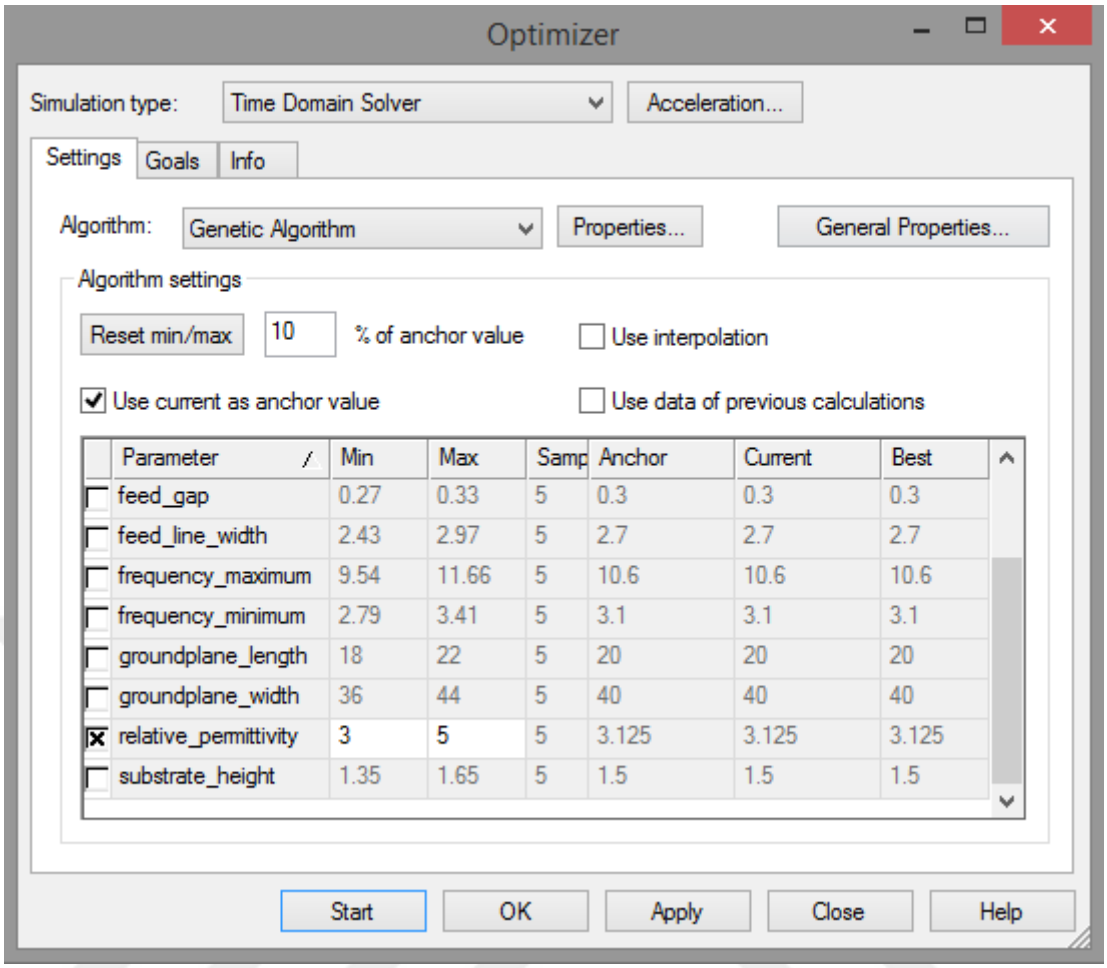

Figure 10.22: The optimization method's input parameter, relative permittivity setting from CST MWS

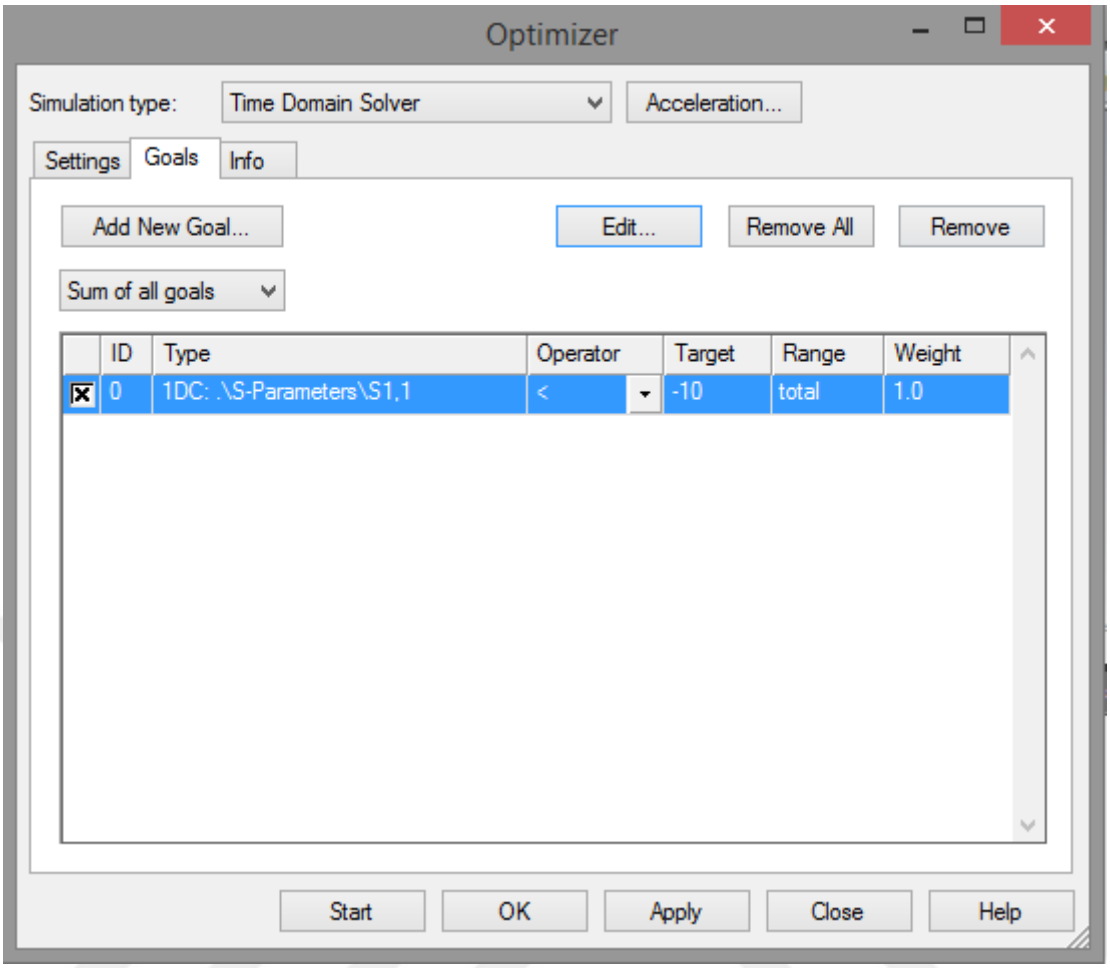

Figure 10.23: The goal function setting from CST MWS

Figure 10.24 outlines the return loss characteristic of the aforementioned elliptic microstrip patch antenna at fist iteration through genetic algorithm. The proposed antenna covers entire UWB frequency range initially. The minimum return loss value of the proposed antenna is obtained from Figure 10.26. The minimum value of -31.72 dB occurs at 9.7674 GHz. Figure 10.25 represents optimized return loss characteristic of the aforementioned elliptic microstrip patch antenna through genetic algorithm. The optimized minimum return loss is obtained from Figure 10.27. The optimized minimum return loss of -49.37 dB occurs at 9.9303 GHz. The comparison of these two values is that the return loss value is decreased by approximately -18 dB which is quite acceptable value so as to prevent power loss due to the reflection from antenna to transmission line. Furthermore, the optimized minimum return loss value, which is handled by genetic algorithm, is more acceptable than handled by particle swarm optimization. Because, the better return loss value is, the more efficiency of the system.

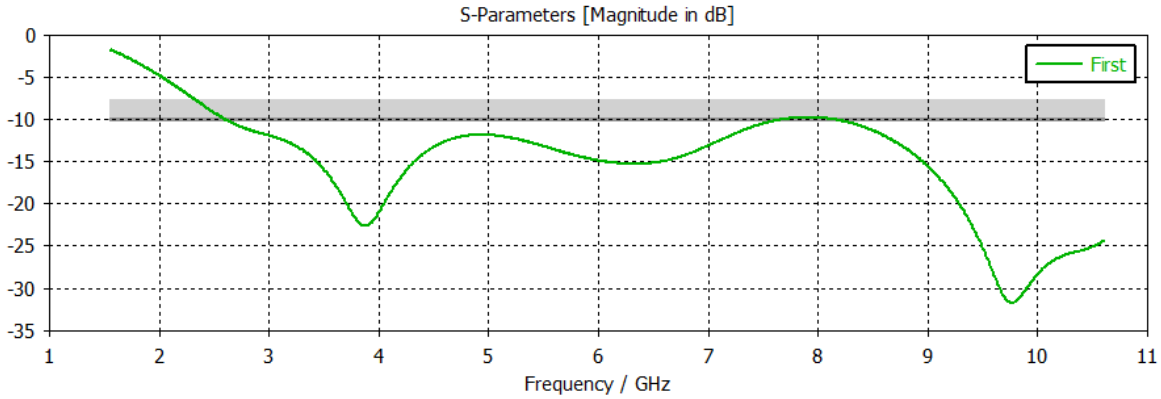

Figure 10.24: Return loss characteristic of the aforementioned elliptic microstrip patch antenna at fist iteration by genetic algorithm

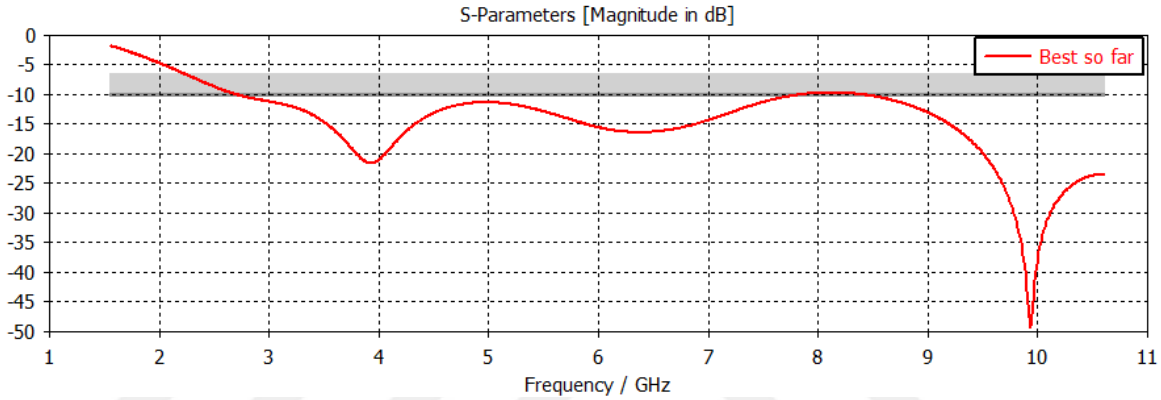

Figure 10.25: Optimized return loss characteristic of the aforementioned elliptic microstrip patch antenna by genetic algorithm

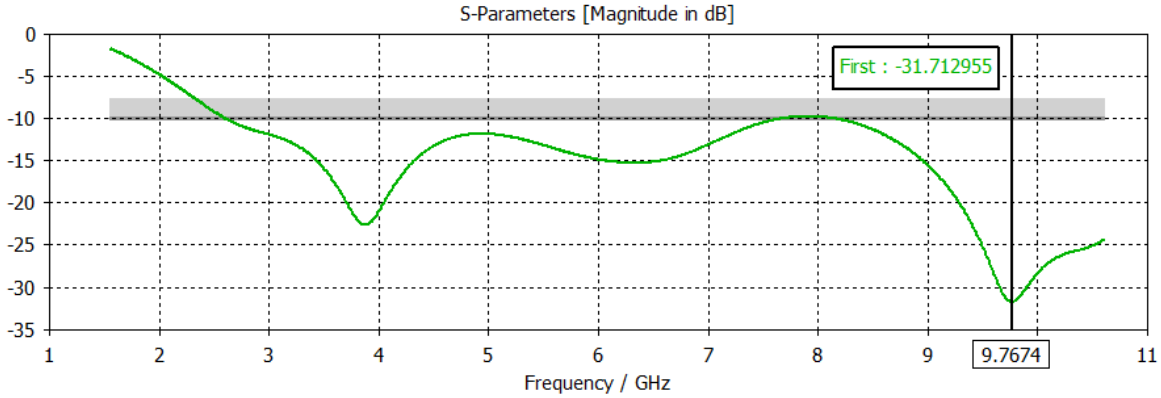

Figure 10.26: Minimum return loss characteristic of the elliptic microstrip patch antenna at first iteration by genetic algorithm

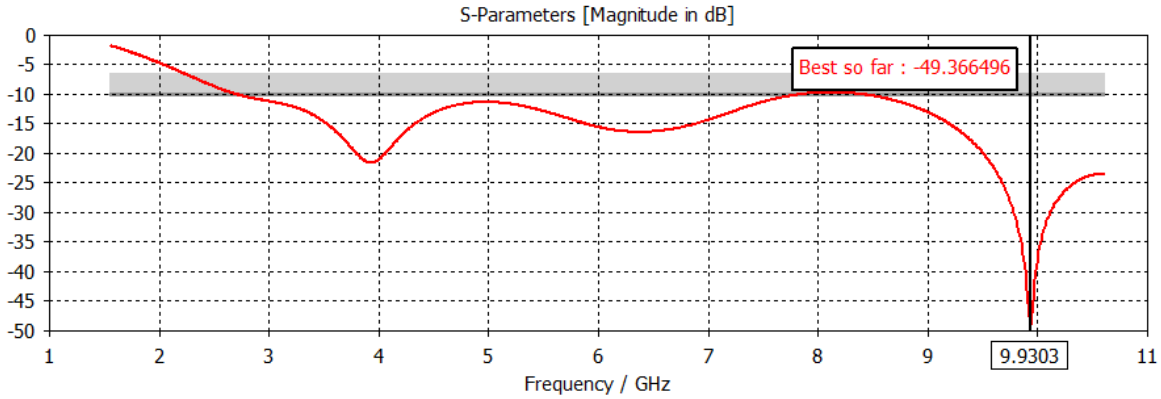

Figure 10.27: Optimized minimum return loss characteristic of the elliptic microstrip patch antenna by genetic algorithm

Again, the maximum number of iterations of genetic algorithm is increased up to 265 so as to clarify the maximum number of iterations might be selected as 25 , which is already mentioned in former sections, i.e. 10.1 and 10.2. The simulation results with 265 iterations shows that the best relative permittivity value is obtained as 3.020833 at 1st iteration. It is conclude that the optimization process with 265 iterations gives almost same results with the 25 iterations as represented in Figure 10.28.

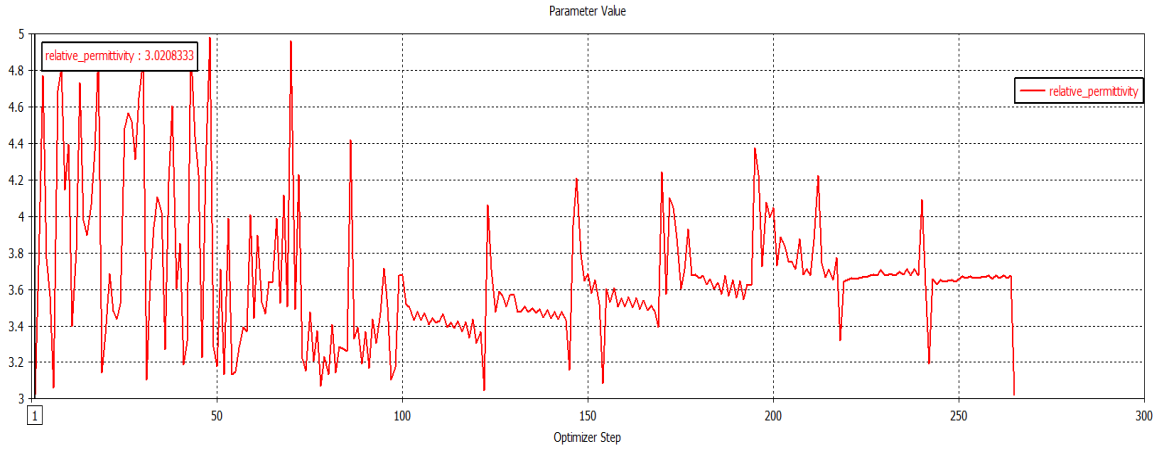

Figure 10.28: Relative permittivity values with 265 iterations

10.4. ENHANCEMENT OF ELLIPTIC MİCROSTRİP PATCH ANTENNA via PARTICLE SWARM OPTIMIZATION

The aim of this section is to prevent major demerits of the microstrip antenna including narrow bandwidth and low efficiency by using evolutionary algorithm such as particle swarm optimization and genetic algorithm. When the relative permittivity of the microstrip antenna is changed, antenna parameters such as return loss, VSWR, gain and radiation pattern are severely altered. Furthermore, these conventional antenna parameters affect the system performance i.e. degrade or upgrade efficiencies.

One of the most crucial parameters which is known as relative permittivity impacts the antenna efficiency and cost of fabrication. There is a great deal of substrate materials in manufacturing sector. However, deciding task is rigorous and vigorous method due to trade-off between cost and efficiency. The most preferable way is to examine the parameter through particle swarm optimization and genetic algorithm. The same procedures are applied to the elliptic microstrip patch antenna with the truncated rounded bowtie antenna introduced by previous section.

Table 10.7 illustrates the lower bound and the upper bound of relative permittivity in order to improve bandwidth and return loss characteristic of the proposed. Using CST MWS optimization toolbox, minimum frequency and maximum frequency are set up as 3.1 GHz and 10.6 GHz, respectively while relative permittivity is varied so as to observe the enhancement of the parameters. Simultaneously, return loss will be optimized regardless of another physical or antenna parameters. The fitness (goal) function which is preferred by optimizer is outlined by Equation (10.1):

Table 10.7- Parameters used for optimization by using particle swarm optimization:

Name	Minimum	Maximum	Anchor
Relative permittivity	3	5	3.21949

$$\text{Goal} = \sum (S_{11} \leq -10\ dB) \tag{10.1}$$

$$\text{Goal} = \sum (VSWR \leq 2) \tag{10.2}$$

Table 10.8- Resulted relative permittivity values after each iteration

Number of iteration	Relative permittivity value after each iteration
1	4.5
2	3.5
3	4.224
4	3.485
5	3.564
6	3.46999
7	3.096
8	3.45499
9	3.756
10	3.10136
11	3.14842
12	3.64987
13	3.51118
14	3
15	3.51694
16	3.66
17	3.14306
18	3.41782
19	3.5811
20	3.24218
21	3.0628
22	3.29687
23	3.68871
24	3.26341
25	3

Figure 10.29 depicts the initial settings of particle swarm optimization. Swarm size is set as 2. Maximum number of iterations and solver evaluations are set as 12 and 25, respectively. The maximum number of solver evaluations will be same with genetic algorithm settings so as to compare each other fairly. Figure 10.30 depict relative permittivity settings as mentioned in Table 10.7. The main aim is to assign return loss value which varies below -10 dB in the entire UWB frequency range. Table 10.8 outline the optimized relative permittivity value in terms of iteration. After 25^{th} iteration, the optimal relative permittivity is obtained as 3 at 14^{th} iteration. Figure 10.31 illustrate relative permittivity values of the proposed antenna with respect to iteration. The graph displays the change in the relative permittivity value of the proposed antenna. Clearly, it can be seen from Figure 10.31 that the optimal result of the relative permittivity is 3.00146.

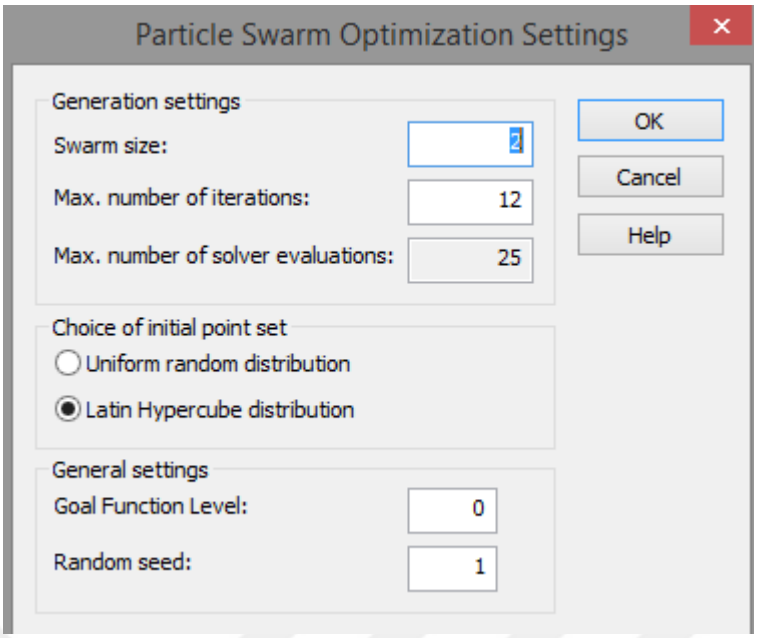

Figure 10.29: Particle Swarm Optimization settings

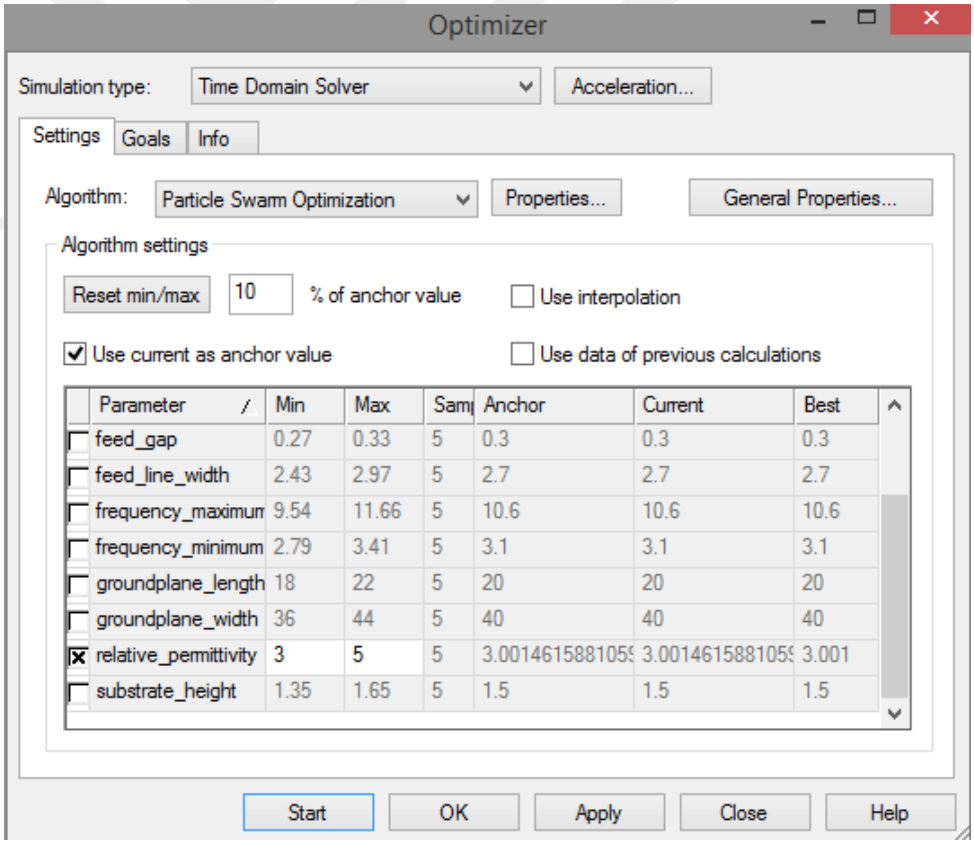

Figure 10.30: The optimization method's input parameter, relative permittivity setting from CST MWS

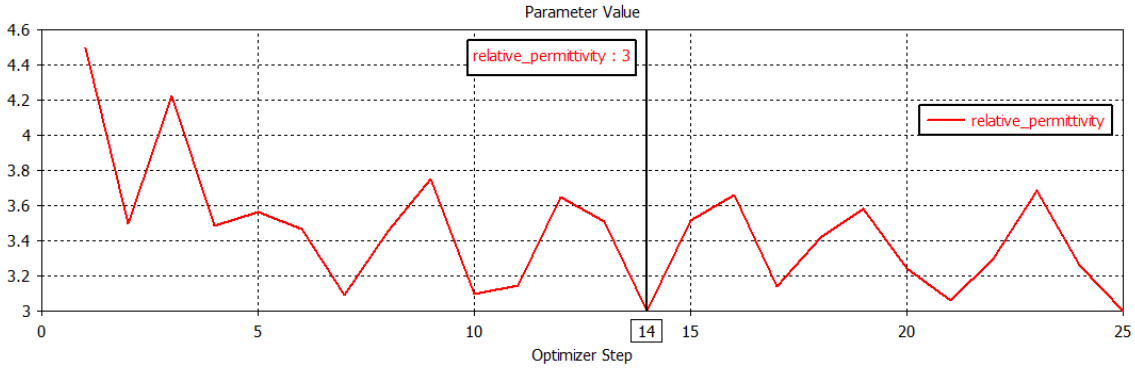

Figure 10.31: Relative permittivity values of each iteration

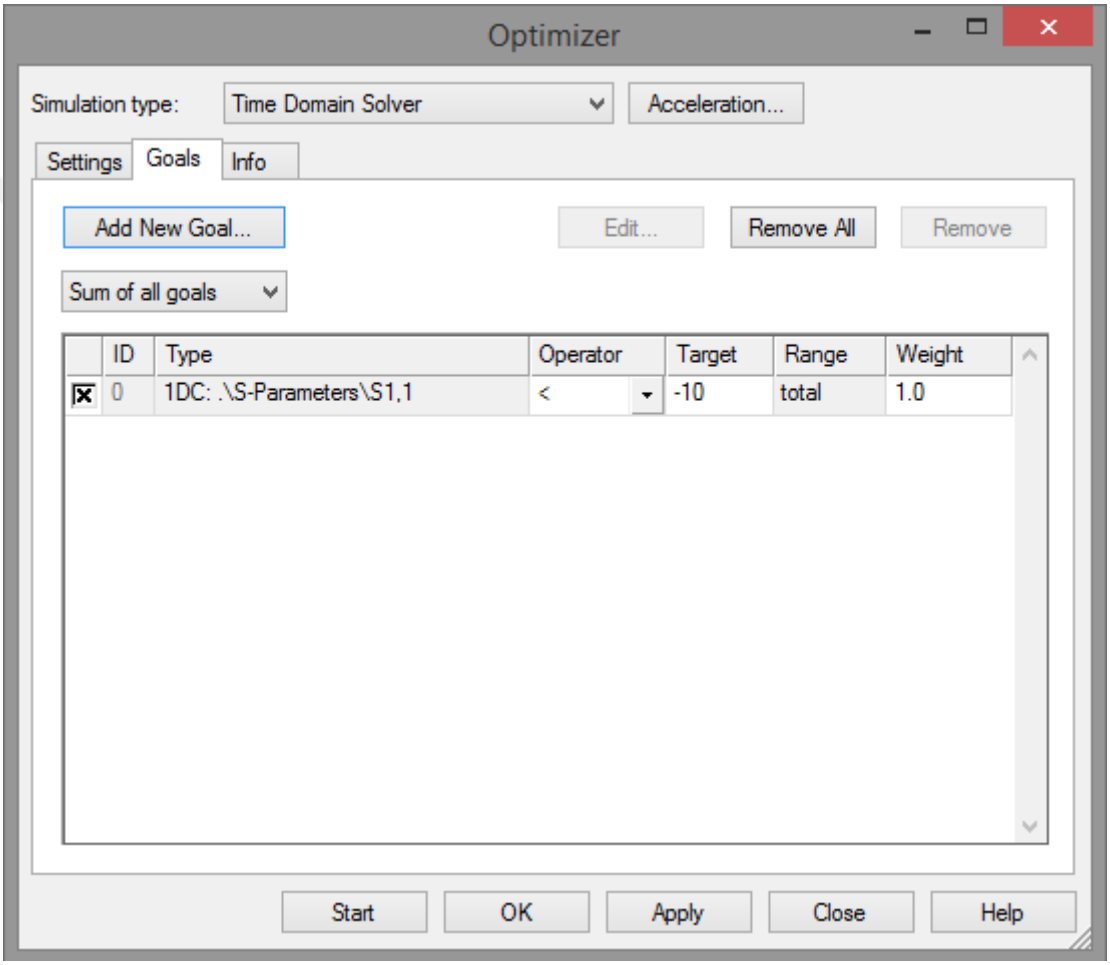

Figure 10.32: The goal function setting from CST MWS

Figure 10.33 and 10.34 illustrate return loss characteristic of the proposed elliptic patch microstip antenna at first iteration and optimized relative permittivity value, respectively. It can be concluded from Figure 10.33 that the proposed elliptic microstrip patch antenna has inherently wider bandwidth regardless of other dimensions of the antenna. Figure 10.34 depicts the optimized return loss characteristic of the aforementioned elliptic microstrip patch antenna. Furthermore, the minimum values of return loss are displayed in Figure 10.35 and 10.36. The minimum return loss of the proposed antenna is -33.11dB at resonance frequency of 9.152 GHz after first iteration

and optimized minimum return loss is -37.29 dB at resonance frequency of 10.084 GHz through optimized relative permittivity value. Consequently, the simulation results outline that return loss is degraded by approximately -4 dB and resonance frequency is increased from 9.152 GHz to 10.084 GHz by almost 1 GHz bandwidth enhancement.

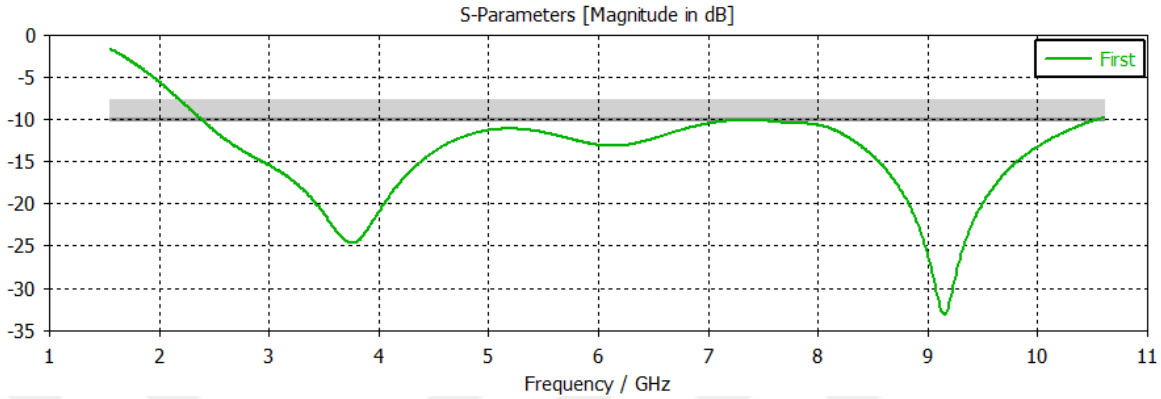

Figure 10.33: Return loss characteristic of the elliptic microstrip patch antenna at first iteration

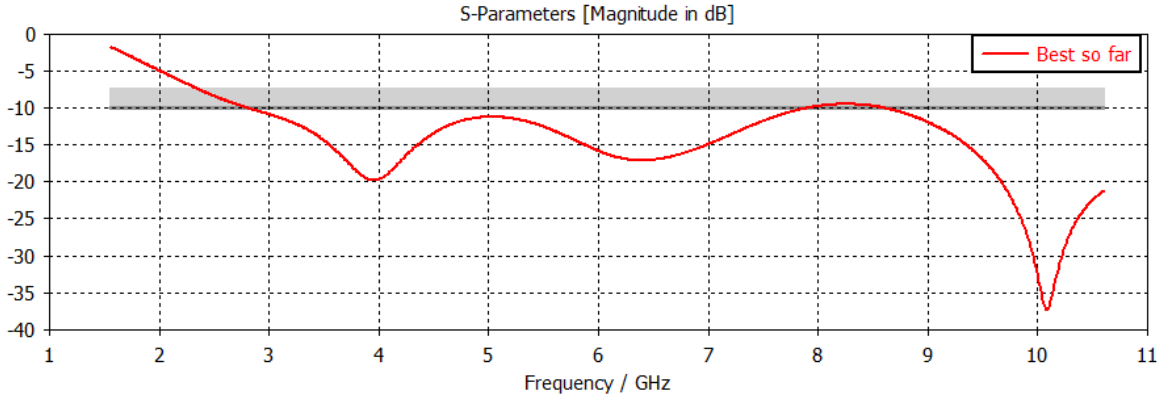

Figure 10.34: Optimized return loss characteristic of the elliptic microstrip patch antenna

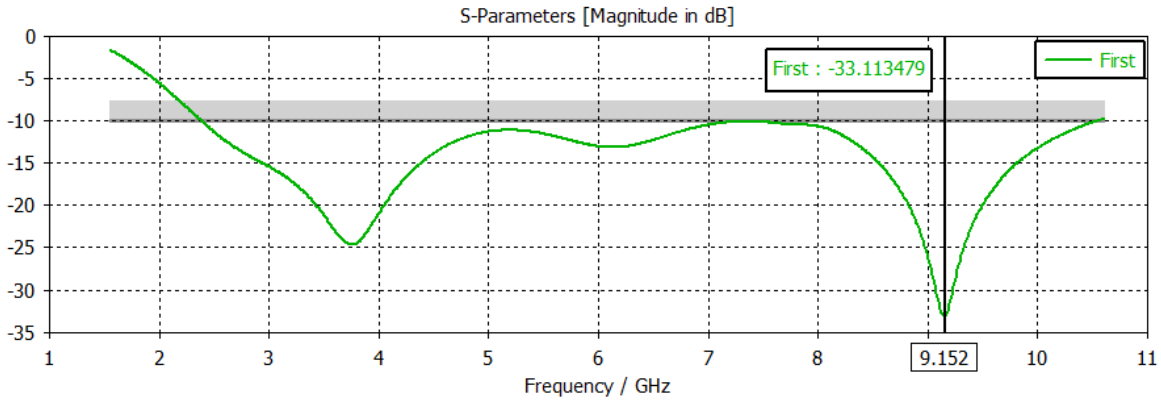

Figure 10.35: Minimum return loss characteristic of the elliptic microstrip patch antenna at first iteration

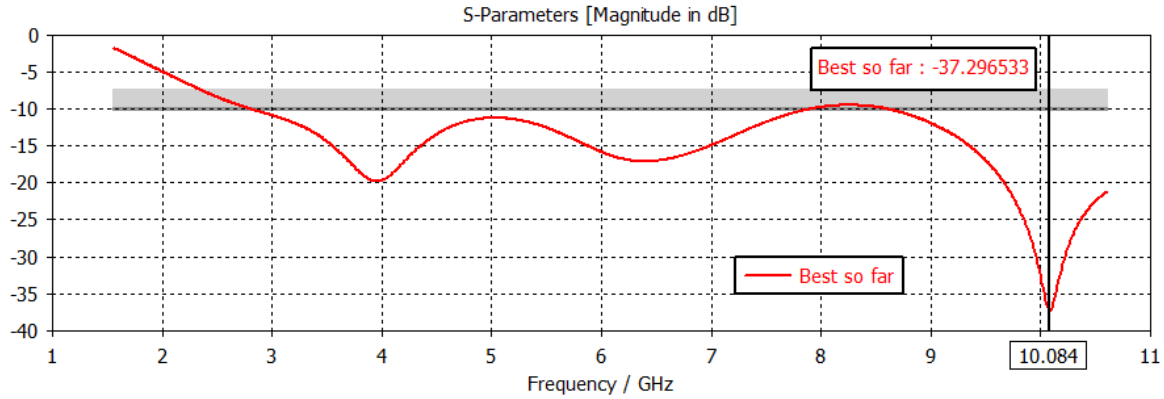

Figure 10.36: Optimized minimum return loss characteristic of the elliptic microstrip patch antenna

Again, the maximum number of iterations is chosen as 265 in order to confirm the iteration number of particle swarm optimization might be selected as 25 which have been already explained the reasons of selecting minimum number of iterations. The best relative permittivity value is obtained as again 3 at 108th iteration which is illustrated in Figure 10. 37.

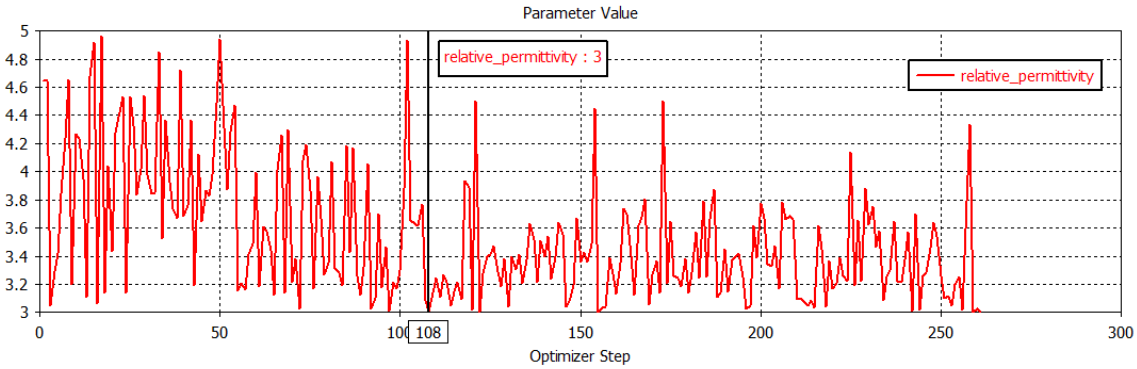

Figure 10.37: Relative permittivity values with 265 iterations

11. CONCLUSION

An antenna is an important component of communication systems for transmitting and receiving signals effectively. Especially in UWB systems, antenna design is a very important task because of its broadband system characteristics. Changes in antenna dimensions and their effect are examined in order to radiate the antenna efficiently, in this thesis. In particular, arm length, substrate length / width and flare angle are also some important parameters that can be optimized to achieve improved bandwidth for the designed antennas. Moreover, the substrate properties, mostly relative permittivity and thickness, have a significant effect on antenna performance. A variety of antenna configurations are depicted in this thesis for UWB communication systems.

This thesis presents to design different antenna structures and define the basic antenna performance parameters including return loss, VSWR and radiation pattern for UWB applications. Additionally, the conventional UWB antennas are modified in order to observe the enhancement of the antenna characteristic. Generally, the crucial treatments of proposed designs require considerable mathematical and theoretical background while the antenna designs in this thesis enhance the bandwidth and radiation characteristics of the antennas in UWB systems. Furthermore, optimization techniques yield the most appropriate antenna dimensions effectively. Half wave dipole, bow tie, rounded bow tie, truncated rounded bowtie, bevelled edge rounded bow tie, microstrip, Rectangular Edge-Fed Patch, and Elliptic Microstrip Patch antenna provide the radiation in the UWB frequency range from 3.1 to 10.6 GHz with 7.5 GHz bandwidth.

Antenna parameters namely Return Loss, Radiation Pattern, Voltage Standing Wave Ratio, Directivity, Gain, and Polarization etc. are crucial restrictions for designing and characterizing the antenna structure in this thesis. Numbers of antennas, which are designed and simulated in this thesis, are appropriate structures so as to provide the features of UWB systems and define the antenna performance.

Some enhancement techniques, including beveling and truncating principle, provide the bowtie antenna bandwidth enhancement.

A rounded bowtie antenna which is obtained from bowtie antenna by truncation process is also presented in this study for UWB applications. The behaviour of the proposed antenna is analysed by modifying thickness and dielectric constant of the substrate. Then, VSWR, S11 and radiation pattern are interpreted in the 3.1-10.6 GHz frequency range. It is additionally observed that the proposed antenna performance is

improved by decreasing thickness and the dielectric constant of the substrate. The proposed rounded bowtie antenna provides significant features for UWB applications.

A different approach namely beveling the arm corners makes the classical bowtie antenna to have broader bandwidth. After this process a novel antenna design is occurred via beveling techniques. This structure provides appropriate performance including better return loss (S_{11}), lower VSWR, flatter input impedance and less distortion radiation pattern as compared to other antenna designs in this thesis. Additionally, transmission line method is applied while the effective antenna structure dimensions are preserved so as to compare with other examined bowtie antenna configurations by using CST Microwave Studio.

Numerous types of microstrip antennas meet demand of the UWB systems and improvement the antenna bandwidth. Two types of the microstrip antenna structures are also considered for UWB. Rectangular patch microstrip antenna has narrow bandwidth which does not meet UWB requirements and restriction of FCC in this thesis. That's why another way of design is considered by changing the patch shape of the proposed antenna. Thus elliptic microstrip patch antenna is considered and it is demonstrated that the structure provides improved bandwidth as compared to rectangular patch antenna.

In order to obtain the most appropriate structures and improve their performance in the frequency range of interest, optimization techniques are used. For this purpose, Genetic Algorithm and Particle Swarm Optimization methods are applied to truncated rounded bowtie and elliptic microstrip patch antennas. According to the obtained results, the effective physical antenna parameters are decided through the optimization methods including Genetic Algorithm and Particle Swarm Optimization so as to exploit these proposed antennas efficiently in the UWB frequency range, i.e. 3.1-10.6 GHz.

REFERENCES

Afyf, A., et al. A Novel Low Cost UWB Antenna for Early Breast Cancer Detection. American Journal of Electromagnetics and Applications, 2015. 3(5): p. 31-37.

Agarwal, A., et al. Ultra-wideband tapered microstrip antenna with modified ground plane. in 2013 INTERNATIONAL CONFERENCE ON SIGNAL PROCESSING AND COMMUNICATION (ICSC). 2013.

Aiello, Roberto and Anuj Batra, eds. Ultra-Wideband Systems: Technologies and Applications. Newnes, 2006.

Antenna Magus, The leading antenna design tool, 2016.

Arokiamary, V.J., Cellular And Mobile Communications. 2009: Technical Publications.

Asghar, M.T., et al., Design and Optimization of an UWB Antenna with 5.8 GHz Band Suppression Using Genetic Algorithm. Journal of Basic and Applied, 2013. 3(7): p. 701-707.

A time-varying electric field, E, will give rise to a perpendicular magnetic field, H, and vice versa. Available from: http://www.dannex.se/theory/1.html

Aydın, E. and D.N Gençoğlan. *A bowtie Antnna Design for Breast Cancer Detection*. in 1st International Energy and Engineering Conference (UEMK 2016)

Bailey, M., Broad-band half-wave dipole. IEEE Transactions on Antennas and Propagation, 1984. 32(4): p. 410-412

BakshiA, U., Antennas and Wave Propagation. 2009: Technical Publications.

Balanis, C.A., Antenna Theory: Analysis and Design. 2005: Wiley.

Baljinder Kaur, L.S.S., A Brief Review on Bowtie Antenna. 2012.

Banerjee, P. and T. Bezboruah, Comparative Study of Transmission Line and Cavity Model of Rectangular Microstrip Antenna. International Journal of Natural Sciences Research, 2015. 3(6): p. 76-82.

Begaud, Xavier, ed. Ultra-wide band antennas. John Wiley & Sons, 2013.

Bernard, V. and J.P. Izuchukwulloh, Microstrip Antenna Design Using Transmission Line Model. International Journal of Emerging Technology and Advanced Engineering, 2013. 3(11).

Blum, C., Ant colony optimization: Introduction and recent trends. Physics of Life reviews, 2005. 2(4): p. 353-373.

Bourqui, J., et al., Antenna Evaluation for Ultra-Wideband Microwave Imaging. International Journal of Antennas and Propagation, 2010. 2010: p. 8.

Bugaj, M., et al., Analysis different methods of microstrip antennas feeding for their electrical parameters.

Černý, Petr, and Miloš Mazánek. "Ultra Wideband Dipole Antenna Optimization." Automatika: Journal for Control, Measurement, Electronics, Computing & Communications 47 (2006).

Choukiker, Y.K., ANALYSIS OF DUAL BAND RECTANGULAR MICROSTRIPANTENNA USING IE3D/PSO. 2009, National Institute of Technology Rourkela.

Chouksey, S. and M. Ghadle, A genetic Algorithm for Optimization of Microstrip Patch Antenna. International Journal of Electrical, Electronics and Computer Engineering, 2012. 1(2): p. 97-99.

Classification of different polarization Available from: http://www.mtiwe.com/?CategoryID=353&ArticleID=163

Çolak, Ş. and D.N. Gençoğlan. Improvement of bowtie antenna parameters for Ultra-Wide Band applications. in 2016 24th Signal Processing and Communication Application Conference (SIU). 2016. IEEE.

Colak, Sule, Tan F. Wong, and A. Hamit Serbest. "Frequency domain analysis of UWB dipole arrays." Journal of Electromagnetic Waves and Applications 28.12 (2014): 1487-1501.

Di Benedetto, Maria-Gabriella, ed. UWB communication systems: a comprehensive overview. Vol. 5. Hindawi Publishing Corporation, 2006.

Dona Mary George, R.R., Design and Analysis of Different Bow-Tie Configurations for Submarines. IJRCCE, 2015. 3(9).

Dyson, John D. "A survey of the very wide band and frequency independent antennas—1945 to the present." Journal of Research of the NBS 66.1 (1962): 1-6.

Federal Communication Commission."FCC Report and Order for Part 15 acceptance of Ultra-Wideband (UWB) systems from 3.1-10.6 GHz." FCC, Washington, DC (2002).

Fereidoony, F., S. Chamaani, and S.A. Mirtaheri, Systematic Design of UWB Monopole Antennas With Stable Omnidirectional Radiation Pattern. IEEE Antennas and Wireless Propagation Letters, 2012. 11: p. 752-755.

Gençoğlan,D.N., Ş. Çolak, Rounded Bowtie Antenna for Ultra-Wideband Communications, International Mediteranean Science and Engineering Congress, IMSEC 2016.

Ghassemi, N., et al., Slot coupled microstrip antenna for ultra-wideband applications in C and X bands. Progress In Electromagnetics Research M, 2008. 3: p. 15-25.

Goudah, M. and M.Y. Yousef, Bandwidth enhancement techniques comparison for ultra-wideband microstrip antennas for wireless application. Journal of Theoretical and Applied Information Technology, 2012. 35(2): p. 184-193.

Hamayoun Nikookar, R. P., Introduction to Ultra-Wideband for Wireless Communications.2009: Springer Netherlands

Harisharan Aggarwal, H. and R. Kumar, Genetic Algorithm Optimization of Bandwidth of Microstrip Patch Antenna.

Hecimovic, N. and Z. Marincic, The improvements of the antenna parameters in ultra-wideband communications

Holland, J.H., Genetic Algorithms and Adaptation, in Adaptive Control of Ill-Defined Systems, O.G. Selfridge, E.L. Rissland, and M.A. Arbib, Editors. 1984, Springer US: Boston, MA. p. 317-333.

Huang, Y. and K. Boyle, Antennas: from theory to practice. 2008: John Wiley &Sons.

Islam, M.T., et al., Curve Fitting Based Particle Swarm Optimization for UWB Patch Antenna. Journal of Electromagnetic Waves and Applications, 2009. 23(17-18): p. 2421-2432.

Jayasinghe, J. and D. Uduwawala, Optimization of the performance of patch antennas using genetic algorithms. Journal of the National Science Foundation of Sri Lanka, 2013. 41(2).

J. Liu, D.Z., and B.-Z. Wang, A beveled and Slot-Loaded Planar Bow-Tie Antenna for UWB Application. Progress In Electromagnetics Research, 2008. 2: p. 37-46.

J. L. Volakis, Antenna Engineering Handbook, 4th Ed., 2007, Chapter 19.3.

Johari, E., et al., Comparative analysis of rectangular and triangular cylindrical microstrip patch antenna.

John, M. and M.J. Ammann. Spline based geometry for printed UWB antenna design. in Antennas and Propagation Society International Symposium, 2007 IEEE. 2007. IEEE.

Karan, S. and V.B. Ertürk, Analysis of Input Impedance and Mutual Coupling of Microstrip Antennas on Multilayered Circular Cylinders Using Closed-Form Green's Function Representations. IEEE Transactions on Antennas and Propagation, 2014. 62(11): p. 5485-5496.

Kaushal, A. and S. Tyagi, MICRO STRIP PATCH ANTENNA ITS TYPES, MERITS DEMERITS AND ITS APPLICATIONS. 2015.

Kennedy, J. and R. Eberhart. Particle swarm optimization. in Neural Networks, 1995. Proceedings., IEEE International Conference on. 1995.

Kshetrimayum, Rakhesh Sing, “An introduction to UWB Communication Systems”. IEEE Potentials 28.2(2009):9-13.

Li, X., E. Pancera, L. Zwirella, H. Wu and T. Zwick, Ultra-Wideband Radar for Water Detection in the Human Body, German Microwave Conference 2010:p.150-153.

Lu, Guofeng, Predrag Spasojevic, and Larry Greenstein. "Antenna and pulse designs for meeting UWB spectrum density requirements." Ultra-Wideband Systems and Technologies, 2003 IEEE Conference on. IEEE, 2003.

Mazhar, W., et al., Compact microstrip patch antenna for ultra-wideband applications.

Nasr, M.A., M.K. Ouda, and S.O. Ouda, Design of star-shaped microstrip patch antenna for ultra-wideband (UWB) applications. International Journal of Wireless & Mobile Networks, 2013. 5(4): p. 65.

Nekoogar,Faranak.Ultra-Wideband Communications: Fundamentals and Applications. Prentice Hall Press, 2005.

Newman, E. and P. Tulyathan, Analysis of microstrip antennas using moment methods. IEEE Transactions on Antennas and Propagation, 1981. 29(1): p. 47-53.

N. Saxena, M.K., N. Kumar and P. Pourush, Application of Genetic Algorithm for Optimization of Important Parameters of Magnetically Biased Microstrip Circular Patch Antenna. 2011. 4: p. 129-136.

Peng, L. and C.-L. Ruan, Design and time-domain analysis of compact multi-band-notched UWB antennas with EBG structures. Progress In Electromagnetics Research B, 2013. 47: p. 339-357.

Powell, Johnna. Antenna design for ultra-wideband radio. Diss. Massachusetts Institute of Technology, 2004.

Punitharaj, D. and S. Kalaimani, Design and fabrication of microstrip antenna for UWB applications. International Journal of Emerging Trends in Electrical and Electronics, 2013. 3(2): p. 60-63.

Prasad, T.D., et al., Comparisons of circular and rectangular microstrip patch antennas.

Rahim, T. and J. Xu, Design of Dual Band Sleeve Dipole Antenna for Mobile Jammer Applications. Indonesian Journal of Electrical Engineering and Computer Science, 2015. 16(1): p. 106-110.

Rani, A. and R. Dawre, Design and Analysis of Rectangular and U Slotted Microstrip Patch using Optimization Program in Java for UHF Applications.

Rumsey, V. Frequency independent antennas. in 1958 IRE International Convention Record. 1957.
Saidulu, V., K.S. Rao, and P.S. Rao, The characteristics of rectangular and square patch antennas with superstrate. Volume. 6: p. 298-307.
Sarkar, Mushlah Uddin, Md Asif Hossain, and Md Imdadul Islam. "The impact of frequency on radiation pattern of bowtie and spiral antenna based on RWG elements." Electronic Computer Technology (ICECT), 2010 International Conference on. IEEE, 2010.
Sayidmarie, K.H. and Y.A. Fadhel, A planar self-complementary bow-tie antenna for UWB applications. Progress In Electromagnetics Research C, 2013. 35: p. 253-267.
Sharma, C., S.B. Rana, and H. Singh, Design and Analysis of Modified Bowtie Antenna. International Journal of Technology Enhancements and Emerging Engineering Research 2015. 3(05): p. 119-121.
Shrestha, S., S.-K. Noh, and D.-Y. Choi, Comparative Study of Antenna Designs for RF Energy Harvesting. International Journal of Antennas and Propagation, 2013. 2013: p. 10.
Singh, Parminder, et al. "Half-Wave Dipole Antenna for GSM Applications." International Journal of Advanced Computer Research 2.4 (2012): 354-357.
Sprungle, Raymond J., and Chi-Chih Chen. "A “UWB” half-wavelength dipole for low-frequency gain reference." Antennas and Propagation Society International Symposium, 2008. AP-S 2008. IEEE. IEEE, 2008.
Studio, M., CST-Computer Simulation Technology. Bad Nuheimer Str, 2008. 19: p. 64289.
Stutzman, W.L. and G.A. Thiele, Antenna theory and design. 2012: John Wiley &Sons.
S, W.Q., L. Ruan, Effect of Round Corners on Bowtie Antennas. Progress In Electromagnetics Research, 2006. 57: p. 179-195.
Tapan Nahar, O.P.S., A Modified Multiband Bow Tie Array Used for L band Applications. International Journal of Engineering Research & Technology, 2014. 3.
Tareq, M., et al., Simple Half-Wave Dipole Antenna Analysis for Wireless Applications by CST Microwave Studio. International Journal of Computer Applications, 2014. 94(7).
Teodorovic, D., et al. Bee colony optimization: principles and applications. in Neural Network Applications in Electrical Engineering, 2006. NEUREL 2006. 8th Seminar on. 2006. IEEE.
Türker, N., F. Güneş, and T. Yildirim, Artificial neural design of microstrip antennas. Turkish Journal of Electrical Engineering & Computer Sciences, 2007. 14(3): p. 445-453.
Wiesbeck, Werner, Grzegorz Adamiuk, and Christian Sturm. "Basic properties and design principles of UWB antennas." Proceedings of the IEEE 97.2 (2009): 372-385.
Win, Moe Z. and Robert A. Scholtz,”Impulse Radio:How it works.” IEEE Communications Letters 2.2(1998):36-38
Zhang, X., et al. Integrated broadband bowtie antenna on transparent substrate. in SPIE OPTO. 2015. International Society for Optics and Photonics.
Zubair, M. and M. Moinuddin, Joint Optimization of Microstrip Patch Antennas Using Particle Swarm Optimization for UWB Systems. International Journal of Antennas and Propagation, 2013. 2013: p. 8.

VITA

Duygu Nazan Gençoğlan was born in Ingolstadt, Germany, in 1990. She received the B.E. degree in electrical and electronics engineering from the Çukurova University, Adana, Turkey, in 2013. She started to study Master of Science in electric and electronic engineering department, in Adana Science and Technology University, in 2014, in September.

In 2017, January, she joined the Department of Electrical and Electronics Engineering, Adana Science and Technology University, as a research assistant. She has been with the department of Electrical and Electronics Engineering Department. Her current interests include antennas and wave propagations, metamaterials, electromagnetic fields and microwave techniques, ultra-wideband communication systems.

She attended the student programme, which is called Work and Travel, so as to learn different cultures and improve the English skill in 2010, from June to September, in U.S.A, in VA, in Williamsburg. She was the recipient of the Certificate of the Honour of the Çukurova University in 2009 and 2010. She was also the recipient of the Certificate of the High Honour of the Çukurova University in 2013, Fall Semester. She got the course of Industrial Electric which was organized by ÇUTED. She also attended the PLC operator training at Çukurova University in 2009.